國立臺灣大學醫學院藥理學研究所

博士論文

Graduate Institute of Pharmacology

College of Medicine

National Taiwan University

Doctoral Dissertation

Dehydrocostuslactone、MPT0G013 與 MPT0B271 對於血管新生抑制作用及抗癌機轉之探討

Investigation of anti-angiogenic and anti-cancer mechanisms of dehydrocostuslactone, MPT0G013 and MPT0B271 *in vitro* and *in vivo*

王之雅

Chih-Ya Wang

指導教授：鄧哲明 博士，潘秀玲 博士

Advisors: Che-Ming Teng, Ph.D., Shiow-Lin Pan, Ph.D.

中華民國 103 年 7 月

July 2014

目錄

國立臺灣大學博士學位論文
口試委員會審定書

Dehydrocostuslactone、MPT0G013 與 MPT0B271 對於
血管新生抑制作用及抗癌機轉之探討

Investigating anti-angiogenic and anti-cancer mechanisms of dehydrocostuslactone, MPT0G013 and MPT0B271 *in vitro* and *in vivo*

本論文係王之雅君（F96443006）在國立臺灣大學藥理學研究所完成之博士學位論文，於民國 103 年 07 月 29 日承下列考試委員審查通過及口試及格，特此證明

口試委員：

鄭哲明（指導教授）

陳育弘（指導教授）

顏茂雄

楊春茂

黃德富

系主任、所長 陳青周

誌謝

一眨眼，台大藥理所七年歲月如梭，我，終於畢業了！回憶起初踏入實驗室興奮的心情，那股悸動仍晃如昨日一般。回首這七年來求學歷程，受到諸位師長、同學、朋友與家人的協助與鼓勵，千言萬語也訴不盡我的感謝。首要感謝的人，是多年來一路帶領我的恩師 鄧哲明老師，感謝老師讓我在這溫馨的實驗室裡學習和成長，老師誠信仁厚的處事態度，虛懷若谷的智慧，是我永遠的典範！更感謝老師送我去美國北卡大學李國雄老師實驗室學習一年，體驗不同的文化和生活，增廣見聞；感謝師母的照顧和祝福，畢業禮物讓我備感溫馨。親愛的阿潘學姐仿佛溫暖的太陽，每當實驗遇到瓶頸與挫折，總引導我到正確的方向，是我信心來源的後盾，學姊樂觀的態度，更是幫助我順利完成這份論文的一大功臣。謝謝雅鈴學姐生活上的照顧，繁冗的行政業務與實驗室相關的一切耗材訂購、管理，都幫我們處理的盡善盡美，使我能心無旁騖，專心進行實驗。特別感謝口試委員黃德富老師、顏茂雄老師、楊春茂老師細心指導改正，使我的論文更臻完善。感謝顧老師實驗上的指導，提供我很多想法；感謝北卡大學的李國雄院士，因為您的指導和幫助，一年的北卡生活，有開心、有辛苦、有成長、更有滿滿的收獲，絕對是我一生珍貴的經歷；感謝所辦梁姐姐和沈姐姐的幫忙、提醒和叮嚀；感謝岸圻學姐的照顧與細心教導，您是我永遠的師父！辛苦您了！

感謝姿璇學姐在實驗上的幫助，很懷念跟您一起去剪頭髮的時光；感謝思穎學姐與我分享許多飼養貓咪的小撇步；感謝美全學姐的建議和幫助，您的健談開朗，和您聊一整天都話題不斷；感謝俊瀚學長在實驗上的指導；感謝清裕學姐的幫助，很懷念一起上畫畫課的日子以及您的開朗和貼心；感謝儷薰學姐的幫助，您的細心認真是我學習的目標；感謝小白的鼓勵和生活心情上的一切分享，一起走過這麼多年的研究生生活！感謝耙子的幫助，祝福妳幸福喔！感謝敏吾的陪

伴，當時一起在 1151 用筆電同步看日劇的情景，仍歷歷在目！感謝玨玨的貼心和幫忙，一起坐 37 回家的日子感謝有妳的陪伴，希望以後可以結伴出遊而不是挑燈夜戰，感謝和穎的生活笑料，增添實驗室的生活樂趣，感謝 Amy、穎萱、亭雲、礦美女、阿蝦、隆隆、阿年一直以來的鼓勵支持和陪伴，給予我信心度過難關；感謝瑞陵、靜琪、Demi、Anita、怡琳在動物實驗上的所有幫助；感謝乖巧的子涵在實驗上的幫助，也感謝俊瑋的幫忙。

感謝親愛的佑維，謝謝你的扶持和鼓勵，在實驗室陪伴我渡過無數的白晝和夜晚，消化我所有的辛酸血淚，支持我撐過多年的研究生活，還長途跋涉到美國來找我，你為我做的一切，真的無法用感謝道盡。

感謝我的父母，您們二十九年來的辛勞、無條件的付出、支持和體諒，讓我無後顧之憂專心在課業上；感謝我的哥哥嫂嫂給予我的支持，鼓勵我完成學業；最後，謝謝所有幫助過我的師長、家人和好友，再一次感謝！謹以此論文，献给我摯愛的父母、師長、朋友惠存，謝謝您們！

縮寫表

Akt	protein kinase B
4E-BP	eukaryotic initiation factor 4E (eIF4E)-binding protein
BrdU	5-bromo-2-deoxyuridine
bFGF	fibroblast growth factor-basic
calcein AM	calcein acetoxymethyl ester
DHC	dehydrocostuslactone
EBM-2	endothelial cell basal medium-2
ECGs	endothelial cell growth supplements
EGF	epidermal growth factor
EGM-2	endothelial cell growth medium-2
ELISA	enzyme-linked immunosorbent assay
MMP	matrix metalloproteinase
mTORC1	mammalian target of rapamycin (mTOR)-C1
NSCLC	non-small cell lung cancer
p70S6K	70-kDa ribosomal protein S6 kinase
PDGF	platelet-derived growth factor
PlGF	placental growth factor
p-gp	p-glycoprotein
Rh-123	rhodamine-123
siRNA	small interfering RNA
TIMP3	tissue inhibitor of metalloproteinase 3
VEGF	vascular endothelial growth factor

中文摘要

血管新生 (angiogenesis) 是從已存在的血管分化形成新血管網路的過程，對於生理器官發育、組織修復及生殖占有重要調控的角色。在病理中，腫瘤的生長、進展都必須仰賴血管新生，來得到足夠的氧氣和養分供應，以及排除細胞的代謝廢棄物。此外，自體免疫疾病、退化性關節炎及老年性黃斑部病變也與血管過度新生相關，因此，抑制血管新生可應用於血管生成相關的疾病。在本論文中，將探討具有發展潛力的血管新生抑制劑之機轉。

本論文的第一個部分主要在探討來自中草藥廣木香 (*Saussurea costus* (Falc.) Lipschitz) 的萃取物 dehydrocostuslactone (DHC) 對血管新生促進因子 (endothelial growth factors；EGM-2) 引起血管新生的抑制作用與分子機轉。實驗發現，DHC 能夠抑制人類臍靜脈內皮細胞的增生及類血管管腔的形成，但是不會影響細胞的移行，在 *in vivo* matrigel plug assay 中，DHC 能抑制體內的血管新生。DHC 能夠透過抑制 Akt/GSK-3β、mTOR 的磷酸化，明顯減少 cyclin D1 的蛋白表現，當細胞過度表現持續性活化的 myristoylated (myr)-Akt，DHC 抑制細胞增生、管腔形成以及減少 cyclin D1 都會被逆轉而回復。若是將內皮細胞共同處理 LiCl 及 DHC，則能夠明顯地逆轉 DHC 抑制細胞生長的作用。總結以上結果，本研究證實 Akt/GSK-3β/cyclin D1 以及 mTOR 訊息路徑是 DHC 重要的標靶，因此能夠應用於如癌症及血管新生相關的疾病。

本論文的第二個部分在探討 arylsulfonamide 衍生物 MPT0G013 在體內及體外具有抗血管新生之活性。MPT0G013 能明顯抑制內皮細胞增生、移行和類血管管腔形成，經由基因晶片檢測分析，MPT0G013 能明顯誘導 tissue inhibitors of metalloproteinases 3 (TIMP3) 的表現，將細胞轉染 TIMP3 siRNA，能夠逆轉 MPT0G013 抑制血管新生的作用及回復 Akt、ERK 蛋白的磷酸化；除此之外，利

用 *in vivo* matrigel plug assay 和腫瘤的異體移植實驗，證實 MPT0G013 在體內具有明顯抑制血管生成的作用。因此，我們推論 MPT0G013 是一個值得進一步研發的抗血管新生藥物。

目前被用來治療癌症的 taxanes 及 vinca 生物鹼等微管結合藥物，缺點為抗藥性的產生及必須透過靜脈注射投與，因此迫切需要研發新的藥物。MPT0B271 是一個口服生體可用的微管標靶全合成藥物，在體內及體外具有強力的抗癌效果，MPT0B271 除了導致微管的去聚合，且能抑制許多癌細胞株生長及降地存活率，包括 multidrug-resistant 癌細胞株 NCI/ADR-RES。利用流式細胞儀分析 rhodamine-123 (Rh-123) 的輸出及利用 calcein acetoxymethyl ester (calcein AM) assay，發現 MPT0B271 不是 p-glycoprotein (p-gp) 的受質；此外，MPT0B271 也會誘導細胞 G2/M 期停滯以及細胞凋亡。我們也發現在體內及體外，與單獨給藥相較之下，MPT0B271 合併 erlotinib (Tarceva) 能明顯抑制人類非小細胞肺癌 A549 細胞的生長，這些結果證實 MPT0B271 是一個具有潛力治療各種癌症的新穎的微管結合藥物。

綜合以上所述，本論文主要以抗血管新生及抗癌為研究對象，證實 DHC 和 MPT0G013 能顯著抑制體內及體外之血管新生作用，MPT0B271 是新穎的抗癌藥物，能夠發展成為治療癌症的先導藥物。

英文摘要

Angiogenesis, which is the process of formation of new blood vessels from pre-existing ones, takes place throughout physiological development, tissue repair, and reproduction. In pathological conditions, angiogenesis is also essential for tumor growth and progression to ensure that more oxygen and nutrients are delivered from the host's vascular system. Therefore, angiogenesis is a promising target for anticancer treatments. In this thesis, we focused on the discovery of potential novel antiangiogenic agents, and further investigated the mechanism of these agents.

In the first part, we investigated the traditional Chinese medicine component dehydrocostuslactone (DHC) isolated from *Saussurea costus* (Falc.) Lipschitz, which has been shown to have anti-cancer activity. DHC has an anti-angiogenic effect in the matrigel-plug nude mice model and an inhibitory effect on HUVEC proliferation and capillary-like tube formation *in vitro*. With respect to the molecular mechanisms underlying the DHC-induced cyclin D1 down-regulation, we demonstrated that DHC significantly inhibited Akt expression, resulting in the suppression of GSK-3β phosphorylation and mTOR expression. Furthermore, the degradation of cyclin D1 and the abrogation of tube formation induced by DHC were significantly reversed by constitutively active myristoylated (myr)-Akt. And the co-treatment with LiCl and DHC significantly reversed the growth inhibition induced by DHC.

Tissue inhibitors of metalloproteinases 3 (TIMP3) were originally characterized as inhibitors of matrix metalloproteinases (MMPs), acting as potent antiangiogenic proteins. In the second part, we demonstrated that the arylsulfonamide derivative MPT0G013 has potent antiangiogenic activities *in vitro* and *in vivo* via inducing

TIMP3 expression. Treatments with MPT0G013 significantly inhibited endothelial cell functions, such as cell proliferation, migration, and tube formation. Subsequent microarray analysis showed significant induction of *TIMP3* gene expression by MPT0G013, and siRNA-mediated blockage of TIMP3 up-regulation abrogated the antiangiogenic activities of MPT0G013 and prevented inhibition of p-AKT and p-ERK proteins. Importantly, MPT0G013 exhibited antiangiogenic activities in *in vivo* Matrigel plug assays, inhibited tumor growth and up-regulated TIMP3 and p21 proteins in HCT116 mouse xenograft models.

MPT0B271, an orally active microtubule-targeting agent, is a completely synthetic compound that possesses potent anticancer effects in vitro and in vivo. MPT0B271 caused depolymerization of tubulin at both molecular and cellular levels and reduced cell growth and viability at nanomolar concentrations in numerous cancer cell lines, including a multidrug-resistant cancer cell line NCI/ADR-RES. Further studies indicated that MPT0B271 is not a substrate of p-gp, as determined by flow cytometric analysis of Rh-123 dye efflux and the calcein AM assay. MPT0B271 also caused G2/M cell-cycle arrest, accompanied by induction of cell apoptosis. We demonstrated that MPT0B271 in combination with erlotinib significantly inhibits the growth of the NSCLC A549 cells as compared with erlotinib treatment alone, both in vitro and in vivo. These findings identify MPT0B271 as a promising new tubulin-binding compound for the treatment of various cancers.

Taken together, the present studies have highlighted the potential application of DHC and MPT0G013 in angiogenesis-related diseases, such as cancer. And the anti-tumor agent MPT0B271 may foster novel therapeutic strategies for various cancer cell lines.

第一章 緒論

第一節 研究動機與目的

根據行政院衛生署公布台灣地區 2013 年最新的 10 大死因排行榜，其中惡性腫瘤連續 31 年蟬聯國人死亡排行榜之首，平均每百人死亡，就有 29.0% 是死於癌症。因此，研發抗腫瘤藥物是研究學者和醫藥專家共同努力的對象。

腫瘤的生長及轉移都必須藉由血管新生達成，其中血管內皮細胞占最重要的地位，因此針對內皮細胞的抗血管新生治療成為有別於傳統毒殺癌細胞的療法。血管新生是由各種血管新生因子來調控的，本論文中將以血管中的內皮細胞為研究對象，探討中草藥成分 DHC 及 arylsulfonamide 衍生物 MPT0G013 對於 EGM-2 內皮生長因子引發血管新生的影響及機轉。

在惡性腫瘤中，氣管、支氣管和肺癌是死因之首，其中，又以非小細胞肺癌為發生率最高，目前肺炎的治療方式主要以手術、化學治療、放射治療、標靶治療或合併治療，化學療法主要以鉑金類藥物 (cisplatin 或 carboplatin) 、抗微管藥物 (paclitaxel 或 docetaxel) 為主；然而微管標靶藥物最大的問題便是其抗藥性的產生及靜脈注射的不便及藥物毒性，因此，開發能避免抗藥性的微管標靶藥物是迫切需要的，以幫助肺癌病患。本篇論文的第三部分是以非小細胞肺癌細胞株為主要對象，探討在體內及體外 MPT0B271 對於細胞微管的影響、引起細胞凋亡及抑制腫瘤生長的機轉。

第二節 文獻回顧

1. 血管新生 (vasculogenesis 及 angiogenesis)

血管的生成可以由兩種方式，vasculogenesis 及 angiogenesis，vasculogenesis 指的是在胚胎中，血管是由中胚層的 endothelial progenitors (angioblasts) 分化形成的原始血管網路，angiogenesis 則是指的是一個已存在的原有血管系統為基礎，形成芽生性 (sprout) 血管，再發展出新的側枝血管網路，將動脈系統架橋連接起來，而形成一個血流供應系統的生理過程 (Figure 1-1)。血管新生在正常生理中的角色除了胚胎中的心血管系統的建立，在成人的生殖系統、卵巢的正常週期和傷口癒合修復都相當重要 (Chung *et al.*, 2010)。然而，不正常或過度的血管新生會導致許多疾病，最常見的是癌症、乾癬症、關節炎和失明，還有許多失調症，例如：肥胖、氣喘、動脈粥樣硬化及感染疾病 (Table 1-1) 。

2. 腫瘤與血管新生

1939 年，Ide 等人利用兔子耳朵的腫瘤異體移植實驗，發現腫瘤生長會伴隨新生成的血管網路，推測腫瘤可能會分泌促血管生長物質 (Ide, 1939)；1945 年，Algire 等人在腫瘤異體移植從動力學進入更深入的研究，發現在缺乏血液供應情況下，腫瘤無法快速生長 (Algire *et al.*, 1950) 。1971 年，Folkman 醫生從腫瘤中分離出了腫瘤血管生成因子 TAF (Tumor Angiogenesis Factor) ，並提出一假說，腫瘤的生長並非持續性的，當腫瘤直徑達到 1 - 2 mm，會釋放出 TAF 促進血管增生，並依賴新生的微血管供給養分、氧氣及排除代謝廢棄物，腫瘤才能繼續成長，因此如果抑制了 TAF 的活性將可以阻礙腫瘤的生長 (Folkman, 1971)，此一假說促使血管新生研究正式啟動，並逐漸成為眾多學者關注的研究熱點。

隨著幾十年來的研究，發現這些腫瘤釋放的血管生成因子主要包括血管內皮

細胞生長因子 (vascular endothelial growth factor；VEGF)、血小板衍生生長因子 (platelet-derived growth factor；PDGF)、鹼性纖維母細胞生長因子 (fibroblast growth factor-basic；bFGF) (Folkman, 2007)，當這些生長因子結合至內皮細胞上的接受器時，會活化內皮細胞並誘導細胞內訊息傳遞，接著癌細胞和活化的內皮細胞都會釋放基質金屬蛋白酵素 (matrix metalloproteinase；MMP) 和 angiopoietin-2，MMPs 和 angiopoietin-2 會增加血管基底膜 (basement membrane) 的水解，對細胞外基質 (extracellular matrix；ECM) 進行再塑 (remodeling) ，使穩定內皮細胞的外被細胞 (pericytes) 分離，進而促進內皮細胞的移行 (migration) 及侵入 (invasion) ，形成血管芽 (sprout) ，其前端內皮細胞會特化為頂端細胞 (tip cell) ，透過 integrins 的訊息傳遞來引導血管芽往生長因子濃度梯度方向移行，後端的內皮細胞會特化成 stalk cell，進行細胞增生，延長血管芽，形成管腔 (tube formation) ；新生的內皮細胞並不是全部來自鄰近血管，有一部分是來自骨髓的內皮原生細胞 (endothelial progenitor cells) ，對血管新生是必須不可或缺的。最後，基質金屬蛋白酵素的組織抑制劑 (tissue inhibitor of metalloproteinases；TIMPs) 抑制基質金屬蛋白酵素的活性，調控細胞外基質的改造，外被細胞及平滑肌細胞聚集並穩定血管，與原本的母血管融合，形成血管網路 (Figure 1-2) (Carmeliet *et al.*, 2011; Folkman, 2007; Potente *et al.*, 2011)。

3. 血管新生的訊息傳遞

血管新生是一個需要眾多血管新生因子與抗血管新生因子參與所調控的過程，這些血管新生因子在內皮細胞內所誘導的訊息傳遞，以 VEGF (VEGF-A) 為例，VEGF 又稱為血管通透因子，ligand 包括 VEGF-A、VEGF-B、VEGF-C、VEGF-D、VEGF-E 及 PlGF (placental growth factor)，receptor 則包括 VEGFR-1 (fms-like tyrosine kinase；Flt-1)、VEGFR-2 (Fetal liver kinase-1/Kinase insert domain containing receptor；Flk-1/KDR)、VEGFR-3 (Flt-4) (Ellis *et al.*, 2008) 。研究發現

VEGF 大部分的 mitogenic 及 chemotactic 作用，是經由 VEGFR-2 的訊息傳遞，這些路徑主要包括：(1) Ras/Raf/MEK/ERK MAP kinase pathway 誘導基因表現促進細胞增生；(2) 透過活化 PLC-γ/PKC，增加細胞內鈣離子濃度、eNOS 的表現以及血管通透性；(3) 透過 focal adhesion kinase (FAK) pathway 導致 focal adhesion turnover 以及細胞移行；(4) 經由 p38/Hsp27 pathway，導致 actin reorganization 以及細胞移行；(5) phosphatidylinositol 3-kinase (PI3K)/Akt pathway 活化維持細胞的存活，PI3K 將 PIP_2 催化轉換成 PIP_3，PIP_3 吸引 Akt 至細胞膜經由磷酸化而活化，Akt 也能夠活化 eNOS，增加細胞通透性，並且也能抑制促細胞凋亡蛋白，增加細胞存活 (Figure 1-3) (Ivy *et al.*, 2009)。

4. 基質金屬蛋白酵素組織抑制劑 (tissue inhibitors of metalloproteinase；TIMPs)

TIMPs 是由 184-194 個胺基酸所組成，是 MMPs 的內生性抑制蛋白，目前在真核生物中發現有四個成員 (TIMP1、TIMP2、TIMP3、TIMP4)，其分布及表現是由器官發育及組織再塑時進行調控，在病理中則被認為與 MMPs 活性的失衡相關。在成人中，TIMP3 持續性的表現在眼睛的視網膜色素內皮層及脈絡膜內皮細胞 (Della *et al.*, 1996; Qi *et al.*, 2002)，TIMP3 的突變會導致 sorsby's 眼底營養不良症 (sorsby's fundus dystrophy)，為體染色體顯性疾病，有研究發現是因為 S156C 的突變使 TIMP3 失去抑制 MMP 的活性，造成脈絡膜的過度血管新生，導致黃斑部病變 (macular degeneration) 以及突發性失去視力 (Langton *et al.*, 2000; Tabata *et al.*, 1998; Weber *et al.*, 1994)。

TIMPs 能夠抑制目前所知所有的 MMPs，與 TIMPs 家族成員不同的是，TIMP3 具有特殊的分子特性和活性，TIMP3 含有與細胞外基質交互作用的特殊介質結合區，從細胞釋放出來後，藉由與 heparan-sulfate-containing proteoglycans 結合聚集在細胞外基質，是唯一能夠抑制細胞膜結合 MMPs (membrane-bound MMPs)、過膜 MMPs (transmembrane MMPs) 的 TIMPs 成員，對象包括去整合素金屬蛋白酵

素 (a disintegrin and metalloproteinases；ADAMs) 以及去整合素金屬蛋白酵素含類凝血酵素區 (a disintegrin and metalloproteinases with thrombospondin-like domain；ADAM-TS)，TIMP3 對於一般的 MMP-2、MMP-9 抑制作用則較弱 (Nagase *et al.*, 2006)。TIMP3 藉由抑制 ADAM-17 (TACE) 對表皮生長因子 (epidermal growth factor receptor；EGFR) 配體 (ligands) 的 ectodomain shedding 作用，進而減少 EGFR 下游 ERK 的訊息傳遞活化 (Murthy *et al.*, 2010) ，另外，TIMP3 能夠穩定細胞表面腫瘤壞死因子受體 (tumor necrosis factor-receptor 1；TNF-α R 1)、Fas (CD95)、TNF-related apoptosis-inducing ligand receptor-1；TRAIL-R1，在許多癌細胞株中具有促細胞凋亡的活性 (Ahonen *et al.*, 2003; Bond *et al.*, 2000; Bond *et al.*, 2002; Koers-Wunrau *et al.*, 2013)。

TIMP3 被認為透過阻礙 VEGF 與 VEGFR2 結合，抑制其下游訊息傳遞，而在體內及體外具有明顯抗血管新生的作用，並且推測與 TIMP3 本身抑制 MMP 的作用不相關 (Qi *et al.*, 2003)，另外，最近也有研究發現，TIMP3 衍生的胜肽能抑制 VEGFR、bFGFR、PDGFR 誘導的血管新生 (Chen *et al.*, 2014)。

5. 細胞週期 (Cell cycle)

細胞週期共分為五個階段，包括 G0、G1 (GAP 1)、S (synthesis)、G2 (GAP 2) 和 M (mitosis) 期，其受到 cyclins、cyclin-dependent kinases (CDKs) 以及 cyclin-dependent kinase inhibitors (CDKIs) 的調控 (Figure 1-4) (Davidson *et al.*, 2010)。CDK 的活化需要與 cyclins 結合形成複合物，在細胞週期進行過程，cyclins 會在特定的時間點合成與分解，來調控 CDK 的活性，當細胞之 DNA 受到傷害時，則可能導致細胞週期停滯在某一時期。當細胞受到生長因子的刺激，會促進 cyclin D 的轉錄及轉譯，cylcin D 會與 CDK4/CDK6 形成複合物，進而磷酸化與轉錄因子 E2F 結合的 retinoblastoma (Rb) 蛋白，使 p-Rb 蛋白釋放出 E2F，促進 E2F 相關基因的轉錄活化，包括 cyclin E 和 cyclin A，對於 DNA 合成是必須的，進而活

化 CDK2，促使細胞從 G1 期進入 S 期 (Figure 1-5) (Musgrove *et al.*, 2011)。目前已知 Akt 訊息路徑能夠透過 glcogen synthase kinase-3β (GSK-3β) 調控 cyclin D1 的表現，GSK-3β 能夠藉由磷酸化促進 cyclin D1 藉由 ubiquitination 而被降解，Akt 將 GSK-3β serine9 磷酸化，抑制 GSK-3β 的活性，增加 cyclin D1 蛋白的穩定性和表現 (Figure 1-6) (Chang *et al.*, 2003)。接著，合成的 cyclin E 與 CDK2 形成複合物，幫助細胞週期從 G1 期進入 S 期，cyclin A/CDK2 複合物則促進細胞週期進入 G2 期 (Figure 1-4) (Davidson *et al.*, 2010)。

細胞週期由 G2 期進入 M 期的調控蛋白質為 cyclin B 及 CDK1 (Cdc2) ，M 期是細胞進行有絲分裂期，又分為 prophase、metaphase、anaphase 與 telophase。首先 CDK activated kinase 會將 Cdk1 Thr161 磷酸化，同時 Cdc25C 去磷酸化酵素會將 Cdk1 抑制性的磷酸根 Thr14/Tyr15，形成活化態的 Cdk1，並與 cyclin B 結合形成複合物，促使細胞進入 M 期，完成有絲分裂 (Figure 1-4) 。

6. 微管與微管標靶藥物 (microtubule-targeting agents)

微管在真核細胞中，增生、運輸蛋白、訊息傳遞、移行占有重要的角色，細胞進行有絲分裂時，必須由微管幫助進行，幫助細胞的染色體確切的分布到兩個子細胞中，因此，如果能夠利用小分子藥物直接干擾微管的功能，就能有效阻止大量分裂的癌細胞存活。微管呈現中空管狀結構的多元體 (polymers) ，由 α 及 β 兩種微管蛋白 (tubulin) 所組成，並由 microtubule-associated proteins 或去穩定蛋白調控微管，使微管能夠在聚合或去聚合之間轉換，呈現動態平衡，微管其中一端是正 (+) 端，生長速率大於解離速率，傾向聚合，另一端為負 (-) 端，生長速率小於解離速率，傾向去聚合，目前微管標靶藥物主要透過干擾微管的穩定度，達到抑制癌細胞生長的作用，這類藥物主要分為微管穩定劑 (microtubule-stabilizers) 及微管去穩定劑 (microtubule-destabilizers) ，根據與微管結合位置不同可分成兩類：vinca 和 colchicine 藥物，能抑制微管聚合；taxol 類藥

物使微管聚合無法分離，來抑制有絲分裂 (Figure 1-7)。

抗微管藥物在臨床上已經成為許多種類癌症的化療藥物，但是由於其藥物腎毒性、骨髓抑制和抗藥性的產生，限制了這一類藥物的效果，抗藥性的產生主要是由於藥物從細胞內排出，而造成藥物無法與標靶結合引發細胞凋亡，細胞膜表面的輸出幫浦 ATP binding cassette (ABC) family 過度表現是癌細胞發展出的主要抗藥性機轉，p-glycoprotein (p-gp) 是 MDR1 基因的產物，屬於 ABC family 中的 ABCB1 subfamily，是傳統微管標靶藥物的運輸蛋白，能夠將 vinca alkaloids 及 taxanes 類藥物排出，降低細胞內濃度及毒殺作用 (Figure 1-7) ，其他的運輸蛋白則只有排出某些種類的抗微管藥物，vinca alkaloids 會被 multidrug-resistance-associated protein 1 (MRP1) 主動運輸出細胞外，taxanes 是 MRP2 及 MRP7 的受質，epothilone B 則是被 MRP7 攜帶排出 (Breuninger *et al.*, 1995; Hopper-Borge *et al.*, 2004; Huisman *et al.*, 2005) ，由於輸出幫浦是造成化療藥物產生抗藥性的重要機轉，因此，迫切需要研發新穎的微管標靶藥物，以改善現有藥物的缺點。

7. 細胞凋亡路徑

已經有許多文獻指出，影響微管的正常功能，破壞癌細胞有絲分裂的進行，能夠使細胞走向凋亡，達到抑制腫瘤生長的作用。細胞凋亡又稱為程序性細胞死亡 (programmed cell death) ，是細胞因應環境的刺激，接受特定的訊號後所自行決定的死亡。細胞凋亡的主要特徵是細胞核內染色質凝結 (nuclear condensation) 以及大量 DNA 水解斷裂成小片段 (< 200 bp) ，屬於細胞凋亡特有的現象 (Taylor *et al.*, 2008)。

細胞凋亡的外生性路徑是藉由細胞外 death ligands (例如 FasL 或 tumour necrosis factor-α (TNFα)) 與 transmembrane death receptors 的結合而啟動，接著吸引 adaptor proteins，例如 Fas-associated death domain protein (FADD) ，並與

procaspase-8 及其他許多分子聚集形成 DISC (death-inducing signaling complex)，活化的 caspase-8 進而活化下游的 caspase-3、caspase-7，以及更進一步的 caspase 活化促使細胞死亡。在某些情況下，外在死亡訊息透過 caspase-8 水解 BH3-only protein BID (BH3-interacting domain death agonist) 形成 Truncated BID (tBID)，與內在死亡路徑進行 crosstalk，使外在路徑與內在路徑連結，tBID 會促使粒線體釋放 cytochrome *c*，並且組成 apoptosome (由 ~7 個 apoptotic protease-activating factor-1 (APAF1) 分子以及相同數目的 caspase-9 homodimers 組成) (Figure 1-8) (Taylor *et al.*, 2008)。

在內在路徑中，不同的刺激造成細胞壓力或損傷 (例如：放射線、失去生長因子、DNA 損傷、自由基的產生)，能活化一或多個 BH3-only protein family 的成員，BH3-only proteins 的活化達到閾值，而能阻礙 anti-apoptotic B-cell lymphoma-2 (BCL-2) family members 的抗凋亡作用，並在粒線體外膜促進 BAK–BAX oligomers (BCL-2-antagonist/killer-1；BCL-2-associated X protein) 的組成，這些 oligomers 能允許粒線體膜間隙的蛋白釋出至細胞質，例如 cytochrome *c*、Endo G (endonuclease G)、Smac/DIABLO (second mitochondrial activator of caspases/direct IAP binding protein with low pI)、AIF (apoptosis inducing factor)，一旦從粒線體釋放出來，cytochrome *c* 就會組成 apoptosome，活化的 caspase-9 進一步切割下游的 executioner caspase，促進細胞凋亡 (Figure 1-8) (Taylor *et al.*, 2008)。

8. 肺癌與 EGFR 標靶治療

由行政院衛生署的統計可知，惡性腫瘤自 1982 年起已連續 32 年高居國人死因之首位。在惡性腫瘤中，肺癌是 2013 年不分男女性癌症死因第一位 (Figure 1-9)。肺癌的分類由細胞型態可以區分為非小細胞肺癌 (non-small cell lung cancer；NSCLC)、小細胞肺癌 (small cell lung cancer；SCLC)、類癌腫瘤 (lung carcinoid tumor)，發生率分別為 85 %、10 – 15%、< 5%，NSCLC 又可再分為

squamous cell carcinoma、adenocarcinoma 以及 large cell carcinoma。

在美國，約有 10% adenocarcinoma 病人帶有 EGFR 突變，亞洲則有 35% adenocarcinoma 病人帶有 EGFR 突變，EGFR 屬於 receptor tyrosine kinase (RTKs)，藉由活化下游的訊息傳遞，促進癌細胞的生長、存活、局部侵犯和遠端轉移，突變最常見於 adenocarcinoma、亞洲女性、非吸菸者的族群，主要突變位置是在 exon 19 的 deletion 以及在 exon 21 的 point mutation (L858R) (Nguyen *et al.*, 2009)，超過 90%的 EGFR kinase mutation 屬於上述突變。目前已經研發出很多針對 EGFR 的小分子標靶藥物和單株抗體，能夠阻斷 EGFR 的訊息傳遞，達到治療效果並降低傳統化療的副作用。FDA 許可用於治療 NSCLC 且具有 EGFR 突變的第一線小分子標靶藥物包括：Gefitinib (Iressa) 和 Erlotinib (Tarceva) ，但是卻發現在超過 50% 的 primarily EGFR TKI-sensitive NSCLC 產生二次突變 (second mutation) ，在 EGFR 的 exon 20 產生 single base pair change (T790M) ，使腫瘤對 EGFR 抑制劑產生了抗藥性 (Kobayashi *et al.*, 2005; Pao *et al.*, 2005) ，其他在 exon 19 的 resistance mutation，包括 D761Y 及 L747S 都有文獻報導 (Balak *et al.*, 2006; Costa *et al.*, 2007) (Figure 1-10)。

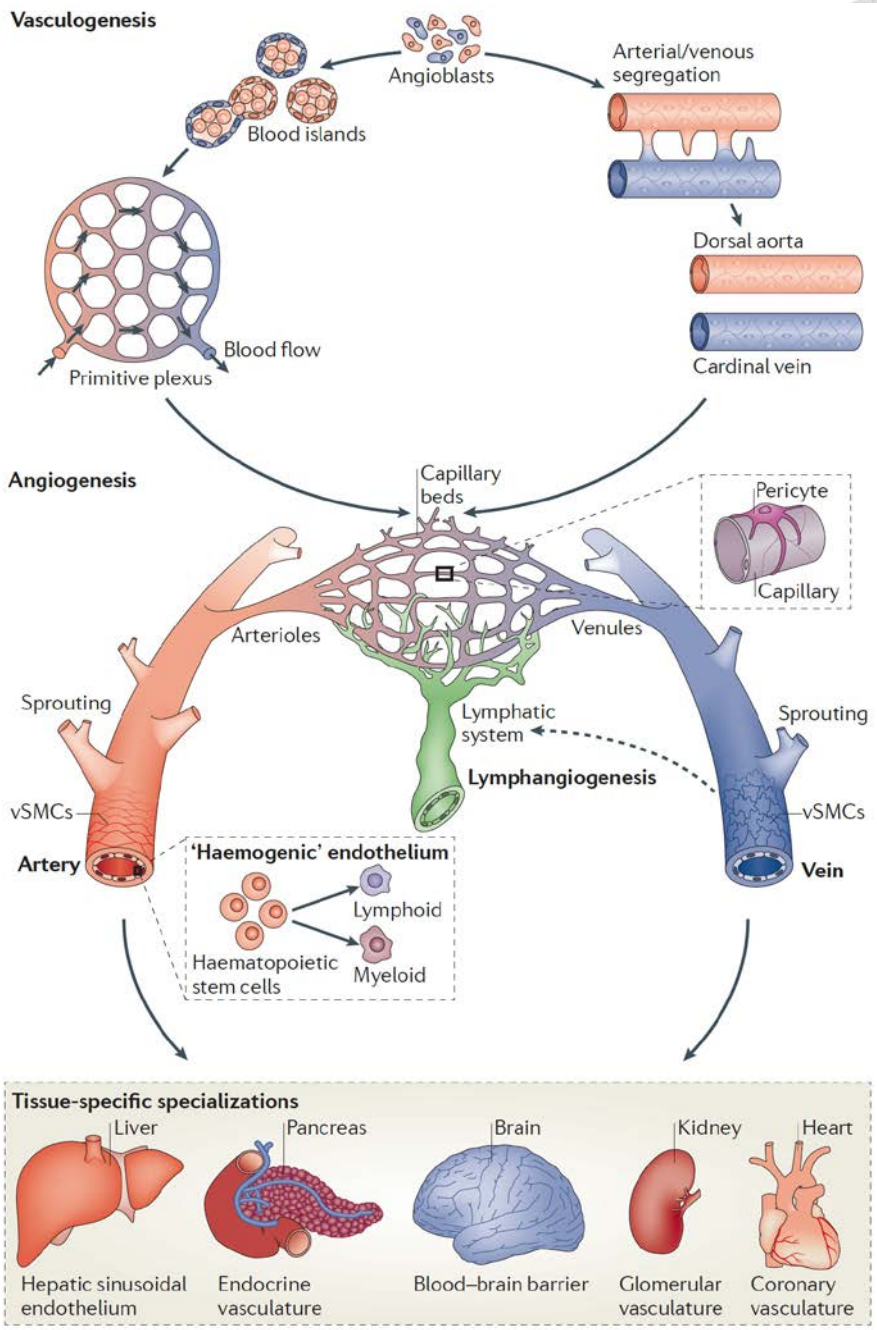

Figure 1-1. Development of a functional vasculature from endothelial progenitor cells. Endothelial progenitors (angioblasts) differentiate from mesodermal cells during early vertebrate development. Once formed, angioblasts may acquire arterial (red) or venous (blue) fates and coalesce to generate the first embryonic blood vessels, the dorsal aorta and cardinal vein. In zebrafish, the coordinated sorting and segregation of arterial and venous angioblasts ensures the assembly of distinct dorsal aorta and cardinal vein vessels. Angioblasts also aggregate to form blood islands, which fuse and remodel in response to haemodynamic stimuli or inherent genetic factors to generate a primitive interlaced network of arterial and venous plexi. Following their vasculogenic

assembly, angiogenic remodelling of the dorsal aorta, cardinal vein and vascular plexi creates a complex hierarchical network of arteries, arterioles, capillary beds, venules and veins. Subsequent recruitment of mural cells (pericytes and vascular smooth-muscle cells (vSMCs)) stabilizes nascent vessels and promotes vessel maturation. In addition, the sprouting of lymphatic endothelial cells from venous vessels (lymphangiogenesis) seeds the lymphatic system (indicated by a dotted arrow). Moreover, the emergence of haematopoietic stem cells from arterial 'haemogenic' endothelium gives rise to all myeloid and lymphoid blood cell lineages. Vessel diversity is further augmented by tissue-specific specializations that alter key properties, such as permeability, or modify endothelial cells to generate vascular networks with new molecular signatures.

Herbert *et al.* (2011) Nat Rev Mol Cell Biol. Aug 23;12(9):551-64.

Table 1-1 Diseases characterized or caused by abnormal or excessive angiogenesis

Organ	Diseases in mice or humans
Numerous organs	Cancer (activation of oncogenes; loss of tumor suppressors); infectious diseases (pathogens express angiogenic genes[112], induce angiogenic programs[113] or transform ECs[114]); autoimmune disorders (activation of mast cells and other leukocytes)
Blood vessels	Vascular malformations (Tie-2 mutation[68]); DiGeorge syndrome (low VEGF and neuropilin-1 expression[33]); HHT (mutations of endoglin or ALK-1 (ref. 69)); cavernous hemangioma (loss of Cx37 and Cx40 (ref. [44])); atherosclerosis; transplant arteriopathy
Adipose tissue	Obesity (angiogenesis induced by fatty diet; weight loss by angiogenesis inhibitors[115])
Skin	Psoriasis, warts, allergic dermatitis, scar keloids, pyogenic granulomas, blistering disease, Kaposi sarcoma in AIDS patients[114]
Eye	Persistent hyperplastic vitreous syndrome (loss of Ang-2 (refs. 65,116) or VEGF164 (ref. 18)); diabetic retinopathy; retinopathy of prematurity; choroidal neovascularization (TIMP-3 mutation[51])
Lung	Primary pulmonary hypertension (germline BMPR-2 mutation; somatic EC mutations[73,75,76]); asthma; nasal polyps
Intestines	Inflammatory bowel and periodontal disease, ascites, peritoneal adhesions
Reproductive system	Endometriosis, uterine bleeding, ovarian cysts, ovarian hyperstimulation[25]
Bone, joints	Arthritis, synovitis, osteomyelitis, osteophyte formation[12]

Carmeliet (2003) Nat Med. Jun;9(6):653-60.

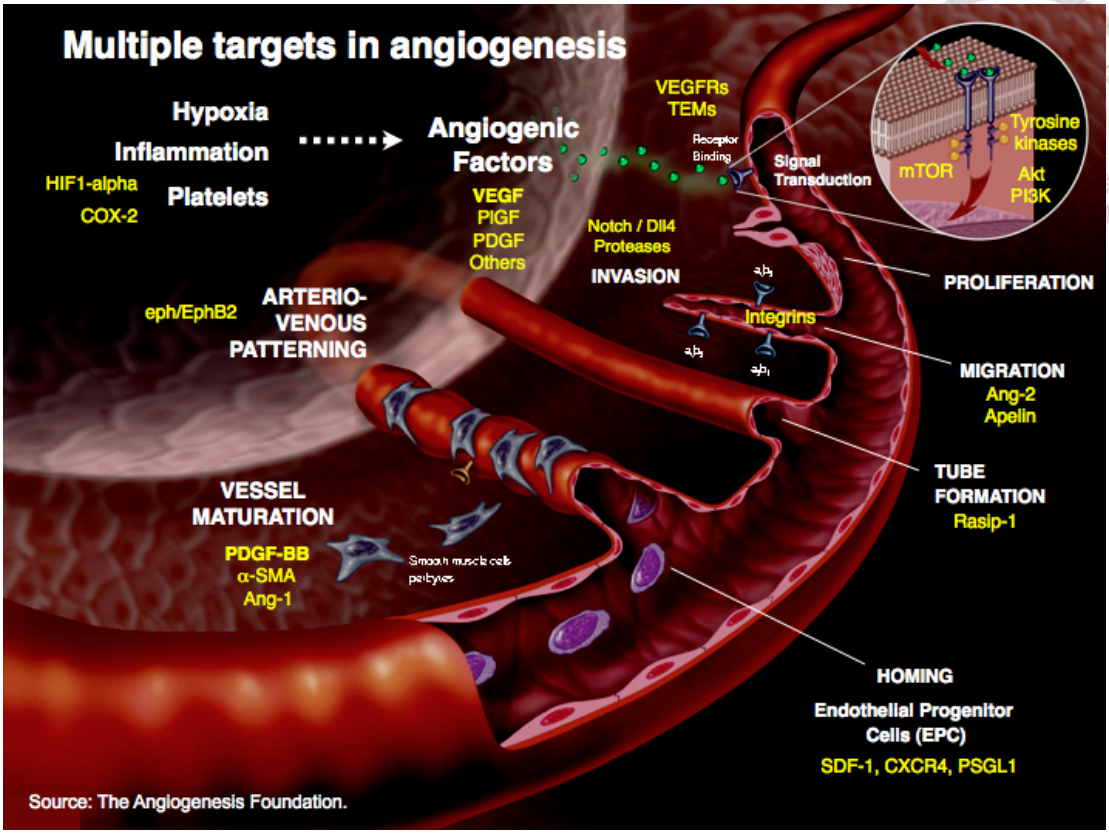

Figure 1-2. The Angiogenesis Process: How Do New Blood Vessels Grow?

The process of angiogenesis in a healthy adult occurs as an orderly series of events:

i. Blood vessels provide nutrients and oxygen throughout the body and are comprised of an inner lining of closely assembled endothelial cells ensheathed by pericytes, (the basement membrane) embedded in the stromal compartment (various stromal cells and extracellular matrix).

ii. In healthy adults, a balance of growth factor signaling maintains endothelial cells in a quiescent, or resting state.

iii. To monitor and supply sufficient amounts of oxygen to surrounding tissues, blood vessels have oxygen and hypoxia-induced sensors, or receptors, which allow vessel remodeling to adjust the blood flow accordingly.

iv. Hypoxia or other endogenous signals activate cells and induce the release signaling factors (such as VEGF, Ang-2, FGF and chemokines) to promote the growth of new blood capillaries from pre-existing vessels – a process called angiogenesis.

v. Pericytes detach from the vessel (Ang-2 signaling), and endothelial cells are activated and lose their close contact as the vessel dilates (VE-cadherin signaling).

vi. In sprout formation, a tip cell is selected (selection influenced by Neuropilin, VEGF/VEGFR and NOTCH / DLL4 and JAGGED1 signaling) which releases

matrix metalloproteases (MT1-MMP) to degrade the basement membrane and remodel the extracellular matrix.

vii. Tip cells are polarized and extend numerous filopodia to guide sprout migration (via semaphorins, ephrins, and integrins guidance signals) toward angiogenic stimuli (VEGF gradient). Tip cells are primarily migratory and do not proliferate.

viii. Stalk cells follow the tip cell and proliferate, extending the sprout. Proliferating stalk cells establish junctions with neighboring endothelial cells and release molecules such as EGFL7 (an endothelial cell chemoattractant expressed by proliferating endothelial cells) that bind to extracellular membrane components and regulates vascular lumen formation.

ix. Fusion of neighboring branches occurs when 2 tip cells encounter each other, establish EC-EC junctions (VE-cadherin, Ang-1) and form a continuous lumen. Extracellular matrix is deposited to establish a new basement membrane (TIMPs), endothelial cell proliferation ceases, and pericytes are recruited to stabilize the new vessel (PDGFR/PDGF-B, Ang-1).

x. Once blood flow is established, the perfusion of oxygen and nutrient reduces angiogenic stimuli (VEGF expression) and inactivates endothelial cell oxygen sensors, re-establishing the quiescent state of the blood vessel.

Source：The Angiogenesis Foundation.

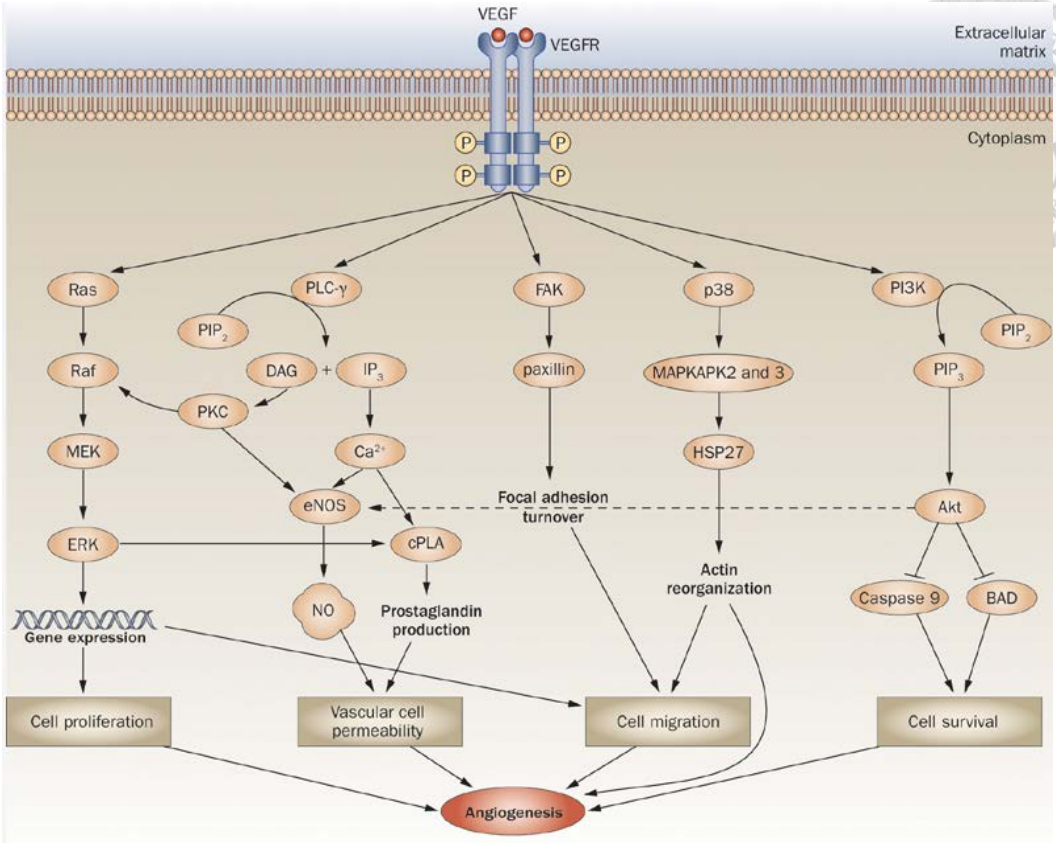

Figure 1-3. Activation of VEGFR mediates proliferation, vascular permeability, cell migration and cell survival, leading to angiogenesis. VEGFR signaling via the Ras/MEK/ERK pathway induces gene expression and results in cell proliferation. VEGFR can also signal through PLC-γ, which activates PKC by the generation of diacylglycerol and increases the concentration of intracellular calcium via inositol triphosphate. Increased intracellular calcium results in induction of vascular permeability via activation of endothelial nitric oxide synthase and generation of nitric oxide, but also via activation of cytosolic phospholipase A and prostaglandin production. Signaling through the focal adhesion kinase pathway leads to focal adhesion turnover and cell migration. VEGFR signaling through p38 results in heat shock protein 27 induction, which leads to actin reorganization and cell migration. Activation of the PI3K pathway maintains cell survival. PI3K catalyzes the conversion of PIP_2 to PIP_3. In turn PIP_3 recruits Akt to the cell membrane where Akt is activated via phosphorylation. Akt can activate endothelial nitric oxide synthase, which leads to vascular cell permeability, but the kinase also inhibits the proapoptotic proteins caspase 9 and BAD, which enhances cell survival. Small-molecule VEGFR inhibitors, such as the VEGFR2 inhibitors, block these pathways and thus inhibit angiogenesis.

Ivy *et al.* (2009) Nat Rev Clin Oncol. Oct;6(10):569-79.

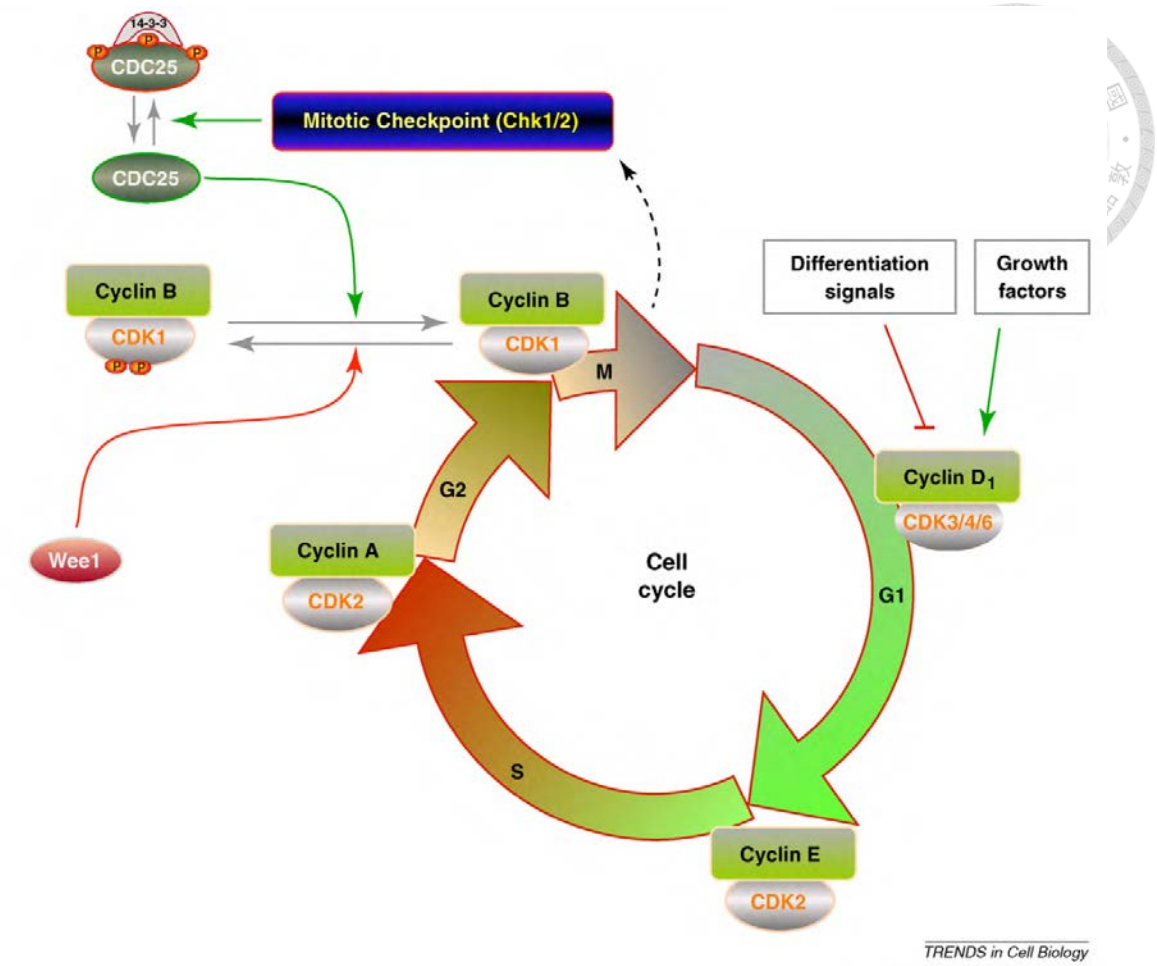

Figure 1-4. Overview of core cell cycle regulation. Different CDK/cyclin heterodimer complexes control entry into, and progression through, the four phases of the cell cycle. Decisions to proliferate (growth factors) or exit the cell cycle (differentiation signals) are made during G1. The initiation of mitosis (M) is highly regulated and requires activation of CDK1. Wee1 mediated phosphorylation keeps CDK1 inactive and removal of these inhibitory phosphates by cell division cycle 25 (CDC25) allows mitosis to proceed. To prevent premature onset of mitosis, CDC25 activity is inhibited by checkpoint kinases (Chk) mediated phosphorylation and 14-3-3 mediated cytoplasmic retention.

Davidson *et al.* (2010) Trends Cell Biol. Aug;20(8):453-60.

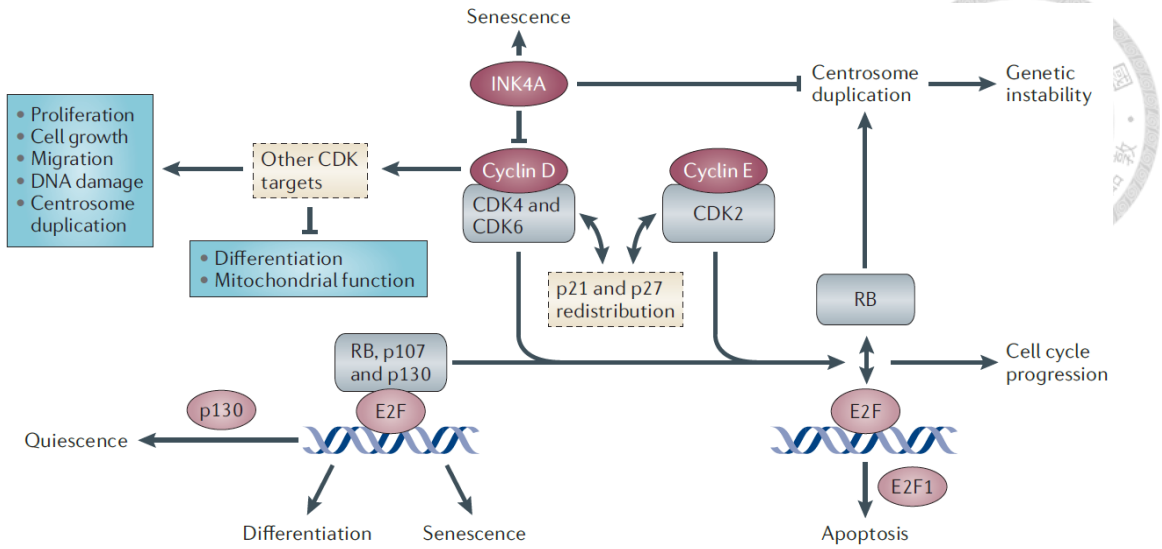

Figure 1-5. CDK-dependent functions of cyclin D. The activation of cyclin D–cyclin-dependent kinase 4 (CDK4) or CDK6 initiates the phosphorylation of the tumour suppressor protein RB and other RB family members (such as p107 and p130), resulting in the release of E2F transcription factors. In turn, this leads to the transcriptional activation of E2F-responsive genes that are essential for DNA synthesis, including cyclin E and cyclin A, which further promote RB phosphorylation by activating CDK2. Cyclin D–CDK4/CDK6 complexes also indirectly activate cyclin E–CDK2 by sequestering the CDK inhibitors p21 and p27. Both INK4A and RB also affect cellular processes other than cell cycle progression, such as centrosome replication, so that their loss can lead to centrosome amplification and genomic instability. Similarly, cyclin D–CDK4/CDK6 phosphorylates substrates in addition to RB, thereby regulating a diverse set of end points (shown in the blue boxes).

Musgrove *et al.* (2011) Nat Rev Cancer. Jul 7;11(8):558-72.

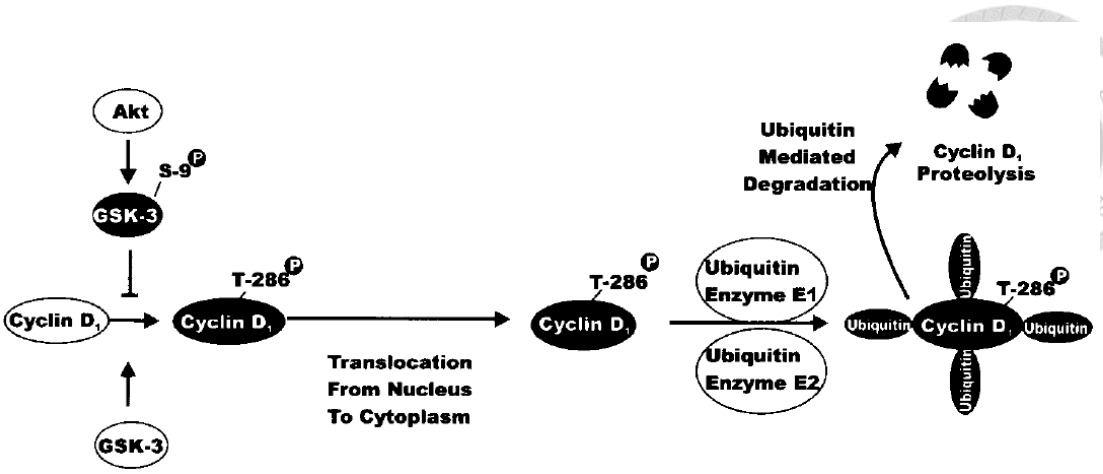

Figure 1-6. Regulation of cyclin D1 protein stability by the PI3K/Akt pathway. Cyclin D1 is phosphorylated by GSK-3, which can be prevented by phosphorylation of GSK-3 by Akt. Phosphorylated cyclin D is translocated from the nucleus to the cytoplasm and targeted for degradation by ubiquitination.

Chang *et al.* (2003) Leukemia. Mar;17(3):590-603.

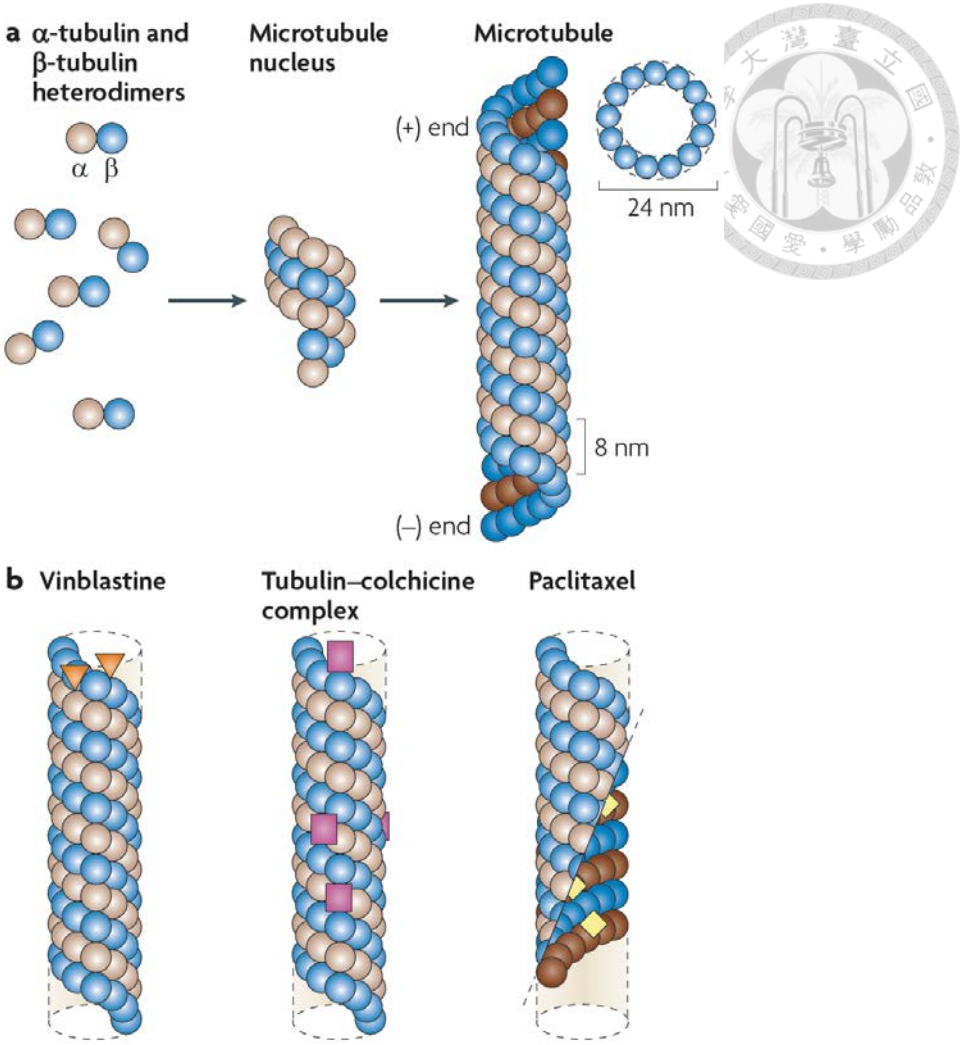

Figure 1-7. Microtubule formation and the binding sites of microtubule inhibitors. a, Soluble tubulin dimers, containing one α-tubulin peptide and one β-tubulin peptide, polymerize to form a microtubule nucleus. Additional dimers are added head-to-tail and the resulting microtubules are highly dynamic structures containing a (+) end, characterized by an exposed β-tubulin peptide and a (–) end, characterized by an exposed α-tubulin peptide. **b,** Binding sites of microtubule inhibitors are shown (orange triangles, purple squares and yellow diamonds). Although vinca alkaloids, such as vinblastine, bind to microtubule ends, colchicine binds to soluble dimers, which can be incorporated in the microtubules. Taxanes, such as paclitaxel, bind along the interior surface of the microtubules.

Dumontet *et al.* (2010) Nat Rev Drug Discov. Oct;9(10):790-803

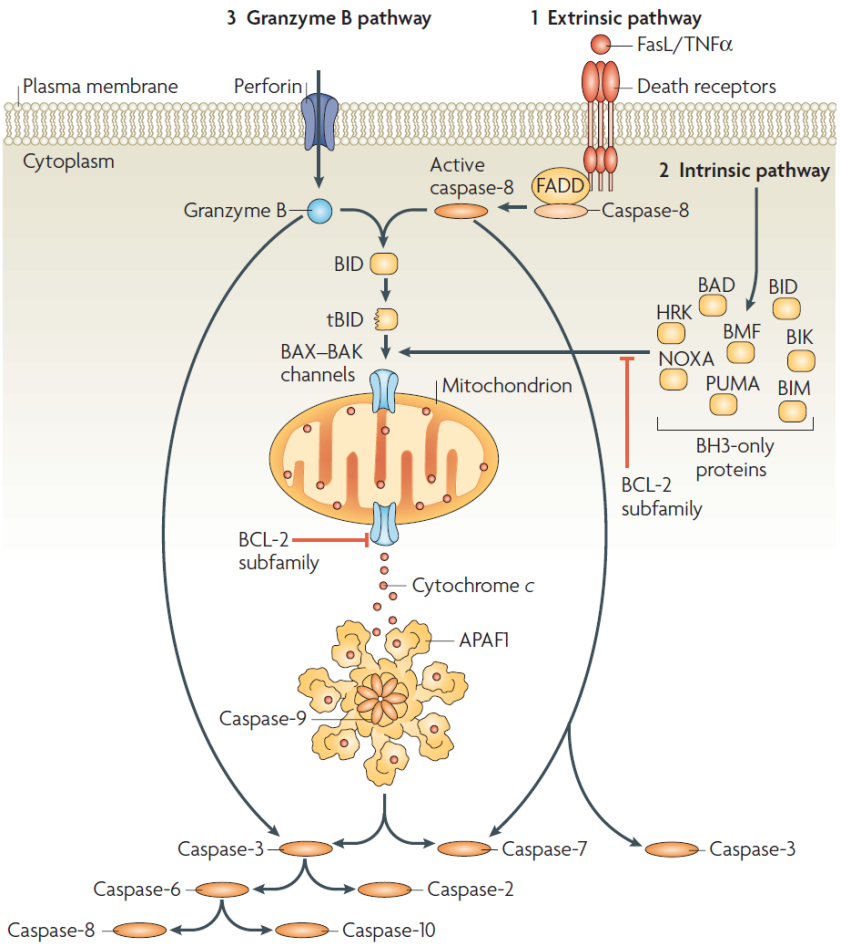

Figure 1-8. Caspase activation pathways. Caspase activation by the extrinsic pathway (route 1) involves the binding of extracellular death ligands (such as FasL or tumour necrosis factor-α (TNFα)) to transmembrane death receptors. Engagement of death receptors with their cognate ligands provokes the recruitment of adaptor proteins, such as the Fas-associated death domain protein (FADD), which in turn recruit and aggregate several molecules of caspase-8, thereby promoting its autoprocessing and activation. Active caspase-8 then proteolytically processes and activates caspase-3 and -7, provoking further caspase activation events that culminate in substrate proteolysis and cell death. In some situations, extrinsic death signals can crosstalk with the intrinsic pathway through caspase-8-mediated proteolysis of the BH3-only protein BID (BH3-interacting domain death agonist). Truncated BID (tBID) can promote mitochondrial cytochrome *c* release and assembly of the apoptosome (comprising ~7 molecules of apoptotic protease-activating factor-1 (APAF1) and the same number of caspase-9 homodimers). In the intrinsic pathway (route 2), diverse stimuli that provoke cell stress or damage typically activate one or more members of the BH3-only protein family. BH3-only proteins act as pathway-specific sensors for various stimuli and are regulated in distinct ways (BOX 1). BH3-only protein

activation above a crucial threshold overcomes the inhibitory effect of the anti-apoptotic B-cell lymphoma-2 (BCL-2) family members and promotes the assembly of BAK–BAX oligomers within mitochondrial outer membranes. These oligomers permit the efflux of intermembrane space proteins, such as cytochrome *c*, into the cytosol. On release from mitochondria, cytochrome *c* can seed apoptosome assembly. Active caspase-9 then propagates a proteolytic cascade of further caspase activation events. The granzyme B-dependent route to caspase activation (route 3) involves the delivery of this protease into the target cell through specialized granules that are released from cytotoxic T lymphocytes (CTL) or natural killer (NK) cells. CTL and NK granules contain numerous granzymes as well as a pore-forming protein, perforin, which oligomerizes in the membranes of target cells to permit entry of the granzymes. Granzyme B, similar to the caspases, also cleaves its substrates after Asp residues and can process BID as well as caspase-3 and -7 to initiate apoptosis. BAD, BCL-2 antagonist of cell death; BAK, BCL-2-antagonist/killer-1; BAX, BCL-2-associated X protein; BID, BH3-interacting domain death agonist; BIK, BCL-2-interacting killer; BIM, BCL-2-like-11; BMF, BCL-2 modifying factor; HRK, harakiri (also known as death protein-5); PUMA, BCL-2 binding component-3.

Taylor *et al.* (2008) Nat Rev Mol Cell Biol. Mar;9(3):231-41.

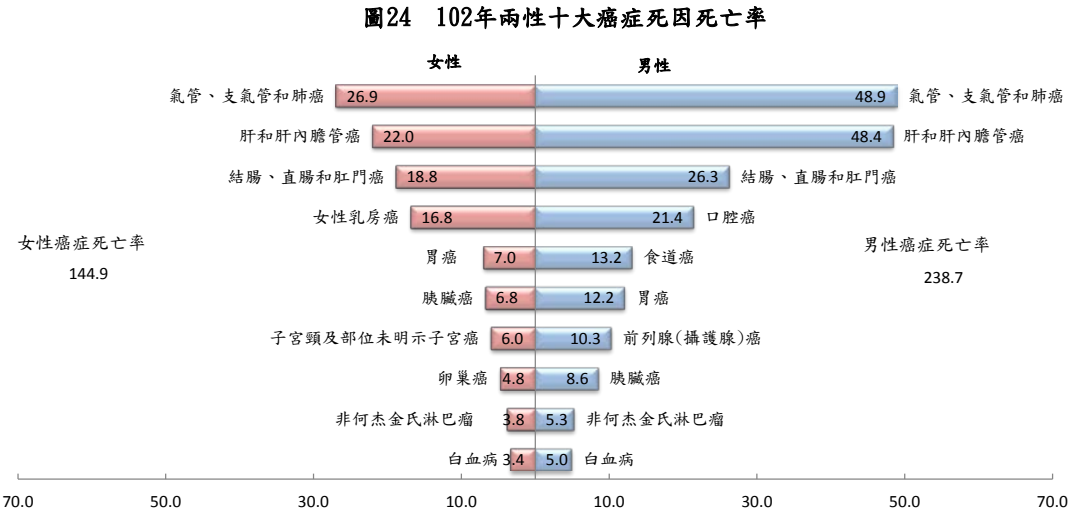

Figure 1-9. 兩性癌症死亡人數占率

來源：行政院衛生署

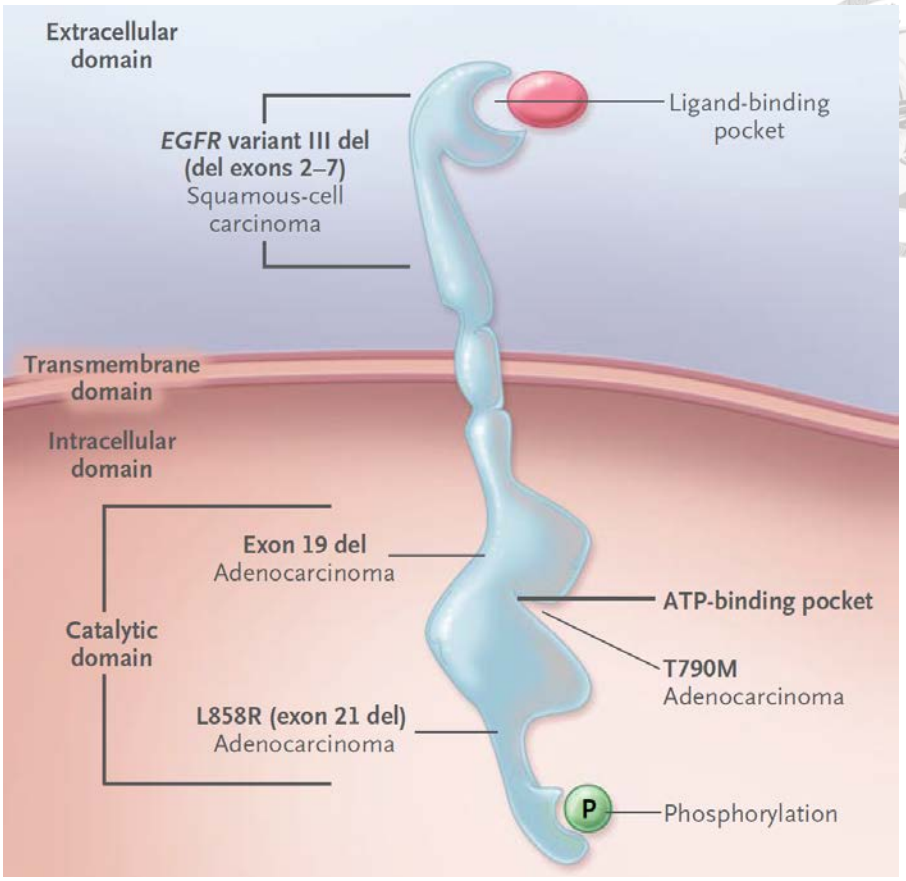

Figure 1-10. Effect of Deletions and Mutations in the Epidermal Growth Factor Receptor Gene (*EGFR*) on Disease Development and Drug Targeting. Ligand binding to the EGFR extracellular domain results in receptor homodimerization and tyrosine phosphorylation, with the phosphate derived from ATP bound within the kinase catalytic domain. *EGFR* mutations have transforming potential in preclinical lung models and can occur early in human lung carcinogenesis. *EGFR* point mutations (e.g., L858R) and exon 19 deletions, which occur predominantly in adenocarcinoma of the lung, are located within the catalytic domain and result in constitutive EGFR activation. These mutations are associated with increased sensitivity to EGFR tyrosine kinase inhibitors, such as erlotinib and gefitinib. In contrast, mutations in T790M (an amino acid located within the ATP binding site of the *EGFR* kinase domain) are associated with acquired resistance to these drugs. *EGFR* variant III mutant deletions occur in the extracellular domain and are associated with squamous-cell cancer.

Herbst *et al.* (2008) N Engl J Med. Sep 25;359(13):1367-80.

第二章 實驗材料與方法

第一節 實驗材料

Dehydrocostuslactone (DHC) 購自於 Wako Pure Chemical Industries, Ltd. (Osaka, Japan)。MPT0G013 及 MPT0B271 由台北醫學大學藥學所劉景平老師合成並提供。3-(4,5-dimethylthiazol-2-yl)-2,5-diphenyltetrazolium bromide (MTT)、Sulforhodamine B (SRB)、FITC-conjugated anti-mouse IgG、Propidium iodide (PI) 與 Drabkin's reagent kit 購自 Sigma-Aldrich Chemical Co. (St Louis, MO, USA)。4',6-diamidino-2-phenylindole (DAPI) 購自 Roche Molecular Biochemicals (Mannheim, Germany)。Medium 199、RPMI-1640、fetal bovine serum (FBS)、penicillin、streptomycin 購自 Gibco BRL Life Technologies (Grand Island, NY)。Endothelial cell growth supplements (ECGs) 購自 Upstate Biotechnology Inc. (Lake Placid, NY, USA)。Endothelial cell basal medium (EBM) and endothelial growth factors (EGM-2) 購自 Clonetics (BioWhittaker, Walkersville, MD)。Matrgel^{TM} basement membrane matrix 購自 BD Biosciences (San Jose, CA, USA)。BrdU labeling and detection enzyme-linked immunosorbent assay (ELISA) kit 購自 Amersham Biosciences (Piscataway, NJ, USA)。TRIzol 試劑、TIMP3 siRNA 與 p53 siRNA 購自 Invitrogen (Carlsbad, CA)。random primer 以及 M-MLV RT 購自 Promega (Madison, WI)。

一級抗體：Cyclin D 購自 Calbiochem (San Diego, CA)。CDK2、CDK4、cyclin A、p27、cyclin B1、cdc25C、cdc2、Bcl-2、Bcl-xL、Bax、Mcl-1、Bak 以及 PARP 購自 Santa Cruz Biotechnology (Santa Cruz, CA)。Phospho-p44/42 MAP kinase (Thr202/Tyr204)、p44/42 MAP kinase (Thr202/Tyr204)、p38 MAP kinase、phospho-mTOR (Ser2448)、phospho-p70S6K (Thr421/Ser424)、phospho-eIF4E

(Ser209)、phospho-4EBP1 (Thr37/46)、phospho-GSK-3β (Ser9)、Akt、TIMP3、p21、caspase-8、caspase-9、cdc2 (Thr161)、cdc2 (Tyr15)、Aurora A、Aurora B、PLK1、p53、Bid 購自 Cell Signaling Technology (Beverly, MA)。phospho-Akt (Ser473) 與 phospho-STAT3 (Tyr705) 購自 Epitomics (Burlingame, CA, USA)。STAT3、p53 以及 caspase-7 購自 BD Biosciences (San Jose, CA)。MPM2 (Ser161/Thr97) 購自 Upstate Biotechnology Inc. (Temecula, CA)。β-actin 購自 Millipore (Temecula, CA, USA)。Caspase-3 購自 Imgenex (San Diego, CA, USA)。二級抗體：HRP-conjugated anti-mouse 和 anti-rabbit IgGs 購自 Santa Cruz Biotechnology (Santa Cruz, CA, USA)。

第二節 實驗方法

細胞培養

本研究中選用的是人類臍靜脈內皮細胞 (Human umbilical vein endothelial cells; HUVECs)，購自 BCRC 生物資源保存及研究中心。將細胞培養在 75 cm^2 的培養瓶中，加入含有 20 % FBS 、ECGs 與抗生素（100 U/ml penicillin 及 100 mg/ml streptomycin）的 M199 培養液，存放於 37 °C、5 % CO_2/95 % air 的培養箱中。細胞密度生長至九分滿時，利用 0.05 % trypsin/0.02 % EDTA 將細胞切下，以 1：3 至 1：4 的比例稀釋進而繼代培養，或計算細胞數目後再均分於培養盤中進行後續的實驗。本研究第五章所使用的細胞株包括：人類非小型細胞肺癌細胞株 A549、H1975、H460、NCI-H1299、NCI-H226、PC-9；人類胰臟癌細胞株 AsPC-1；人類大腸直腸癌細胞株 HCT-116；人類肝癌細胞株 Hep3B；人類乳癌細胞株 MDA-MB-231；人類前列腺癌細胞株 PC-3；人類卵巢癌細胞株 SKOV3 以及人類前骨髓細胞白血病細胞株 HL60。上述細胞株皆購自 American Type Culture Collection (ATCC) (Manassas, VA)。NCI/ADR-RES 細胞株來自於 DTP Human Tumor Cell Line Screen (Developmental Therapeutics Program, NCI)。將細胞株培養於含有 10% FBS、penicillin (100 U/ml)/streptomycin (100 μg/ml)/amphotericin (0.25 μg/ml) 的 RPMI-1640 培養液或 DMEM 培養液中，存放於 37 °C、5 % CO_2/95 % air 的培養箱中。

細胞轉染

細胞轉染是利用 Lipofetamine 2000 進行，操作方式依照原廠說明書的建議執行。根據實驗設計將細胞種於 dish 或 plate 中， cDNA 與 Lipofetamine 2000 的混合比例根據實驗稍做調整，過程以 OPTI – MEM (Invitrogen) 為溶解試劑，

將混合液 vortex 後置於室溫 40 分鐘，而後加入細胞進行轉殖反應。於培養箱靜置 6 小時後，將轉殖試劑移除，並加入原來細胞培養液中止反應。轉殖後的細胞於培養箱靜置過夜，即可依實驗需求進行後續動作。Myr-Akt plasmids 由台北醫學大學的林建煌老師提供。

結晶紫染劑細胞增生實驗

將細胞種在 96-well 的細胞培養盤中，放入細胞培養箱，待細胞完全貼附後，吸掉上清液，加入混合 DMSO 或待測藥物的培養液，持續培養。待細胞處理刺激劑或藥物 72 小時後，移除培養液，加入 50 µl 結晶紫染劑，室溫下靜置 10 分鐘，將細胞固定染色，接著利用清水移除多餘結晶紫染劑，待風乾後，加入 100 µl 0.1 M sodium citrate solution 溶解結晶紫，以分光光度計 (spectrophotometer) OD_{550} 讀取容易之吸光值。

DNA 合成的測定

5-溴 2-脫氧尿嘧啶核苷 (5-bromo 2-deoxyuridine, BrdU) 為胸腺嘧啶 (thymidine) 類似物，當 DNA 合成時，BrdU 可當作是原料被接合到 DNA 中，再利用特異性抗體 (anti-BrdU Ab) 辨識，以評估細胞增生的情形。將 HUVECs 以 5 x 10^3 cells/well 的細胞密度種在 96-well 的細胞培養盤中，放入細胞培養箱。待細胞完全貼附，移除上清液，換上 EBM-2 培養液處理 24 小時。之後，對照組單獨給予 EGM-2 培養液，實驗組則同時加入待測藥物刺激 48 小時，收集細胞前 18 小時加入 BrdU (10 µM)，最後利用 BrdU labeling and detection kit 來測定 DNA 合成量，以評估細胞增生的密度。

細胞毒性定量（MTT）的測定

細胞毒性定量的測定是參照 Monsmann（1983）發表的 MTT 偵測法；利用

MTT 在活細胞中會被粒腺體的酵素 dehydrogenase 作用，而產生紫色的 formazan 產物的特性來測定細胞存活率。細胞在培養瓶中長滿後，以 0.05 % trypsin/0.02 % EDTA 收集細胞並離心，將收集的細胞以密度 10^4 cells/well 將細胞種在 96-well 的細胞培養盤中。加入待測試藥物處理 24 小時後，改換為 100 ml 含有 10 % MTT solution（0.5 mg/ml）的 culture medium，於 37 °C 的細胞培養恆溫箱中作用 1 小時。吸掉上清液後以 DMSO 將細胞打破，於室溫下作用 10 分鐘，使用 enzyme-linked immunosorbent assay (ELISA reader) 讀取波長 550 nm 吸光值的變化。

細胞存活率 (SRB) 的測定

細胞存活率的測定是參照 Skehan (1989) 發表的 SRB 偵測法。細胞在培養瓶中長滿後，以 0.05 % trypsin/0.02 % EDTA 收集細胞並離心，將收集的細胞懸浮在 RPMI (5 % FBS) 中，以密度 5,000 cells/well 將細胞種在 96-well 的細胞培養盤中。隔天將第一排細胞以 10 %的 TCA 固定，視為 Tz，其餘的加入待測試藥物處理 48 小時，再以 10 %的 TCA 固定，以自來水清洗後陰乾，加入溶於醋酸的 4 mg/ml sulforhodamine B (SRB)，之後以 10 % 醋酸清洗後陰乾，再加入 Trizma base 溶解結晶，以 ELISA reader 讀取波長 515 nm 吸光值的變化。其吸光值的數據是根據 Tz 及對照組求出細胞生長的比例，藉此評估藥效。

細胞凋亡的評估

本實驗是 Cell Death Detection ELISA^{PLUS} kit (Roche) 來評估細胞凋亡。細胞以藥物處理後，利用 lysis buffer 將細胞打破，以 200×g 離心十分鐘，取 20 ml 上清液加入 streptavidin-coated microplate，再加入 anti-histone-biotin 及 anti-DNA-POD 的第一級抗體，置於室溫兩小時，wash 之後加入呈色劑，在波長 405 nm 讀取吸光值。

細胞移行試驗 (Boyden chamber migration assay)

先將 8-μm 孔徑大小的之濾膜使用 0.5 % gelatin coating 24 小時，第二天在 chamber 下層加入 100 μL EGM-2，將 Boyden chamber 組合好，並將 HUVECs 培養在 EBM-2 或外加待測藥物之 EBM-2 培養液中並置入 chamber 上層，經過持續處理 6 小時後，移除所有培養液，將濾膜取出後置入 4 % 甲醛液中固定 20 分鐘，並以棉花棒移除濾膜上層的細胞，再將 membrane 置入結晶紫染劑中染色 10 min，接著利用 PBS 清除多餘結晶紫染劑。待風乾濾膜，在顯微鏡下拍照，並以 0.1 M sodium citrate solution 溶解結晶紫，以分光光度計 (spectrophotometer) OD_{550} 讀取容易之吸光值以量化細胞遷移程度。

類血管管柱形成試驗 (Tube formation assay)

Matrigel 的特性為 -20 °C 為固體狀、0 ~ 4 °C 為液體狀、> 4 °C 為膠體狀，因此實驗前一天必須將 Matrigel 冷藏到 4 °C 冰箱中，以利實驗進行。實驗當天將 Matrigel 加至 96-well 之細胞培養盤 (50 μl/well)，過程中需避免氣泡以及注意要均勻平鋪於 well 中，之後放入 37°C 的細胞培養箱中 30 分鐘至 1 小時待凝膠。將 HUVECs 混合於 EGM-2 或外加待測藥物之 EGM-2 培養液中，隨後將細胞 (5×10^4 cells/well) 加至已經 coated Matrigel 之 96 孔盤中，置於 37°C 的細胞培養箱中培養 6-18 小時後，在顯微鏡下觀察管柱生成的情況，並以 Image-pro plus 軟體量測五個不同視野下管柱的長度總和來量化管柱形成的程度。

HDAC Biochemical Assay

藥物對於不同種類 HDAC 的抑制活性是由 HDAC Biochemical Assay kit (BPS Biosciences, San Diego, CA, USA)進行。利用 HDAC1、HDAC2、HDAC4、HDAC6、HDAC8 的重組蛋白，測試其移除受質上的乙醯基所產生的

7-amino-4-methylcoumarin。首先將待測試的藥物、HDAC、HDAC substrate 以及 BSA 加入 96 孔黑盤，於 37 °C 反應 30 分鐘。之後加入 2X HDAC assay developer，於室溫反應 15 分鐘。最後於 ELISA reader 中測定螢光讀值 (Ex/Em = 350 - 380/440 - 460 nm)。

Total HDACs Enzymatic Activity Assay

細胞處理過藥物之後，收集 total cell lysate，經過蛋白質定量之後，利用 Fluorometric HDAC Activity Assay kit (BioVision, Mountain View, CA, USA)測定細胞中 HDAC 活性。先將待測試的藥物、10X HDAC Assay Buffer、 Protein Extract 以及 HDAC Fluorometric Substrate 加入 96 孔的黑盤中，於 37°C 反應 30 分鐘。之後加入 Lysine developer 終止反應，並於 37 °C 反應 30 分鐘。最後於 ELISA reader 中測定螢光讀值 (Ex/Em = 350 - 380/440 - 460 nm)。

體外微管聚合實驗

微管聚合實驗是以 CytoDYNAMIX Screen kit (BK006P, Cytoskeleton Inc., Denver, CO, USA) ，依照公司的 protocol 來進行。首先將 300 μg tubulin (純度> 99%) 懸浮於 100 μl 的 G-PEM buffer (80 mM PIPES, 2 mM $MgCl_2$, 0.5 mM EGTA, 1 mM GTP, pH 6.9 plus 15% glycerol)，在藥物存在之下保存在 4°C。其後將樣品轉置於 96 孔盤中，在 37°C 中觀察 340 nm 的吸光值 (SpectraMAX Plus, Molecular Devices Inc., Sunnyvale, CA, USA)，每分鐘一次，觀察 30 分鐘。

免疫螢光染色與共軛焦顯微鏡

A549 細胞培養在 chamber slight 中，藥物處理 24 小時後，以冷凍於-20 °C 的甲醇固定 15 分鐘，以 PBS wash 三次後加入 0.1 % Triton-X-100 在 37°C 處理三十分鐘，再加入 monoclonal anti-β-tubulin 在 37°C 處理一小時。以

FITC-conjugated-a-microtubule 與 DAPI 加以染色，PBST wash 後，以 Crystal mount 封片，在 Leica TCS SP2 Confocal Spectral Microscope (Leica, Wetzlar, Germany) 觀察。

流式細胞儀測定細胞週期 (Flow cytometric analysis)

細胞藥物處理後，將收集的細胞以冰的 70 % v/v ethanol 再懸浮後放置於-20 °C，至少 30 分鐘以上。細胞在室溫下加入 0.1 ml DNA 萃取液 (0.2 M Na_2HPO_4- 0.1 M citric acid buffer, pH 7.8) 30 分鐘後離心，再加入 1 ml DNA 染色液－propidium iodide staining buffer (0.1 % Triton X-100、100 μg/ml RNase A、80 μg/ml propidium iodide (PI) in PBS)，避光下染色 30 分鐘。將細胞過濾後跑流氏細胞儀，以 FACScan 和 CellQuest program (Becton Dickinson) 分析細胞週期。

西方點墨法 (Western blot)

取一定量的蛋白質樣品加入 1/4 體積的 5X sample buffer，於滾水中煮沸 5 分鐘。將此蛋白質混合液注入電泳膠片內，以 12 % sodium dodecyl sulfate-polyacrylamide gel (SDS-PAGE) 作垂直電泳。蛋白質樣品用 SDS-PAGE 法分離後，取下電泳膠片，將其緊密貼合於 polyvinylidene difluoride (PVDF) membrane 上，並依序疊上 3M papers 及海綿，然後裝置於轉印槽中。注意膠片、PVDF membrane、3M papers 及海綿均須用 transfer buffer 充分潤濕。在轉印槽內注滿 transfer buffer，以 350 mA 的固定電流進行蛋白質轉印，過程中須冰溶，2 小時後將 PVDF membrane 取出，進行免疫顯色。首先將 PVDF membrane 浸泡在含 3 % BSA in TBST buffer (20 mM Tris pH7.4，150 mM sodium orthovanadate 和 0.05 % Tween-20) 中至少 1 小時, 以阻斷非特異性結合。接著，用 TBST 溶液清洗並搖晃 30 分鐘，再注入以 3 % BSA 溶液適當稀釋的第一抗體，輕搖至隔天，同樣以 TBST 溶液洗去殘餘的第一抗體，再加入合適的第二抗體 (anti-mouse

immunoglobulin (IgG) -HRP) 作用 1 小時後，再以 TBST 溶液浸洗 30 分鐘，加入 ECL™ 溶液以 X 光片偵測特定蛋白質。

RNA extraction

細胞以藥物處理後，將上清液吸掉，以 TRIZOL 將細胞刮下，加入 0.2 ml chloroform 混合均勻後靜置冰上十分鐘，以 4 °C 離心 12,000 rpm 十五分鐘，取出上清液與 0.5 ml isopropenol 混合均勻後靜置冰上十五分鐘，以 4 °C 離心 12,000 rpm 十五分鐘，去除上清液，pellet 為 RNA 與鹽類，以 75 % 酒精洗掉鹽類，待酒精揮發後以 DEPC-H_2O 溶解，並加以定量。

Quantitative reverse transcription-polymerase chain reaction (QRT-PCR)

取 1 μg total RNA 加入 0.5 μg oligo (dT) primer 在 70 °C 下加熱 10 分鐘，以破壞 RNA 的二級結構，並將 oligo (dT) primer 結合至 mRNA 上。再加入 RT buffer (500 mM、KCl 25 mM $MgCl_2$ 和 200 mM Tris-HCl pH 8.4) 、10 mM deoxynucleoside triphosphates (dNTPs) 和 0.1M DTT，在 42 °C 下加熱 5 分鐘，接著加入 SuperScript II RT (200 units) 經 42 °C 50 分鐘後再加熱 70 °C 15 分鐘，然後再加入 RNase H 於 37 °C 20 分鐘後，即合成 cDNA。取 2 μl first strand complementary DNA (cDNA) 加入 10X CYBR green PCR master mix (Applied Biosystems) 及待測之 5'、3'-primer 1.5 mM 各 4μl 至最後體積為 20 μl，mastermix (TaqMan One Step RT-PCR; ABI) 進行 quantitative PCR。TIMP3 的 primer 序列為：5'-TGCTCTCTGTCTCTTTTTTCAGCTT-3' (forward) 以及 5'-CTACAGTGTGTTGTCTGCTGCTTTT-3' (reverse)。GAPDH 為內生性控制組。

干擾性核醣核酸轉染 (Small interfering RNA (siRNA) transfection)

所使用的 stealth RNA duplexes 是由 Invitrogen 所合成。在轉染過程中，控

制細胞種在 6-cm dishes 時大約 80 % 的滿度，隔天將 siRNA duplexes (200 nM) 利用 lipofectamine® *RNAiMAX* 送入細胞，經過約 16 到 18 小時，就可以加入待測藥物，然後檢驗細胞生長率或存活率，以及西方墨點法測定 silence 蛋白的表現量。

新生 RNA 標的與分離

利用 Click-iT Nascent RNA Capture kit (Invitrogen, Carlsbad, CA, USA) 來分離新合成的 RNA 並按照製造商 protocol 進行。將細胞同時給予 MPT0G013 (1 μM) 和 0.2 mM 5-ethymyluridine (EU, 是一種 alkyne-modified uridine analog，能夠有效率並自然的嵌入新合成的 RNA 中)，六小時後，以 TRIZOL 將 total RNA 分離，接著以 5 μg of EU-labeled RNA 加入 0.5 mM biotin azide 進行 click reaction，混合物在室溫下反應 30 分鐘，經過 RNA 沉降後，將 RNA 溶於 RNase-free water，加入 12 μl of Dynabeads® MyOne™ Streptavidin 進行 Biotin-labeled EU-RNA-binding pull-down assay，接著以緩衝液清洗與 beads 結合的 RNA。使用 Superscript VILO cDNA synthesis kit (Invitrogen)，立即將與 beads 結合的 RNA 進行 cDNA synthesis，最後以 QRT-PCR 分析結果。

血管新生動物實驗

以皮下注射方式打入混合 heparin (10 U/ml)，EGM-2，DMSO 或藥物的 0.5 ml Matrigel™ basement membrane matrix 至 BALB/c-nude 老鼠下腹部，在植入 Matrigel 七天後，將老鼠麻醉、犧牲，將 Matrigel plug 取下，並隨即拍攝，接著，將一部分 plug 進行組織切片染色 (H&E staining)，另一部分 plug 放入 100 μl PBS，利用超音波震盪器將 plug 均質化後，再以 4,000 rpm，4°C 離心 10 分鐘，取得上清液，利用 Drabkin's reagent kit (Sigma) 測量其血紅素含量，以量化血管新生作用。

動物腫瘤移植評估 (Tumor xenograft model)

首先培養大量的癌細胞，將 HCT116 腫瘤細胞或 A549 腫瘤細胞以皮下注射的方式植入 BALB/c-nude (或 SCID) mice 背部。待腫瘤細胞長大至 150 mm^3 時開始給予藥物，每週測量腫瘤大小兩次，藥物以口服方式給予。實驗組總共分成 3 組，第一組為 control 組，5 隻小鼠植入腫瘤細胞後僅給予溶劑 (1% carboxymethyl cellulose + 0.5% Tween 80，0.2 mL/mouse)。第 2、3 組為加藥組，每小組各 5 隻，停藥後將小鼠犧牲，取出腫瘤組織，部分以 10 %中性福馬林固定，以 paraffin 作包埋，組織切成 5 mm 薄片，進行後續 H&E 及 CD31 染色。部分組織將保存於液態氮中，萃取其中的蛋白質，進行西方點墨法的分析。

動物腫瘤轉移實驗 (*In vivo* metastatic model)

在癌症轉移實驗中，大腸癌細胞 HCT-116 (1 x 10^7 cells/ml) 直接打入 4 週大 male SCID mice 的尾靜脈，將小鼠分成兩組，每組 4 隻，並立即開始口服給予溶劑 (1% carboxymethyl cellulose + 0.5% Tween 80，0.2 mL/mouse) 或藥物 MPT0G013 (25 mg/kg) ，兩天餵藥一次。在第 42 天犧牲小鼠，取出肺臟，照像並固定於 4% formaldehyde，在解剖顯微鏡 (Optima) 下計數肺臟表面的轉移節結 ($\Phi > 1$ mm) ，並將肺臟秤重及定量。

藥物動力學分析

CD-1 (Crl.) 公鼠 (每組n = 4) 來自於Lasco (Taipei, Taiwan) 用來測平 MPT0B271的藥物動力學，MPT0B271溶於polyethylene glycol 400/ethanol/water (60/5/35, v/v)，並以靜脈注射方式 (2.0 mg/kg) 打入小鼠尾靜脈，口服溶劑則為 0.5% methylcellulose (MC) /water，每隻小鼠口服給予MPT0B271 0.26 ml (10 mg/kg) ，小鼠在給予藥物之前禁食16小時，給予後正常飲食4小時，靜脈注射組

別的小鼠，血液樣本在藥物給予前、給予2、5、15、30分鐘及1、1.5、2、4、6、9、24、27小時後收集，口服組別則是在藥物給予前、15、30分鐘及1、1.5、2、4、6、9、24、27小時後收集，接著利用LC-MS/MS (API4000; PE Sciex, Concord, ON, Canada) 及反相柱 (reverse-phase ODS column) 來分析MPT0B271的血中濃度，並使用WinNonlin Professional program (version 5.2, Pharsight Corp., Mountain View, CA, USA) 計算出平均血中濃度及藥物動力學相關參數。

統計分析

所有實驗結果以平均值 ± 標準誤差 (mean ± SD) 或平均值 ± 平均值標準誤差 (mean ± SEM) 表示，並使用 one-way ANOVA 和 *t* test；當 $P < 0.05$ 時即視為其具有統計意義。

第三章

Dehydrocostuslactone藉由抑制Akt/GSK-3β及mTOR的訊息路徑阻礙體內及體外的血管新生

Dehydrocostuslactone Suppresses Angiogenesis *In Vitro* and *In Vivo* through Inhibition of Akt/GSK-3β and mTOR Signaling Pathways

PLoS One. 2012;7(2):e31195.

中文摘要

傳統中藥成分 dehydrocostuslactone (DHC) 是從 *Saussurea costus* (Falc.) Lipschitz 分離出來的，目前已經知道其抗癌的活性。而血管新生是癌症生長及進展的必經過程，本研究主旨在首次發現 DHC 能夠經由抑制 Akt/glycogen synthase kinase-3β (GSK-3β)/cyclin D1 以及 mTOR signaling pathway 而造成細胞週期停留在 G0/G1 phase，產生抗血管新生作用。首先，在 matrigel-plug 動物實驗模式，DHC 具有明顯抑制血管新生的作用，此外，作用在人類臍靜脈內皮細胞 (human umbilical vein endothelial cells；HUVECs) 可呈現濃度相關性地抑制由 EGM-2 所引起的細胞增生及管腔形成。DHC 能夠造成細胞週期停留在 G0/G1 phase，減少 cyclin D1、cyclin A、cdk2 蛋白質表現、抑制 retinoblastoma 蛋白的磷酸化，此外，DHC 能夠明顯抑制 Akt、GSK-3β、mTOR 的磷酸化，當細胞過度表現持續性活化的 myristoylated (myr)-Akt，DHC 抑制細胞增生、管腔形成的抑制作用以及減少 cyclin D1 的表現都能夠被逆轉而回復。另外，將內皮細胞共同處理 LiCl 及 DHC，也能夠明顯地逆轉 DHC 抑制細胞生長的作用。總結以上結果，本研究證實 Akt/GSK-3β/cyclin D1 以及 mTOR signaling pathway 是 DHC 重要的標靶，因此能夠應用於如癌症及血管新生相關的疾病。

英文摘要

The traditional Chinese medicine component dehydrocostuslactone (DHC) isolated from *Saussurea costus* (Falc.) Lipschitz, has been shown to have anti-cancer activity. Angiogenesis is an essential process in the growth and progression of cancer. In this study, we demonstrated, for the first time, the anti-angiogenic mechanism of action of DHC to be via the inhibition of cell cycle progression at the G0/G1 phase due to abrogation of the Akt/glycogen synthase kinase-3β (GSK-3β)/cyclin D1 and mTOR signaling pathway. First, we demonstrated that DHC has an anti-angiogenic effect in the matrigel-plug nude mice model and an inhibitory effect on human umbilical vein endothelial cell (HUVEC) proliferation and capillary-like tube formation *in vitro*. DHC caused G0/G1 cell cycle arrest, which was associated with the down-regulation of cyclin D1 expression, leading to the suppression of retinoblastoma protein phosphorylation and subsequent inhibition of cyclin A and cdk2 expression. With respect to the molecular mechanisms underlying the DHC-induced cyclin D1 down-regulation, this study demonstrated that DHC significantly inhibits p-Akt expression, resulting in the suppression of GSK-3β phosphorylation and p-mTOR expression. These effects are capable of regulating cyclin D1 degradation, but they were significantly reversed by constitutively active myristoylated (myr)-Akt. Furthermore, the abrogation of tube formation induced by DHC was also reversed by overexpression of Akt. And the co-treatment with LiCl and DHC significantly reversed the growth inhibition induced by DHC. Taken together, our study identified Akt/GSK-3β and mTOR as important targets of DHC and thus highlighted its potential application in angiogenesis-related diseases, such as cancer.

第一節 緒言

Dehydrocostuslactone (DHC) 是傳統中藥雲木香的成分之一，屬於 sesquiterpene lactone 的衍生物，主要是從 *Saussurea costus* (Falc.) Lipschitz 分離出來的活性成分，已有許多研究證實 DHC 具有抗發炎、保肝利膽、免疫調節及抗氧化的作用，被使用於治療潰瘍等疾病。在最近的研究中發現，DHC 能明顯抑制卵巢癌細胞的增生，誘導許多不同腫瘤的細胞凋亡，並發現機轉如下：在 human promyelocytic leukemia cells (HL-60) 中，DHC 會阻止 tumor necrosis factor (TNF)-α 誘導 IκBα 的磷酸化和降解作用，在 hepatoma 及肺癌細胞中，誘導 endoplasmic reticulum stress，在乳癌細胞中能抑制 signal transducers and activators of transcription 3 (STAT3) 的活化。雖然 DHC 已被知道能在 *in vitro* 及 *in vivo* 中，抑制腫瘤生長的作用，但是目前尚未有研究探討 DHC 是否能調控腫瘤的血管新生。因此，本實驗以內皮細胞為對象，探討 DHC 抑制血管新生的機轉。

第二節 結果

Dehydrocostuslactone 抑制體內血管新生的作用

為了確定 DHC 是否可以抑制血管新生，我們首先以 Matrigel plug assay 動物實驗來評估 DHC 在老鼠體內的藥效。本實驗利用 co-plug 將 Matrigel 與血管新生生長因子混合以及 DHC 藥物混合後打入 C57BL/6 小鼠皮下，從目測可見未加藥組明顯誘發血管生成 (Figure 3-1A)，相反的，DHC 明顯抑制血管新生並且呈現濃度相關性的抑制作用。此外，我們將取出的 Matrigel plug 部分進行組織切片染色 (Masson's Trichrome staining)，發現 DHC 能明顯抑制血管生長因子所誘導形成的紅血球填充的管腔 (Figure 3-1A)。最後使用 Drabkin's reagent kit 來定量血紅素的含量，結果顯示 DHC 能明顯抑制血管新生因子所誘發的血管生成而減少血紅素的含量 (Figure 3-1B)。

Dehydrocostuslactone 抑制體外血管新生的作用

在血管新生的過程中，內皮細胞必須經由細胞外基質的降解，移行，增生，以及形成管柱以進行血管的新生。本實驗利用一系列的 functional assays 來探討 DHC 在體外是否會抑制血管生成的步驟，首先在結晶紫染色法 (crystal violet assay) (Figure 3-2A) 及 BrdU incorporation labeling assay (Figure 3-2B) 中，DHC (0.3-10 μM) 能明顯有濃度相關性的抑制 EGM-2 誘導的細胞增生及 DNA 的合成，其 GI_{50} 分別是 2.4 及 3.0 μM。接下來利用 transwell assay 及 tube formation assay 來探討 DHC 對內皮細胞移行及型態分化的影響。Figure 3-2C 顯示 DHC 能夠濃度相關性明顯抑制類血管管柱分化的形成。利用 Image-pro plus 軟體定量後，DHC 在 3，5，10 μM 能分別有 54.0%，76.2%，98.6% 的抑制程度 (Figure 3-2D)。然而，DHC 卻對內皮細胞移行沒有明顯的影響 (Figure 3-2E and 2F)。

Dehydrocostuslactone 能影響內皮細胞的細胞週期

為了探討 DHC 抑制細胞生長的作用，本研究利用流式細胞儀確認 DHC 是否透過影響細胞週期來造成生長抑制。當給予細胞 DHC 處理 18 小時後，能夠增加內皮細胞在 G0/G1 期的百分比，減少在 S/G2/M 期的百分比 (Figure 3-3A, 3B, and 3C)。另外也測試了 DHC 在細胞飢餓狀態下，對細胞凋亡的作用，然而，控制組的細胞與 DHC 處理的細胞並沒有明顯的差異，在 DHC 處理的細胞組別的細胞凋亡現象，推測是因為缺少了生長因子和血清 (Supplementary Figure 3-1)。接者探討 DHC 對於細胞週期 G0/G1 調控蛋白的影響，發現 DHC 能夠以具有時間及濃度相關性地明顯減少 cyclin D1 的表現 (Figure 3-4A and 4B)，並且抑制其下游蛋白 Rb 的磷酸化，cyclin A 及 cdk2 的表現也在 12 小時減少，然而，不論在任何時間點，DHC 對於 cdk4 只有些微的影響 (Figure 3-4A)。

DHC 藉由 Akt/GSK-3β pathway 造成 cyclin D1 減少及生長抑制

過去的研究已顯示許多不同種類的生長因子，包括 platelet-derived growth factor (PDGF) 、bFGF (Burgering *et al.*, 1995; Franke *et al.*, 1995) 、VEGF (Gerber *et al.*, 1998) ，都能夠活化 serine/threonine kinase Akt。為了進一步釐清 DHC 抑制血管新生的機轉，藉由西方墨點法來觀察 DHC 對於 Akt 活化的影響，將內皮細胞處理 DHC 能夠具有時間及濃度相關性地抑制 EGM-2 誘導 Akt 在 serine 473 的磷酸化 (Figure 3-5A) 。為了確認 Akt 參與調控細胞生長及細胞週期蛋白 cyclin D1 的表現，將 HUVECs 轉染持續性活化型態的 myristoylated (myr) - Akt，然後探討其對於 DHC 抑制細胞生長作用的影響。本實驗先進行轉染證實效果 (Figure 3-5B)；利用 LY294002 (Akt 抑制劑) 作為 positive control，與轉染 vector 的控制組比較，over-expression Akt 經 DHC 處理後，能明顯增加 cyclin D1 的表現 (Figure 3-5C)。

Akt 能夠藉由在 GSK-3β 的 serine 9 磷酸化來負向調控其活性，GSK-3β 促進 cyclin D1 被 proteasome 降解進而調控細胞週期 (Diehl *et al.*, 1998)。本研究繼續探討 DHC 抑制 Akt 的磷酸化是否會導致 GSK-3β 磷酸化減少，並造成生長抑制。將細胞處理 DHC 後，會明顯抑制 GSK-3β 的磷酸化，並且具有時間及濃度相關性的作用 (Figure 3-5D)；然而，與轉染 vector 的控制組別比較，over-expression Akt 的細胞處理 DHC 後，會明顯增加 GSK-3β 的磷酸化 (Figure 3-5D)。另外，利用結晶紫染劑細胞增生實驗，DHC 誘導的生長抑制作用則會被 Akt 的轉染所反轉 (Figure 3-6A)；除此之外，over-expression Akt 也能部分反轉 DHC 阻礙類血管管腔形成的作用 (Figure 3-6B)。為了進一步證實在 DHC 抑制血管新生得作用過程中，GSK-3β 有參與並作為 Akt 下游的 effector，將細胞同時處理 GSK-3β 活性抑制劑 LiCl 與 DHC，發現能明顯反轉 DHC 的生長抑制作用約 50% (Figure 3-6C)。總結以上結果，在 DHC 抑制細胞生長和類血管管腔形成的作用中，Akt/GSK-3β/cyclin D1 pathway 扮演了相當重要的角色。

DHC抑制cyclin D1表現與mTOR pathway相關

Akt的訊息傳遞路徑對於生長因子誘導mammalian target of rapamycin (mTOR)-C1的活化是必須的，另外在缺乏Akt的細胞中，mTORC1是不具有活性的 (Gingras *et al.*, 1998; Hahn-Windgassen *et al.*, 2005)。mTORC1的活化也會導致4-emopamil-binding protein (EBP)-1磷酸化，因而活化了eIF4E，並增加cyclin D1的轉錄 (Rosenwald *et al.*, 1995)。為了評估mTORC1在DHC抑制cyclin D1表現的角色，利用西方墨點法來觀察mTORC1下游的訊息蛋白，發現DHC能夠明顯抑制EGM-2誘導mTOR訊息路徑的磷酸化，例如：mTOR、p70S6K、4EBP以及eIF4E，並且具有時間及濃度相關性的作用 (Figure 3-7A)。在over-expression Akt的內皮細胞中，與轉染vector的控制組別比較，DHC對於mTOR下游訊息分子磷酸化的蛋白表現抑制作用，會被明顯的反轉 (Figure 3-7B)。利用結晶紫染劑細胞增生實

驗，與單獨處理DHC的組別比較之下，將細胞共同處理rapamycin及DHC，能增加DHC的生長抑制作用 (Supplementary Figure 3-2) 。綜合以上結果，Akt/mTOR signaling pathway可能有參與在DHC藉由抑制cyclin D1表現而造成生長抑制的作用中。

第三節 討論

腫瘤的進展與轉移都必須依賴血管新生 (Folkman, 2002)，因此，在最近幾年，抗血管新生的藥物發展日趨重要，最近的文獻也報導指出天然產物在正常細胞週期具有細胞毒殺作用，根據文獻報導，約只有十一種天然產物或是天然修飾化合物進入臨床試驗 (El Sayed, 2005)。在本研究中，發現傳統中藥成分DHC，在體內和體外皆具有抗血管新生的作用。首先，利用matrigel plug assay，證實DHC在體內具有濃度相關性地抑制血管新生，過去的研究已知，在xenograft mouse models中，DHC能抑制許多不同種類的腫瘤生長 (Hsu *et al.*, 2009; Hung *et al.*, 2010; Kuo *et al.*, 2009) ，因此，DHC抑制血管新生的作用，可能是阻礙腫瘤進展的其中一個主要機轉，經由利用一系列的*in vitro* assays，顯示DHC抑制類血管管腔形成及內皮細胞生長之作用，與本研究之體內結果具有一致性。相反的，DHC在transwell assay中對於細胞移行則沒有明顯的抑制作用，利用西方墨點法，發現DHC能活化內皮細胞中的p38及ERK1/2的訊息 (Supplementary Figure 3-3A) ，使用scratch wound healing assay來再度確認DHC對於HUVECs移行的作用，發現只有在將細胞共同處理SB203580 (p38抑制劑) 及DHC能明顯抑制HUVECS的移行 (Supplementary Figure 3-3B) 。這些結果顯示DHC雖能夠抑制PI3K/Akt pathway，當Akt訊息被抑制時，p38的活化卻可能貢獻於HUVECs移行的訊息。總結以上，推測DHC應是透過選擇性抑制內皮細胞生長及類血管管腔結構形成來阻礙血管生成。

細胞增生在血管新生中是極重要的過程之一，本研究發現DHC延緩了HUVECs從G0/G1期進入S期，此結果與之前的研究一致，DHC能造成乳癌細胞的生長抑制 (Kuo *et al.*, 2009)。Cyclin D1是必須不可或缺的有絲分裂訊號感受蛋白以及細胞週期調節者，藉由與CDK4結合而促使細胞從G0期進入增生階段，

cyclin D1在內皮細胞中占有重要的角色，最近的研究顯示over-expression cyclin D1與各種癌症的發展有關聯 (Fu *et al.*, 2004)，因此，減少cyclin D1表現的策略被報導認為在體內及體外可以抑制腫瘤血管新生 (Hanai *et al.*, 2002; Yasui *et al.*, 2006)。本研究結果顯示在處理DHC三小時後，就能明顯減少cyclin D1的表現，並具有濃度及時間相關性，其他細胞週期調控者則在12小時開始減少，所以推測DHC是透過減少cyclin D1的表現造成HUVECs生長抑制，並且此作用在阻礙血管新生扮演重要的角色。

目前有許多文獻意味著Akt的訊息路徑對於正常細胞G1/S期的過渡以及內皮細胞的增生是必要不可或缺的 (Jiang *et al.*, 2008; Jiang *et al.*, 2000; Kanda *et al.*, 1997; Skeen *et al.*, 2006)，從臨床前的研究已知PI3K/Akt訊息路徑的抑制劑是強力的抗血管新生制劑而能達到抑制腫瘤生長之效益 (Hamada *et al.*, 2005; Phung *et al.*, 2006; Schnell *et al.*, 2008; Tsai *et al.*, 2010; Yuan *et al.*, 2008)。當內皮細胞受到生長因子的刺激，Akt會立即活化，PDK1磷酸化Akt的T308 residue，mTORC2則在Akt的S473 residue磷酸化 (Sarbassov *et al.*, 2005)，這兩個磷酸化的位置具有相同重要性，並且導致Akt protein kinase的完全活化。Akt下游的主要訊息蛋白是mTORC1及GSK-3β，活化的mTORC1會藉由直接磷酸化轉譯調節蛋白S6K1及4EBP1，來誘導cyclin D1表現以促進細胞生長 (Nelsen *et al.*, 2003; Rosenwald *et al.*, 1995)，另外Akt也能磷酸化及抑制GSK-3β的活性來阻止cyclin D1降解 (Diehl *et al.*, 1998; Diehl *et al.*, 1997)，因此，抑制Akt的訊息路徑會導致cyclin D1經由GSK-3β降解或是減少mTORC1的轉譯作用，進而減少cyclin D1的蛋白表現。本研究首次證實DHC在Akt/GSK-3β/cyclin D1訊息路徑的作用，除此之外，DHC在HUVECs中，能抑制Akt在Ser473的磷酸化，推測DHC可能與mTORC2是互相競爭的關係。如同前面文獻所述，Akt的活化必須由各種不同的生長因子所誘發，並且必須透過PI3K的刺激。而在本研究中，發現轉染myr-Akt明顯增加細胞內的p-Ser473 Akt，實驗結果與PI3K抑制劑LY294002的相關研究結果是相似的，此

外，利用Akt kinase activity assay，發現DHC並不能抑制Akt磷酸化受質的能力(Supplementary Figure 3-4)，因此，本研究推測DHC可能是一個PI3K kinase抑制劑或PDK1 kinase抑制劑，而能夠在體內及體外發揮抗血管新生的作用。

過去的研究顯示mTORC1的活化不只是受到Akt的調控，其他例如生長因子、缺氧、低能量和胺基酸含量都會影響mTORC1，並且這些因素都會共同調控細胞的反應 (Engelman, 2009)。然而，本研究結果顯示轉染myr-Akt能反轉DHC對於mTOR訊息路徑的抑制作用，表示Akt/mTOR轉譯路徑是DHC減少cyclin D1另一個重要的標靶。過去的文獻曾經報導DHC在癌細胞中的其他標靶包括NF-kB、STAT3以及誘導內質網壓力 (ER stress) (Hsu *et al.*, 2009; Kuo *et al.*, 2009; Oh *et al.*, 2004)，除此之外，NF-kB的活化會調控血管新生因子基因的表現，因此，這些機轉仍對DHC所產生的抗血管新生作用有一定的貢獻，無法排除。然而，over-expression myr-Akt會明顯回復DHC的生長抑制作用，表示DHC抑制Akt活化是DHC阻礙內皮細胞增生的主要機轉，有鑑於此，前述DHC的機轉可能都會協同性地在體內和體外發揮抗血管新生的作用。

總結以上結果，本研究發現DHC透過新穎的機轉來抑制生長因子所誘發的血管新生，DHC造成HUVECs的細胞週期滯留在G0/G1期，並藉由抑制Akt/GSK-3β及mTOR路徑來阻礙體內及體外的血管新生。因此，這些結果顯示DHC是具有發展潛力的傳統中草藥物成分，來治療血管新生相關的疾病。

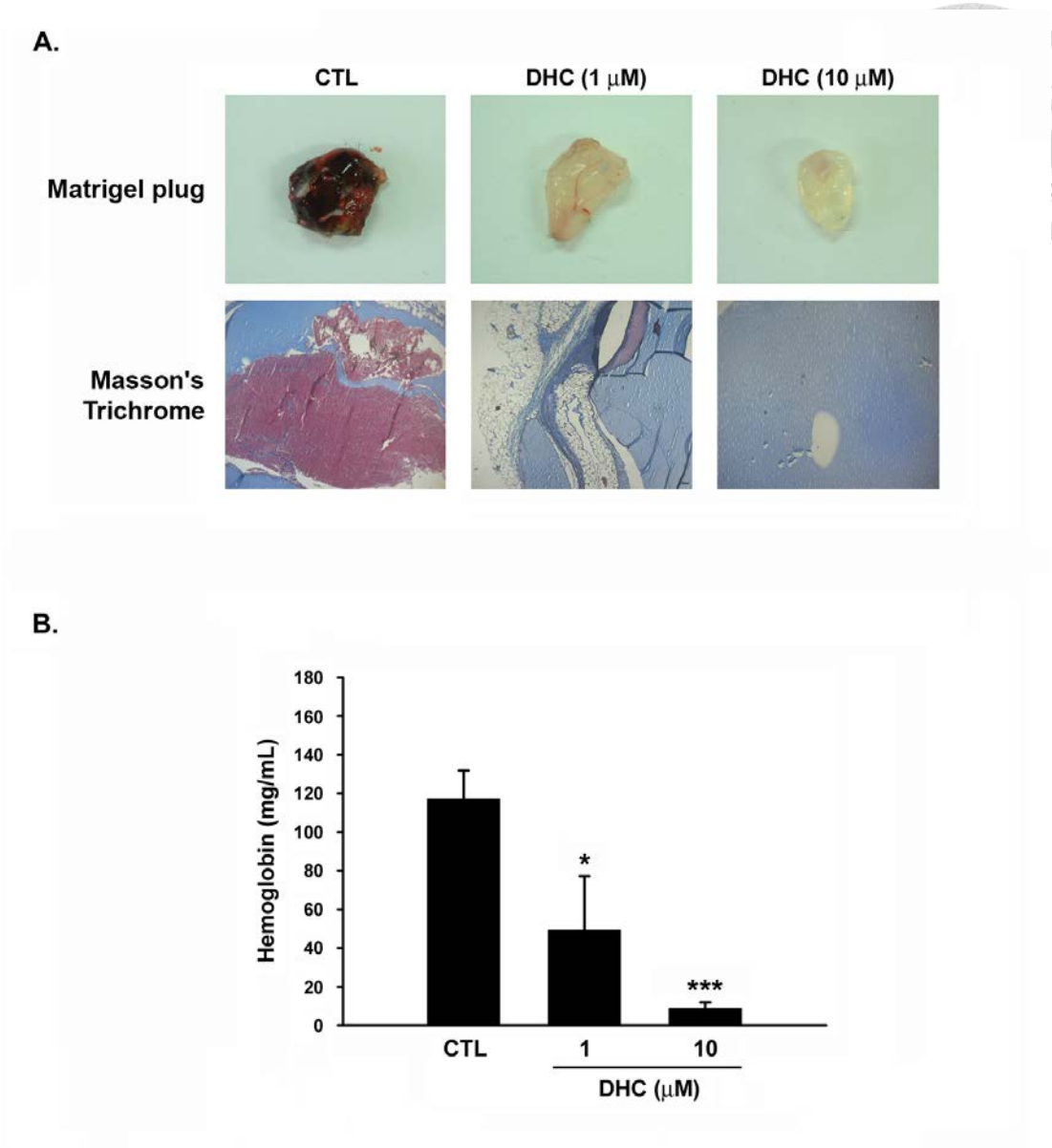

Figure 3-1. DHC inhibits angiogenesis in a mouse matrigel model. C57BL/6 mice were injected subcutaneously with matrigel mixed without (control, CTL) or with DHC (1 μM and 10 μM). A, upper panel, plugs were excised from the mice after a week and photographed. Bottom panel, histological analysis was performed using Masson-Trichrome staining from the excision of matrigel plug. B, Quantification of the hemoglobin content of matrigel plugs by spectrophotometer measured at 540 nm. Data represent the mean ± SEM from five independent experiments. * $P < 0.05$ and *** $P < 0.001$ versus control.

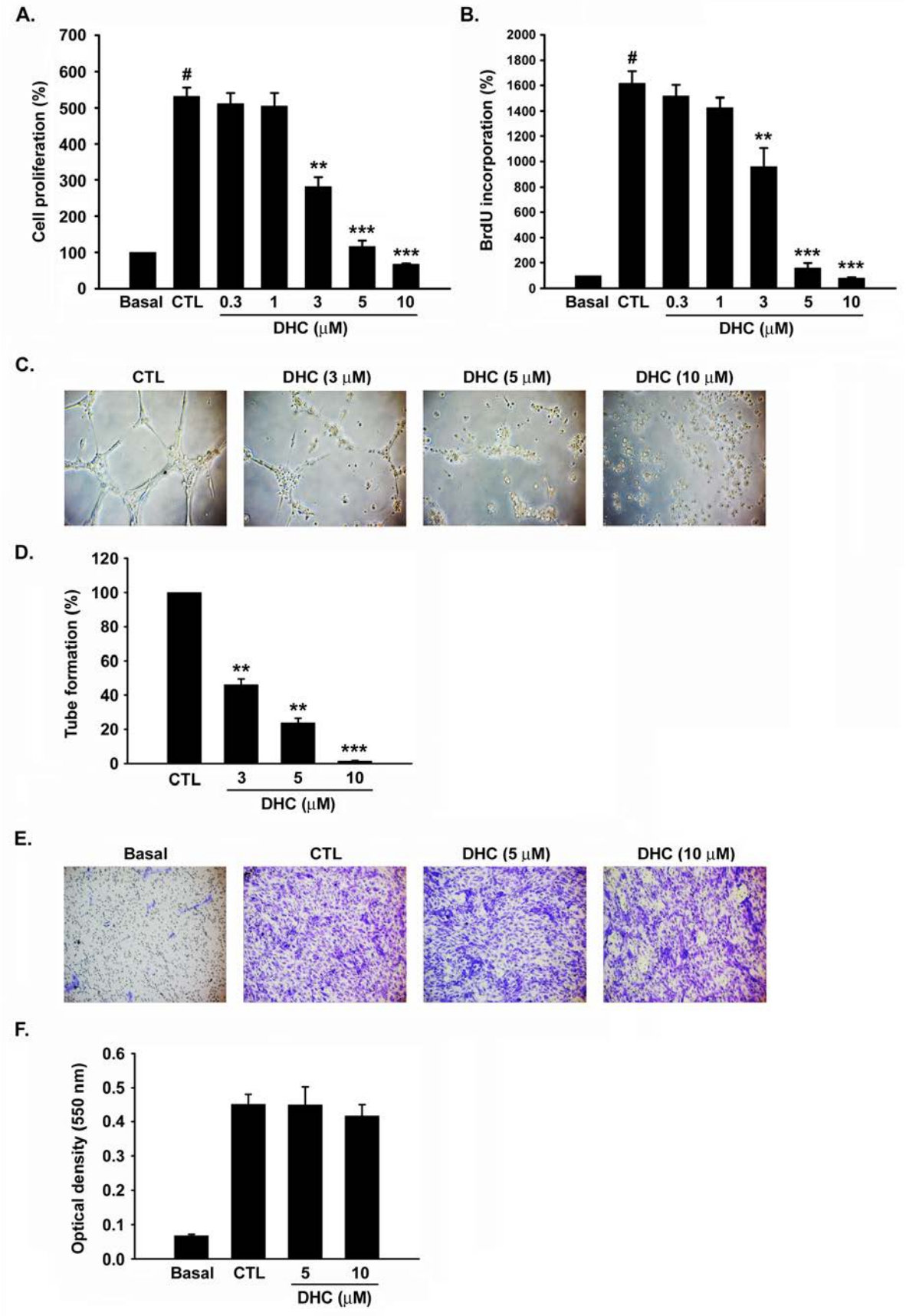
A.
Cell proliferation (%)
700
600
500
400
300
200
100
0
#
**
***
***
Basal CTL 0.3 1 3 5 10
DHC (μM)
B.
BrdU incorporation (%)
2000
1800
1600
1400
1200
1000
800
600
400
200
0
#
**
***
***
Basal CTL 0.3 1 3 5 10
DHC (μM)
C.
CTL
DHC (3 μM)
DHC (5 μM)
DHC (10 μM)
D.
Tube formation (%)
120
100
80
60
40
20
0
**
**
***
CTL 3 5 10
DHC (μM)
E.
Basal
CTL
DHC (5 μM)
DHC (10 μM)
F.
Optical density (550 nm)
0.6
0.5
0.4
0.3
0.2
0.1
0.0
Basal CTL 5 10
DHC (μM)

Figure 3-2. Impairment of *in vitro* angiogenesis by DHC. HUVECs were treated without (control, CTL) or with DHC (0.3-10 μM) in EGM-2 medium. A, After 72 h of incubation, cells were stained with crystal violet and determined the inhibition of cell proliferation by the absorbance at 550 nm. B, DNA synthesis was assessed by BrdU incorporation assay. C, representative photographs of capillary-like structures formation of CTL and DHC-treated HUVECs on matrigel under microscope (magnification is X100). D, Quantification of the total tube length of capillary-like structures by image analysis software. Data represent the mean ± SEM from three independent experiments. ** $P < 0.01$ and *** $P < 0.001$ versus control. E, effect of DHC on cell migration using a transwell assay. F, the graph shows quantitative analysis of the migrated cell numbers in tranwell assay. Data represent the mean ± SEM from three independent experiments. ## $P < 0.01$ versus basal.

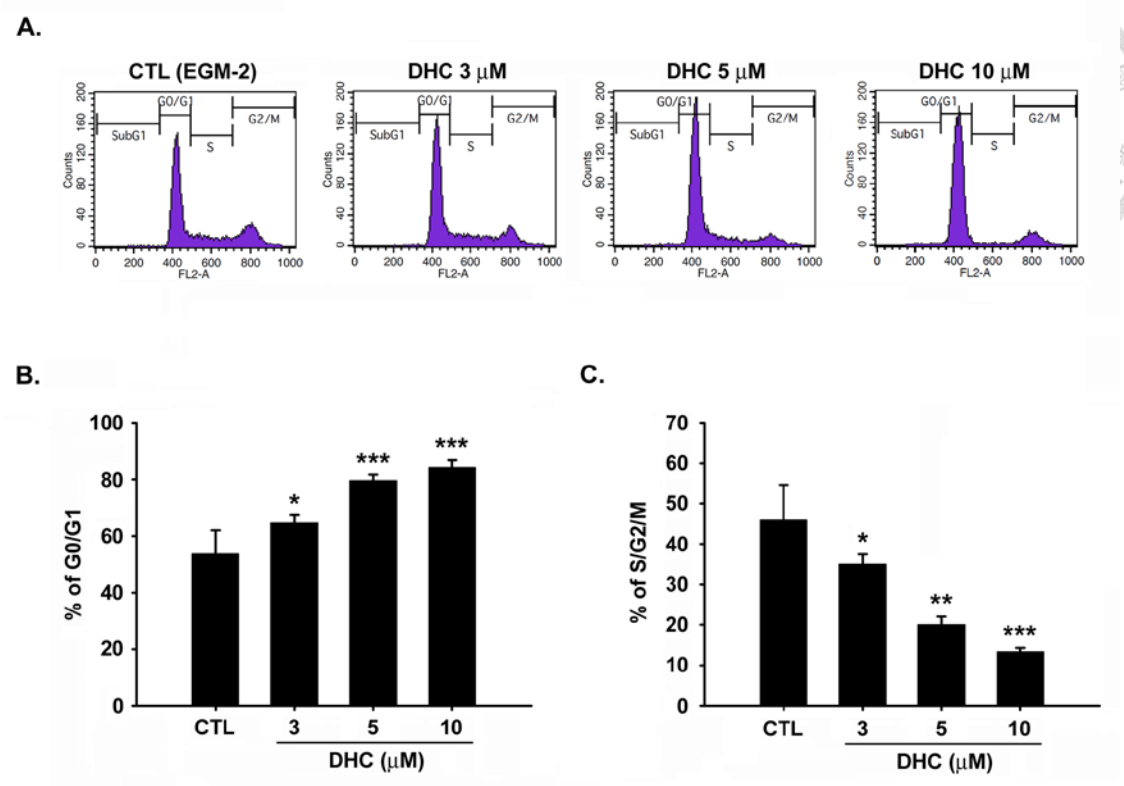

Figure 3-3. Effect of DHC on cell cycle. A, HUVECs were starved for 24 h, and then were treated without (control, CTL) or with DHC (3-10 μM) for 18 hr. After cells were labeled with propidium iodide, DNA content was analyzed by flow cytometry. B and C, cell population in G0/G1 and S/G2/M phase were quantified. Data represent the mean ± SEM from four independent experiments. * $P < 0.05$, ** $P < 0.01$ and *** $P < 0.001$ versus control.

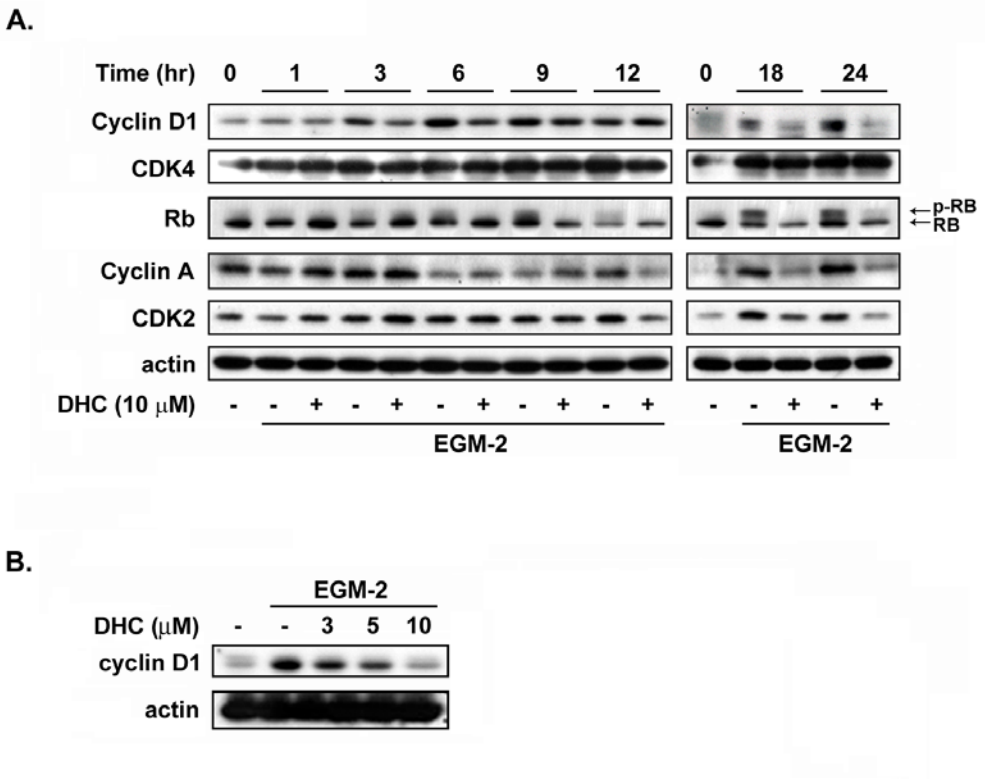

Figure 3-4. Effect of DHC on expression levels of cyclins and CDKs. A, after starvation for 24 hr, HUVECs were pretreated without (control, CTL) or with DHC for 60 min and then incubated with EGM-2 at indicated time. Cells were harvested, analyzed by western blot and probe with antibodies. B, cyclin D1 expression was inhibited by DHC in a concentration dependent manner. Actin expression served as a loading control. Data represent from three independent experiments.

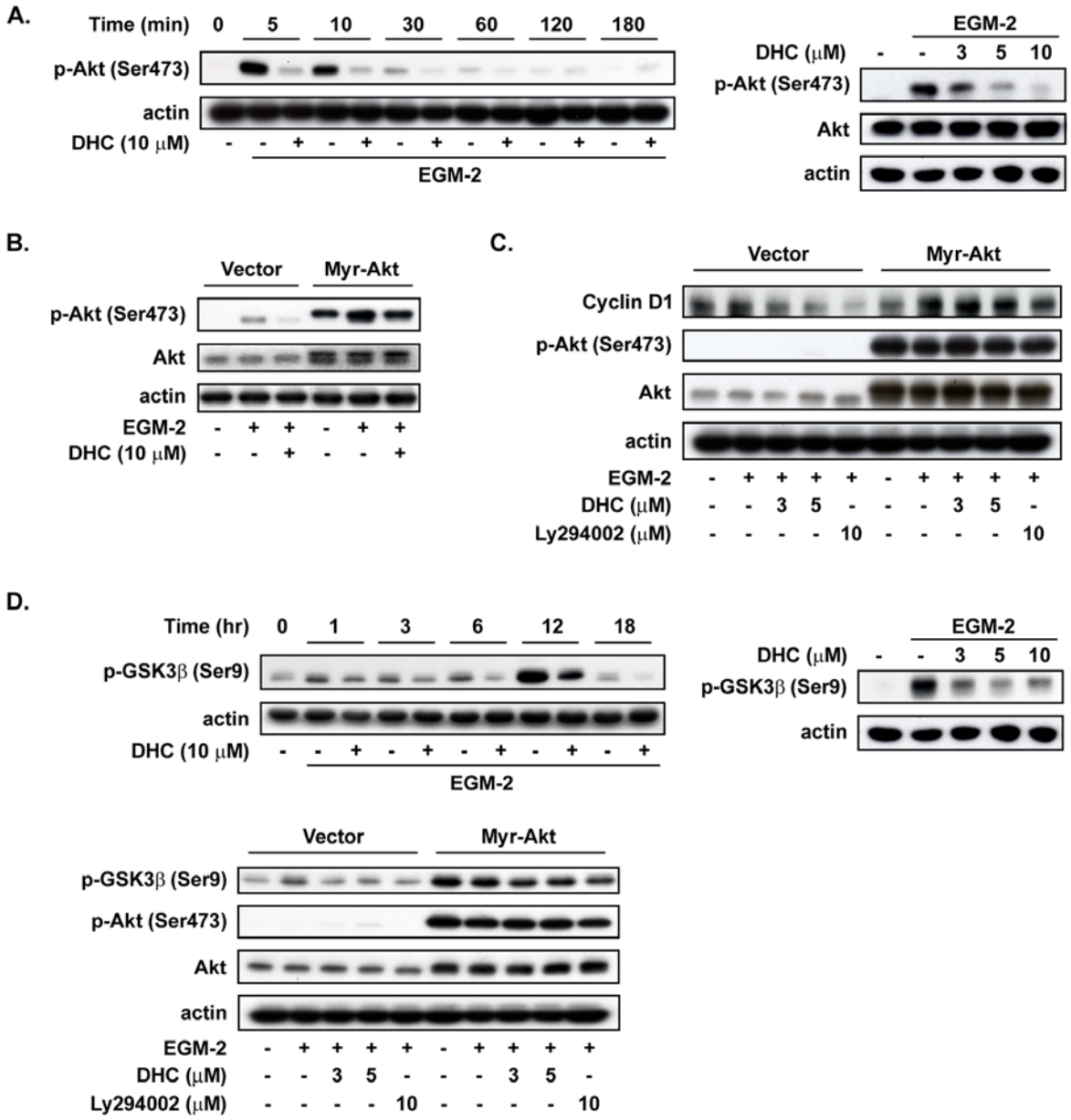

Figure 3-5. Cyclin D1 is a critical target of DHC-mediated cell cycle arrest through Akt/GSK-3β pathway. A, Western blot analysis of Akt phosphorylation inhibited by DHC with the indicated times and concentrations. B, HUVECs were transfected with either vector or myr-Akt, starved for 24 hr, and then pretreated with DHC for 1hr followed by incubation in EGM-2 medium for 10 min. Cells were harvested and analyzed protein expression by western blot. C and D, western blot analysis of cyclin D1 expression and GSK-3β phosphorylation in HUVECs transfected with the indicated plasmids and then treated with DHC (3 and 5 μM) and Ly294002 (10 μM) for 6 hr. Data represent from three independent experiments.

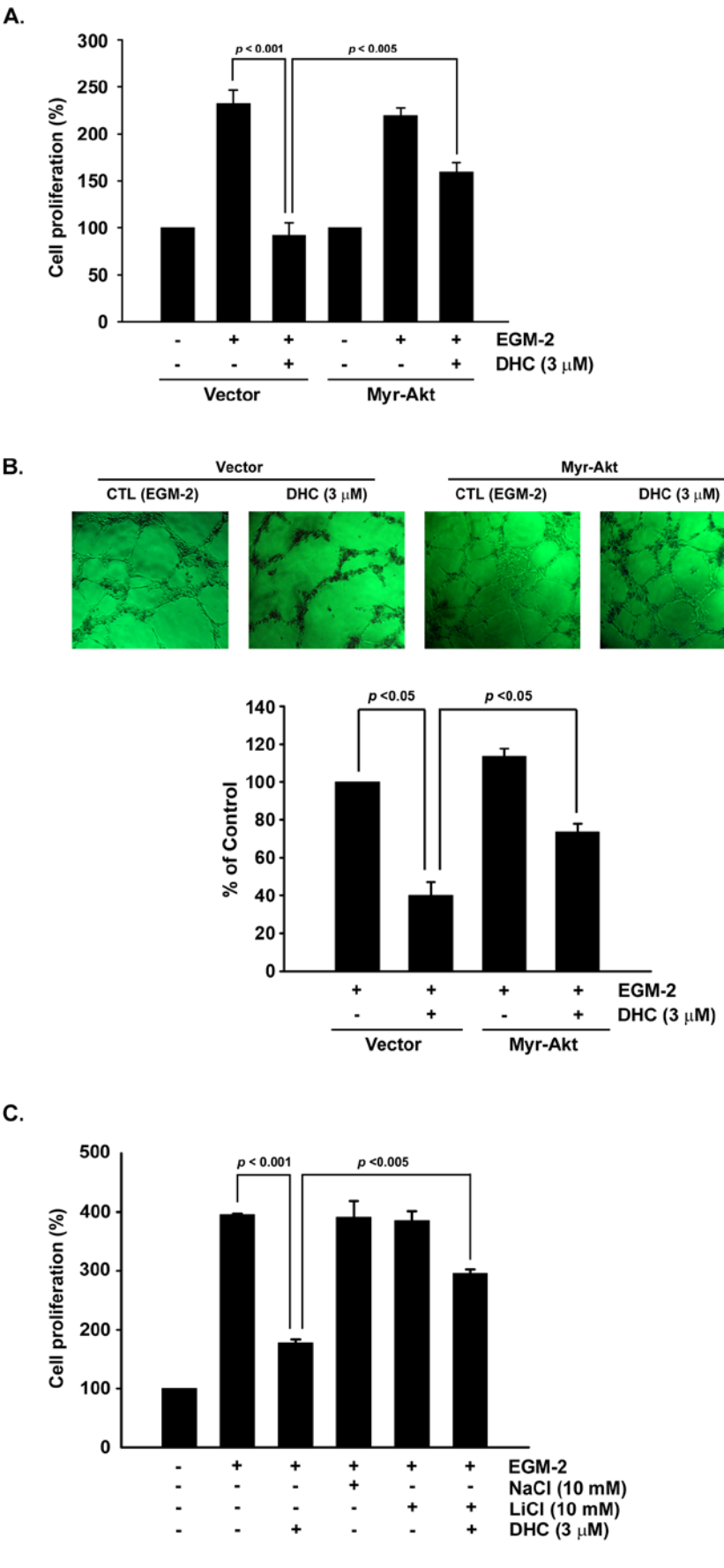
A.
Cell proliferation (%)
300
250
200
150
100
50
0
p < 0.001
p < 0.005
- + + - + + EGM-2
- - + - - + DHC (3 μM)
Vector
Myr-Akt
B.
Vector
Myr-Akt
CTL (EGM-2)
DHC (3 μM)
CTL (EGM-2)
DHC (3 μM)
% of Control
140
120
100
80
60
40
20
0
p <0.05
p <0.05
+ + + + EGM-2
- + - + DHC (3 μM)
Vector
Myr-Akt
C.
Cell proliferation (%)
500
400
300
200
100
0
p < 0.001
p <0.005
- + + + + + EGM-2
- - - + - - NaCl (10 mM)
- - - - + + LiCl (10 mM)
- - + - - + DHC (3 μM)

Figure 3-6. DHC inhibited cell proliferation and tube formation through Akt/GSK-3β pathway A, crystal violet assay. Treatment of vector group with DHC (3 μM) in EGM-2 medium significantly decreased cell proliferation numbers compared with untreated vector group. Akt overexpression significantly increased cell proliferation in DHC-treated group. B, tube formation assay. Treatment of vector group with DHC (3 μM) abrogated tube formation compared with vector control (CTL) group. Akt overexpression partial reversed the inhibitory effect. C, crystal violet assay. HUVECs were treated with DHC (3μM) and/or LiCl (10 mM). NaCl (10 mM) was as an osmolality control. Data represent from three independent experiments.

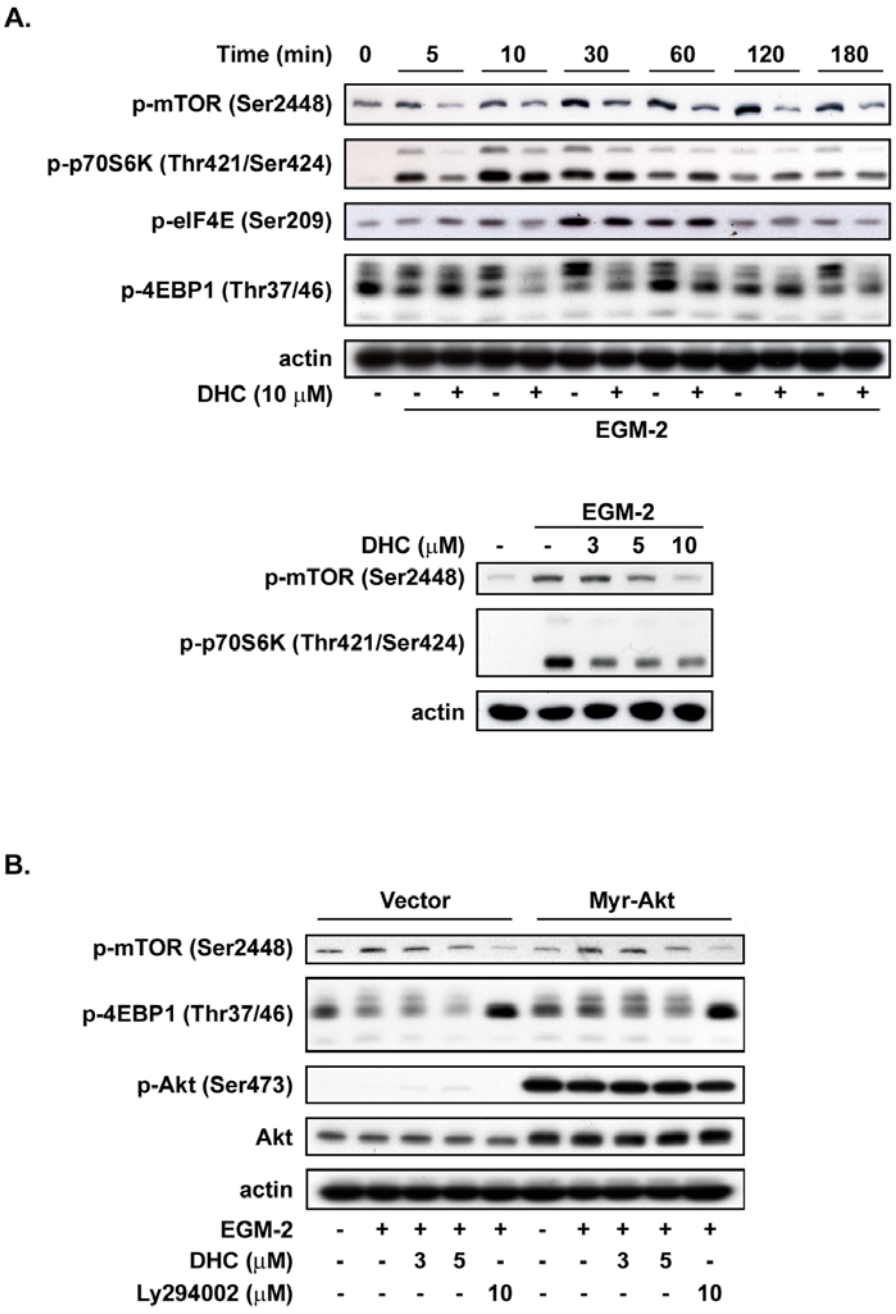

Figure 3-7. Effect of DHC on mTOR signaling downstream pathway. A, Western blot analysis of phosphorylation of mTOR, p70S6K, eIF4E and 4EBP in HUVECs treated with DHC for the indicated times and concentrations. B, after transfected with the indicated plasmids, HUVECs were starved for 24 hr and then pretreated with DHC followed by 10 min of EGM-2 incubation. Phosphorylation of mTOR and 4EBP were analyzed by western blot. Data represent from three independent experiments.

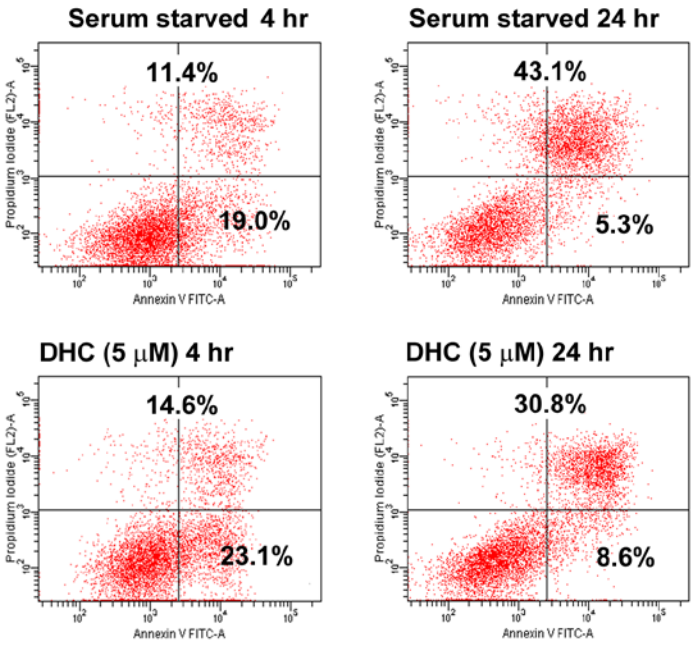

Supplementary Figure 3-1. Effect of DHC on early and late stage of HUVECs apoptosis was detected by flow cytometry with Annexin-V-FITC/PI dual staining. A representative histogram of flow cytometric analysis using double staining with annexin-V (FITC-A) and PI (PE-A). HUVECs were treated with DHC (5 μM) in EBM-2 basal medium for 4hr or 24hr. The lower right quadrants represent the cells in the early stage of apoptosis. The upper right plus left quadrants contain the cells in the late stage of apoptosis and necrosis. Data represent from three independent experiments.

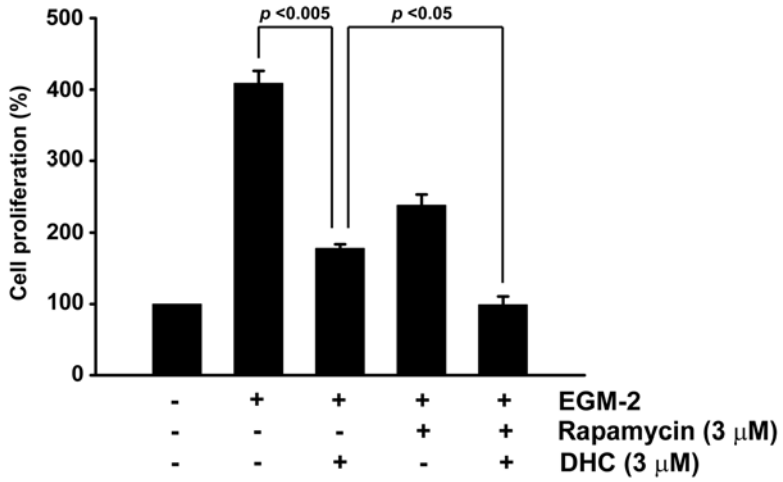

Supplementary figure 3-2. Rapamycin increased the anti-proliferative effect induced by DHC. Crystal violet assay. HUVECs were treated with DHC (3 μM) and/or rapamycin (3 μM). Inhibition of mTOR activity increased the anti-proliferative effect of DHC. Data represent from three independent experiments.

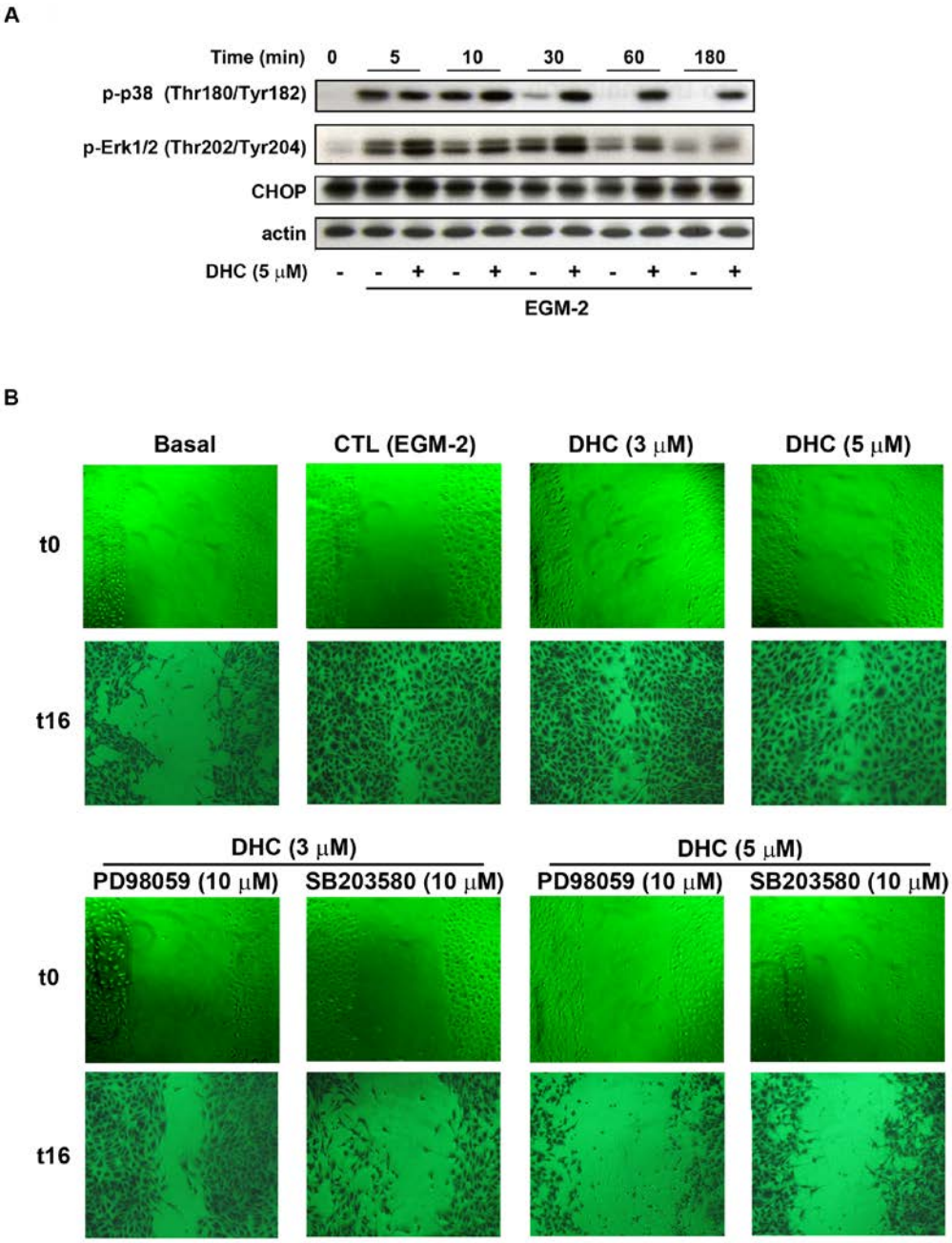

Supplementary figure 3-3. Effect of DHC on HUVECs migration. A, Western blot analysis of the protein expression of p-p38, p-ERK1/2, CHOP in DHC-treated HUVECs with the indicated times and concentrations. Data represent from three independent experiments. B, HUVECs migration after DHC treatment was accessed by wound-healing assay. Upon reaching 95% confluence, the HUVEC monolayer was scratched and cell debris was removed. Cells were cultured with EGM-2 medium and preteated with PD98059 (10 μM) or SB203580 (10 μM) for 30 min, and then cells were treated with DHC (3 or 5 μM). After incubation for 16 h, cells were stained with crystal violet and photographed.

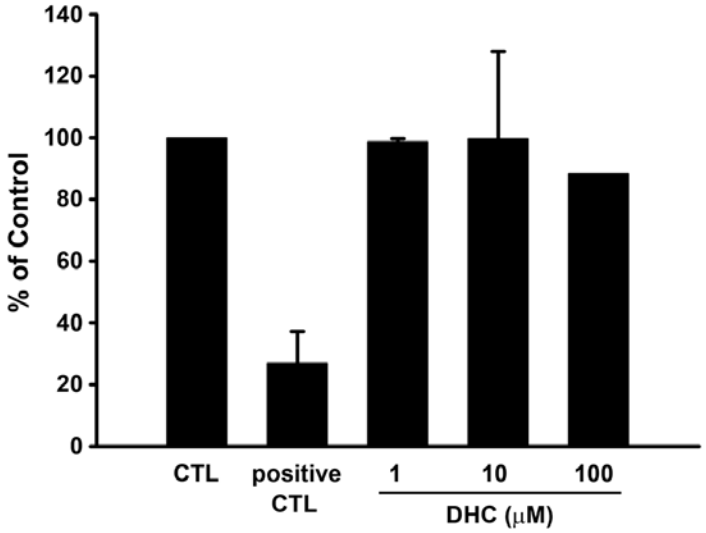

Supplementary figure 3-4. DHC did not inhibit Akt kinase activity. Akt Kinase activity kit was purchased from Enzo Life Sciences. Data represent from three independent experiments.

第四章

Arylsulfonamide 衍生物 MPT0G013 藉由增加 TIMP3 的表現抑制腫瘤血管新生

A novel action mechanism for MPT0G013, a derivative of arylsulfonamide, inhibits tumor angiogenesis through up-regulaiton of TIMP3 expression

Oncotarget 2014 revised

中文摘要

Tissue inhibitors of metalloproteinases 3 (TIMP3) 是具有強力抗血管新生作用的 matrix metalloproteinases (MMPs) 抑制性蛋白，在本研究中，發現 arylsulfonamide 衍生物 MPT0G013 在體內及體外透過誘導 TIMP3 的表現來達到抗血管新生的作用，將內皮細胞處理 MPT0G013 能明顯抑制細胞增生、類血管管腔形成及細胞移行，並且誘導 p21 蛋白表現，造成細胞週期停滯在 G0/G1 期。從 DNA 基因晶片表達檢測分析中，發現 MPT0G013 能明顯增加 TIMP3 基因的表現，藉由 siRNA TIMP3 可明顯地反轉 MPT0G013 抑制血管新生的作用以及回復了 MPT0G013 減少 p-AKT、p-ERK 蛋白表現。更重要地，在 *in vivo* Matrigel plug assay 及 HCT-116 腫瘤異體移植實驗中，MPT0G013 抑制體內血管新生及腫瘤生長，並且增加腫瘤細胞的 p21 及 TIMP3 的蛋白表現。總結以上結果，本研究證實 MPT0G013 做為抗血管新生藥物，可能對於治療過度血管生成之疾病有所助益。

英文摘要

Tissue inhibitors of metalloproteinases 3 (TIMP3) were originally characterized as inhibitors of matrix metalloproteinases (MMPs), acting as potent antiangiogenic proteins. In this study, we demonstrated that the arylsulfonamide derivative MPT0G013 has potent antiangiogenic activities *in vitro* and *in vivo* via inducing TIMP3 expression. Treatments with MPT0G013 significantly inhibited endothelial cell functions, such as cell proliferation, migration, and tube formation, as well as induced p21 and cell cycle arrest at the G0/G1 phase. Subsequent microarray analysis showed significant induction of *TIMP3* gene expression by MPT0G013, and siRNA-mediated blockage of TIMP3 up-regulation abrogated the antiangiogenic activities of MPT0G013 and prevented inhibition of p-AKT and p-ERK proteins. Importantly, MPT0G013 exhibited antiangiogenic activities in *in vivo* Matrigel plug assays, inhibited tumor growth and up-regulated TIMP3 and p21 proteins in HCT116 mouse xenograft models. These data suggest potential therapeutic application of MPT0G013 for angiogenesis-related diseases such as cancer.

第一節 緒言

過去文獻指出，血管新生在胚胎發育、組織修復和血管疾病是必要不可或缺的步驟 (Ferrara *et al.*, 2005)，在過去幾十年來，血管研究專家先驅發現腫瘤的生長及轉移必須依賴血管生成。腫瘤會釋出血管新生蛋白，例如：vascular endothelial growth factor-A (VEGF-A) 及 basic fibroblast growth factor (bFGF)，並藉由促進微血管基底膜的降解來啟始血管新生，因此促進內皮細胞移行、增生以及血管管腔的形成 (Folkman, 2007)，所以，血管新生是重要且具發展性的抗腫瘤治療標的 (Miao *et al.*, 2012)。

過去的研究顯示血管新生的首要步驟是藉由 matrix metalloproteinase (MMP) family 將細胞外基質降解，因此，MMP 與 MMP 抑制蛋白在腫瘤的侵略、轉移、血管新生佔有重要的角色 (Lockhart *et al.*, 2003; Nagase *et al.*, 2006)。Tissue inhibitor of metalloproteinase-3 (TIMP3) 屬於 TIMP 家族中，廣泛分布表現的內生性的 MMP protease 抑制蛋白，與其他的 TIMP 家族的成員蛋白不同，TIMP3 是與細胞外基質結合的分泌型蛋白 (Pavloff *et al.*, 1992)。在正常生理中，TIMP3 是由眼睛脈絡膜內皮細胞及視網膜色素上皮細胞持續性製造分泌及表現 (Della *et al.*, 1996; Qi *et al.*, 2002)，由於 TIMP3 有效抑制 MMP 的活性，進而影響了生理組織的重塑以及藉由影響細胞生長、侵略及移行來調控發育過程 (Zeng *et al.*, 1998)。在病理情況下，TIMP3 被認為是強力的血管新生和腫瘤生長抑制蛋白 (BenEzra, 1997)，因此，在腫瘤中，常見 TIMP3 基因表現低下，並且藉由增加腫瘤中 MMP 的活性來促進腫瘤進展和轉移 (Shinojima *et al.*, 2012)。此外，TIMP3 的突變與 Sorsby's fundus dystrophy 疾病相關，其為一種黃斑部退化與黃斑下脈絡膜新生血管膜的疾病 (submacular choroidal neovascularization) (Langton *et al.*, 2000; Tabata *et al.*, 1998; Weber *et al.*, 1994)。

在本篇研究中，探討了 arylsulfonamide 衍生物 MPT0G013 (3-[1-(3,4-dimethoxy-benzenesulfonyl)-1H-indol-5-yl]-N-hydroxy-acrylamide) (Figure 4-1 A) 在體內與體外的抗血管新生作用，MPT0G013 過去曾被報導是一個強力的 HDAC 抑制劑 (Lai *et al.*, 2012)，然而，此化合物對腫瘤血管新生的作用尚未被證實，因此，本實驗以內皮細胞為對象，探討 MPT0G013 抑制血管新生的機轉。

第二節 結果

MPT0G013 在體外抑制血管新生

內皮細胞增生、管腔形成和移行都是血管新生必要的過程，此外，生長因子藉由促進內皮細胞有絲分裂而在其中占有相當重要的角色 (Folkman, 2007)。首先，本研究利用結晶紫染劑細胞增生實驗篩選了一系列 arylsulfonamide 衍生物的抗血管新生活性，將細胞在 EGM-2 medium 中處理此系列的化合物 72 小時後，利用結晶紫染劑並測量藥物對細胞生長的作用。從結果可知，在這些化合物中，MPT0G013 (Figure 4-1A) 具有最強抑制細胞增生的作用，GI_{50} = 0.14 ± 0.01 μM (Table 4-1 及 Figure 4-1B)，因此，本研究選擇 MPT0G013，在體內與體外進行更深入的抗血管新生活性和機轉之探討。為了觀察 MPT0G013 對於血管新生的影響，我們利用了一系列已建立之技術實驗；首先，利用 5-bromo-2-deoxyuridine (BrdU) incorporation assays 觀察影響細胞生長之 DNA 合成步驟。以 MPT0G013 處理 48 小時，BrdU-labeling reagent 在最後 18 小時加入，Figure 4-1C 顯示 MPT0G013 能以濃度相關性抑制內皮細胞 DNA 合成 (GI_{50} = 0.19 ± 0.02 μM)。接著，本研究利用 Matrigel assay 來評估 MPT0G013 對於類血管管腔網路形成的作用，將 MPT0G013 處理過 6 小時之 HUVECs 種在有 Matrigel-coated 的 96 well 孔盤，並以 MPT0G013 處理 18 小時，在 EGM-2 控制組中，能夠明顯誘導 HUVECs 的分化，形成高度分支狀態的類血管管腔結構，相反地，MPT0G013 以濃度相關性地明顯抑制管腔形成 (Figure 4-1D)，利用影像分析軟體 (Image-Pro® Plus) 在五個隨機的樣本區域計算及分析管腔長度，與 Figure 4-1D 左圖結果一致，MPT0G013 在 0.3、1、3 μM 的抑制程度分別為 44.3% ($P < 0.05$)、68.8% ($P < 0.005$)、90.6% ($P < 0.001$)。由於內皮細胞的趨化移行能力在芽生性血管新生 (angiogenic sprouting) 是必須的，我們利用 Boyden chamber assays 來觀察

MPT0G013 對於細胞移行的影響，將細胞以 MPT0G013 處理 6 小時後，能以濃度相關性抑制 EGM-2 誘導的細胞移行 (Figure 4-1E)。綜合以上結果，顯示 MPT0G013 在體外具有強力的抗血管新生作用。

MPT0G013 誘導 HUVECs 停滯在 G0/G1 期

為了探討 MPT0G013 是否能阻礙細胞增生，我們利用流式細胞儀檢測細胞週期，結果顯示，MPT0G013 能夠濃度及時間相關性地增加 HUVECs 在 G0/G1 期的細胞百分比，並減少 S/G2/M 期的細胞百分比 (Figure 4-2A, B and C)。接下來，本研究利用西方墨點法來探討 MPT0G013 對於 G0/G1 期調控蛋白表現的影響，MPT0G013 能以濃度及時間相關性地明顯增加 p21 (Waf1/Cip1) 及 p27 的蛋白表現，並減少 cyclin D1 的表現 (Figure 4-2D)。此外，Cyclin A 及 phosphorylated Rb 蛋白表現在 12 和 18 小時後都有明顯下降，然而，MPT0G013 對於 CDK4 並沒有明顯的影響。

MPT0G013 藉由增加 *TIMP3* 來抑制血管新生

為了進一步探討MPT0G013在體內及體外調控血管新生的作用機轉，首先，我們利用microarray analyses來評估在內皮細胞中，MPT0G013影響的血管新生相關的基因表現模式，在細胞處理MPT0G013 24小時後，Supplementary Figure 4-1顯示基因表現的聚類分析 (clustering analysis)，結果指出MPT0G013能夠增加抗血管新生基因的表現，例如：*IGFBP3*及*TIMP3*，並減少促進血管新生的基因，包括*ANGPT2*、*FGF2*、*Fltl*以及*PLAUR* (Table 4-2)。

為了確認microarray的結果，本研究利用quantitative RT-PCR assay以及西方墨點法來分析TIMP3的mRNA及蛋白表現。Figure 4-3A及4-3B顯示MPT0G013能顯著增加*TIMP3* mRNA的表現，約為控制組的18倍，並且以濃度及時間相關性地誘導TIMP3的蛋白表現。為了進一步探討MPT0G013增加TIMP3的表現是透過

transcriptional或是post-transcriptional levels，我們利用Click-iT® Nascent RNA Capture kit (Invitrogen, Carlsbad, CA, USA) 來標記新生成的RNA，並將其分離出來。Figure 4-3C表示MPT0G013能明顯誘導增加新合成的TIMP3 mRNA表現，約為控制組的14倍，此結果指出MPT0G013是透過轉譯活化 (transcriptional activation) 來誘導TIMP3的表現。為了確認TIMP3參與在MPT0G013抑制血管新生的作用中以及是否扮演重要的角色，本研究利用特定的siRNA使內皮細胞的TIMP3表現低下，轉染效率如Figure 4-3D所示。另外，Figure 4-3E左圖顯示在內皮細胞以MPT0G013處理18小時後能以濃度相關性抑制BrdU的嵌入，而siTIMP3卻能明顯的反轉MPT0G013抑制DNA合成的作用 (Figure 4-3E 右圖)；除此之外，siTIMP3也能夠明顯逆轉MPT0G013抑制細胞移行的作用 (Figure 4-3F)，過去的研究顯示TIMP3透過抑制VEGF的下游蛋白，PI3K/Akt及ERK訊息路徑，來調控血管新生 (Qi *et al.*, 2003) 。更甚者，與siCTL組別相較之下，Figure 4-3D顯示在處理MPT0G013的細胞中，TIMP3基因的沉默可以明顯增加Akt及ERK的磷酸化表現，這些結果發現指出MPT0G013是藉由增加TIMP3表現，並且抑制下游蛋白PI3K/Akt及ERK訊息路徑，造成血管新生的抑制。

MPT0G013 藉由增加 TIMP3 表現來抑制腫瘤血管新生及生長

本研究為了探討在體內 MPT0G013 對於血管新生生長因子的影響而使用了 Matrigel plug assays。首先，將 nu/nu mice 分成兩組，一組為生長因子、Matrigel 與 MPT0G013 (1 μM 及 10 μM) 或溶劑 (DMSO) 混合後，植入到小鼠皮下；另一組為只有生長因子與 Matrigel 混合，植入皮下，接著口服給予小鼠溶劑或 MPT0G013 (25 mg/kg/day 及 50 mg/kg/day)。七天後，將小鼠犧牲後取出 Matrigel plug，並且進行切片染色 hematoxylin and eosin (H&E) 以及免疫組織染色血管標記蛋白 CD31。接著，利用 NIH Image J software (Bethesda, MD) 定量 CD31-positive 的區域，在這些實驗結果中，從 Matrigel plug 外觀來看，Figure 4-4A

顯示口服 MPT0G013 以及 co-plug MPT0G013 都能明顯地抑制血管新生，與只含有生長因子的控制組比較之下，hematoxylin and eosin (H&E) 染色以及 CD31 染色也都顯示 MPT0G013 減少了 Matrigel plug 中的血管結構 (Figure 4-4B)。將這些取出的 Matrigel plug 進行血紅素含量測定來評估血管新生，MPT0G013 在 10 μM 濃度下抑制血管新生的程度約 96%，此外，口服給予 25 mg/kg/day 及 50 mg/kg/day MPT0G013 能達到明顯抗血管新生的作用，抑制程度約為控制組的 84%及 97% (Figure 4-4C)。

大量的研究已顯示腫瘤的生長必須仰賴血管新生，而抑制血管新生能夠減少腫瘤生長。在本研究中，我們利用大腸直腸癌 HCT116 細胞進行腫瘤異體移植實驗，進一步評估 MPT0G013 是否能直接影響腫瘤的生長及血管新生。在這實驗過程中，口服給予 MPT0G013 的小鼠沒有產生任何毒性症狀，包括體重減輕 (n = 8; Figure 4-4D 下圖)，表示小鼠可以忍受藥物處理。未給予藥物的控制組 HCT116 腫瘤體積在 15 天生長到超過 2,000 mm^3，然而在同一個時間點，給予 MPT0G013 (50 and 100 mg/kg/day) 的小鼠腫瘤體積則小於 1,000 mm^3 (Figure 4-4D 上圖)。為了更進一步探討 MPT0G013 對於腫瘤生長和血管新生的抑制作用，我們利用免疫組織染色血管新生來標記蛋白 CD31，與控制組相較之下，口服給予 MPT0G013 能明顯減少表現 CD31 的血管數目 (Figure 4-4E)。此外，以西方墨點法分析藥物誘導腫瘤內的標的蛋白，確鑿了 MPT0G013 在體內抗血管新生和抑制腫瘤生長的作用，Figure 4-4F 顯示來自於給予 MPT0G013 小鼠身上的腫瘤組織，與控制組比較之下，MPT0G013 能明顯增加 TIMP3 的蛋白表現，並且也伴隨著 p21 蛋白的增多。儘管血管新生對於腫瘤生長及轉移是必須的，且在調控腫瘤進展占有相當重要的角色 (Folkman, 2002) ，過去有文獻指出抗血管新生療法會增加癌細胞的侵略和轉移，小分子 receptor tyrosine kinase 抑制劑 Sunitinib 以及 anti-VEGFR2 antibody DC101 雖然皆具有抑制原位癌生長的作用，在一些案例中卻會促進腫瘤的轉移 (Ebos *et al.*, 2009; Paez-Ribes *et al.*, 2009)。

因此，本研究使用 lung tumor metastases model 來評估在體內 MPT0G013 對於癌細胞轉移的影響。首先將大腸癌細胞 HCT-116 注射至 severe combined immunodeficiency (SCID) mice 的尾靜脈，在癌細胞接種後，立刻開始口服給予溶劑或 MPT0G013 (25 mg/kg) ，每兩天一次，在實驗終點，將小鼠犧牲並取出肺臟以評估轉移。與控制組相較之下，給予 25 mg/kg MPT0G013 明顯減少了肺臟表面的轉移數目及程度 (Figure 4-4G, 4H)，並且也減少了肺臟的重量 (Figure 4-4I)。綜合以上結果，MPT0G013 在體內及體外能夠藉由增加抗血管新生蛋白 TIMP3 的表現，阻礙生長因子誘導的血管新生，而造成腫瘤生長的抑制。

第三節 討論

TIMP3 在 1997 首先被證實在體內及體外是血管新生的抑制性蛋白 (BenEzra, 1997)，而許多年以來，TIMPs 被認為是透過抑制 MMP 的活性來調控血管新生 (Akahane *et al.*, 2004; Hoegy *et al.*, 2001)。然而，最近有越來越多文獻指出，TIMPs 蛋白的眾多功能與其本身抑制 MMP 活性的作用是獨立不相關的。此外，TIMP3 抑制血管新生的作用也被證實主要透夠抑制 VEGF 與 VEGFR 結合，來達到抑制 VEGF 誘導細胞增生和移行的作用，與本身 MMP 抑制活性無關 (Qi *et al.*, 2003)。在小鼠胚胎纖維母細胞 mouse embryonic fibroblasts (MEFs) 失去 *TIMP3* 基因的表現，被認為會提升 hepatoprotective EGFR ligand shedding 以及其下游蛋白 ERK1/2 的磷酸化 (Murthy *et al.*, 2010)，此外，利用 lentivirus 使間質細胞 (mensenchymal cells) 過度表現 TIMP3 會導致 ERK 和 Akt 磷酸化的減少 (Koers-Wunrau *et al.*, 2013) ，而在許多不同種類的癌症中，*TIMP3* 經常表現下降 (Gu *et al.*, 2008; Shinojima *et al.*, 2012)。此外，眾多文獻指出生長因子活化的 PI3K/Akt 及 Ras/Raf/ERK 訊息路徑，在正常細胞 G1/S 期的轉換、細胞增生及內皮細胞移行中，不僅僅只是參與，更是必要的調控訊息 (Jiang *et al.*, 2008; Skeen *et al.*, 2006; Ussar *et al.*, 2004)。臨床前的研究顯示 PI3K/Akt 及 ERK 訊息路徑的抑制劑是強力的抗血管新生藥物，並且能夠抑制腫瘤生長 (Murphy *et al.*, 2006; Wang *et al.*, 2012a)。在本研究中，siTIMP3 明顯地反轉 MPT0G013 抑制 Akt 和 ERK 磷酸化的作用，表示 TIMP3 是 MPT0G013 重要的標靶蛋白，縱使 Table 4-2 顯示 MPT0G013 減少了許多血管新生相關的基因表現，siTIMP3 能明顯拯救 MPT0G013 抑制的 DNA 合成及細胞移行，所以推論 MPT0G013 所誘導增加的 TIMP3 在所發現的抗血管新生作用中，扮演了主要的角色。我們也發現了 MPT0G013 些微的減少 MMP-2 和 MMP-9 的蛋白表現，然而，由於在 boyden

chamber 細胞移行實驗中，siTIMP3 能增加內皮細胞移行，穿過有雙面明膠塗層的 membranes，因此，我們推測對於 MPT0G013 抑制 MMPs 作用的貢獻，屬於 MPT0G013 較為次要的作用。

Microarray 的分析顯示 MPT0G013 誘導了許多不同的血管新生的基因表現，包括 *IGFBP3* 以及 *TIMP3*。其中，insulin-like growth factor binding-protein 3 (IGFBP3) 在抑制 VEGF 誘導的內皮細胞生長以及抗血管新生作用之角色，已經在過去文獻證實 (Franklin *et al.,* 2003; Iwatsuki *et al.,* 2005)。本研究利用 quantitative RT-PCR 確認 MPT0G013 對於 IGFBP3 mRNA 表現的影響，發現 MPT0G013 能誘導 IGFBP3 mRNA 增加約為控制組的七倍左右 (Supplementary Figure 4-2A)。然而，在 BrdU incorporation assays 中，siIGFBP3 只能部分反轉 MPT0G013 造成 DNA 合成抑制的作用 (Supplementary Figure 4-2B)。因此，我們推測 IGFBP3 也有貢獻於 MPT0G013 抗血管新生的作用，但是扮演相較於 TIMP3 次要的角色。

過去有研究報導 MPT0G013 是一個新穎的 HDAC 抑制劑，並且在體內及體外能抑制腫瘤生長 (Lai *et al.,* 2012)。本研究也確認了 MPT0G013 抑制 HDAC 活性之強度大於 HDAC 抑制劑 SAHA (Supplementary Figure 4-3 and Supplementary Table 4-1)，此外，MPT0G013 在內皮細胞及腫瘤中，都能明顯增加 TIMP3 mRNA 及蛋白質表現，雖然 SAHA 與 MPT0G013 具有相似 HDAC subtypes 抑制活性的模式，但是 SAHA 難以在體外及體內誘導 TIMP3 基因或蛋白質的表現 (Supplementary Figure 4-4) 。因此，本研究推測此作用是 MPT0G013 特有新穎的作用。

本研究利用 SRB assay 來評估 MPT0G013 對於各種不同人類癌細胞生長的作用，Supplementary Table 4-2 顯示 MPT0G013 能抑制 A549、HCT-116、Hep3B、MDA-MB-231、PC-3 以及 SK-OV-3 的生長，GI_{50} 依序分別為 0.44、0.34、0.57、0.32、0.42、0.35 μM，由於 MPT0G013 在癌細胞中的 GI_{50} 約為在內皮細胞中的

三倍左右，因此，在腫瘤異體移植實驗中，本研究無法排除 MPT0G013 同時對於癌細胞的影響。

綜合以上發現，以我們目前所探討的結果可知，本研究是首先發現新穎的抗血管新生藥物 MPT0G013，在內皮細胞中誘導腫瘤抑癌基因 (tumor suppressor gene) TIMP3 的表現，而能夠抑制其下游 PI3K/Akt 及 ERK 的訊息路徑。利用 Matrigel plug assays 以及腫瘤異體移植實驗，本研究證實了 MPT0G013 在體內抑制腫瘤血管新生的作用，此外，腫瘤組織西方墨點法分析顯示口服給予小鼠 MPT0G013 能明顯增加 p21 及 TIMP3 蛋白的表現。因此，目前的結果表示 MPT0G013 有潛力作為一個新穎的候選藥物，來治療血管新生相關的疾病，例如癌症。

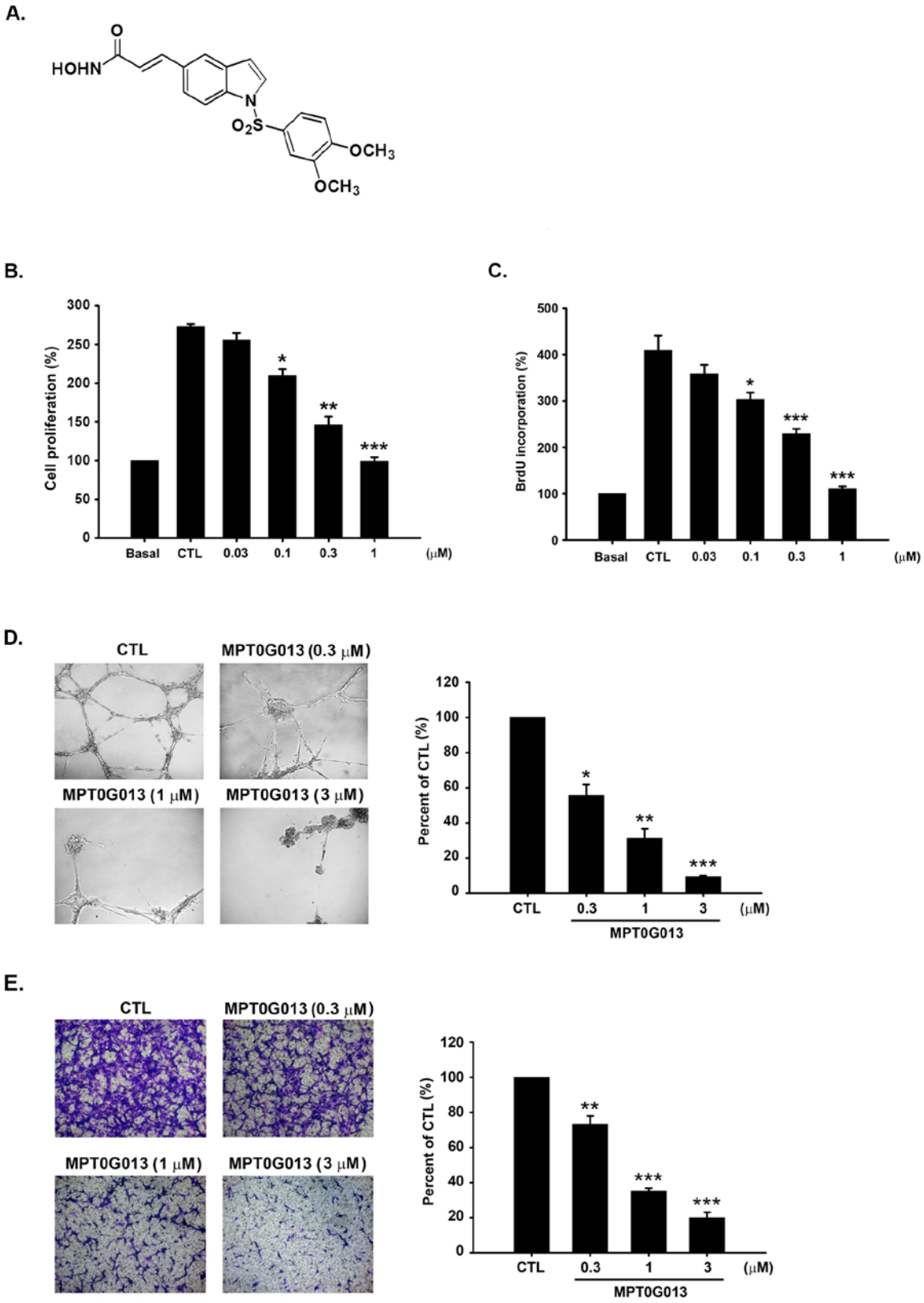

Figure 4-1. MPT0G013 inhibits angiogenesis *in vitro*.

A, Chemical structure of MPT0G013. B, HUVECs were treated without (control,

CTL) or with MPT0G013 at the indicated concentrations in EGM-2 medium. Inhibition of cell proliferation was measured by crystal violet assay after 72 hrs. C, DNA synthesis was determined by BrdU incorporation assay. In B and C, 100% = OD. D, *Left panel*, representative photographs of tube formation of HUVECs treated with or without MPT0G013 on matrigel under microscope (magnification is X100). *Right panel*, quantitative analysis of the total tube length by Image analysis software (Image-Pro® Plus). For total tube length 100% = μm. E, *Left panel*, inhibitory effect of MPT0G013 on cell migration using a boyden chamber assay. *Right panel*, quantitative analysis of the migrated cell numbers. 100% = number of migrating cells. Data represent the mean ± SEM from three independent experiments. * $P < 0.05$, ** $P < 0.01$ and *** $P < 0.001$ versus control.

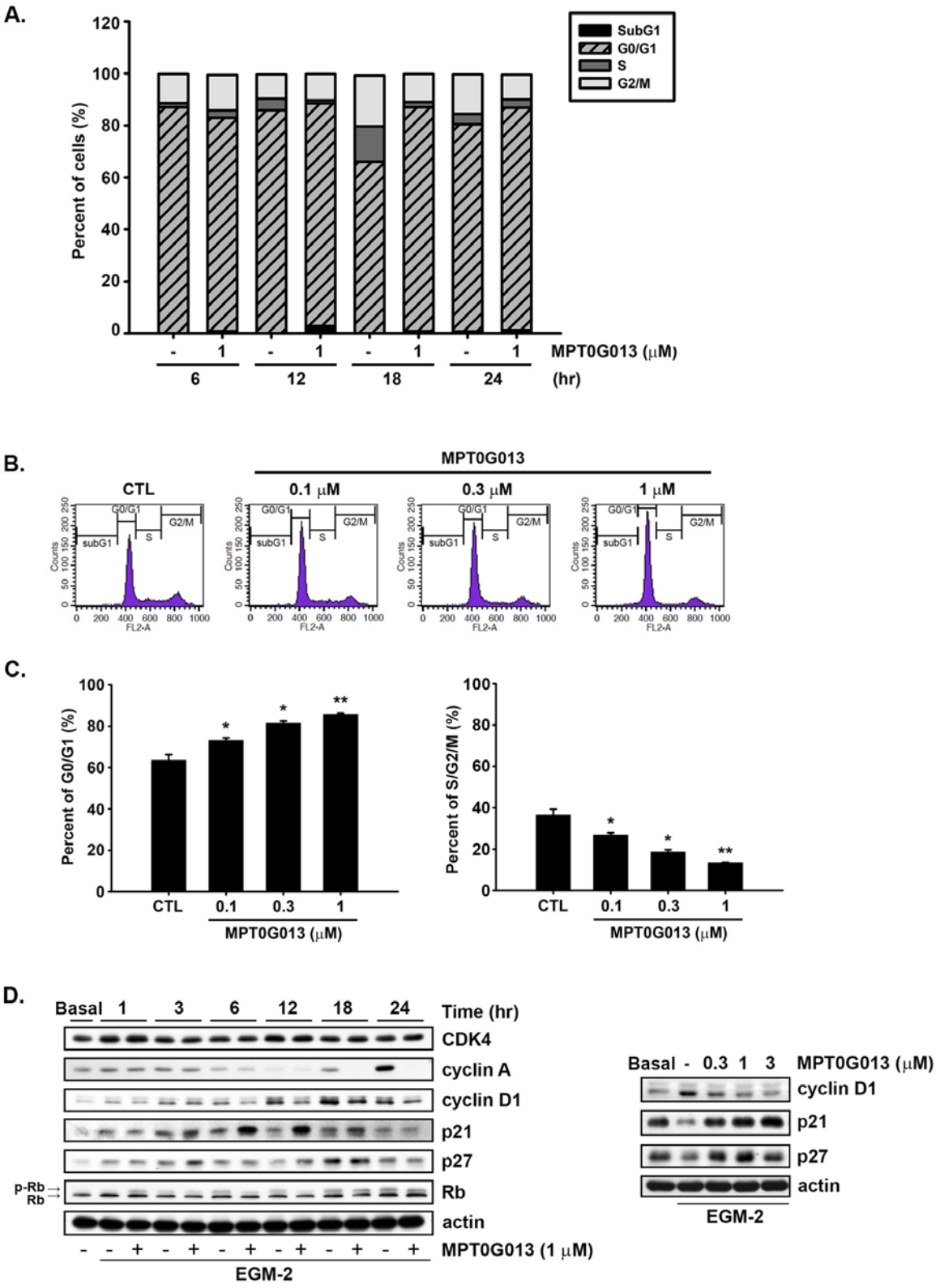

Figure 4-2. MPT0G013 induces cell cycle arrest in the G0/G1 phase.

A, After starvation for 24 h, HUVECs were then treated without (control, CTL) or

with MPT0G013 (1 μM) for the indicated time interval. After labeling with propidium iodide, DNA content was analyzed by flow cytometry. B, HUVECs were treated with or without the indicated concentrations of MPT0G013 for 18 h and were analyzed by flow cytometry for cell cycle distribution. C, Quantification of cell population in G0/G1 and S/G2/M phase. In A, B and C, 100% = percent of cells. D, HUVECs incubated in EGM-2 medium were treated with or without MPT0G013 at indicated times. Cells were harvested and analyzed protein expression by western blot. Data represent the mean ± SEM from three independent experiments. * $P < 0.05$ and ** $P < 0.01$ versus control.

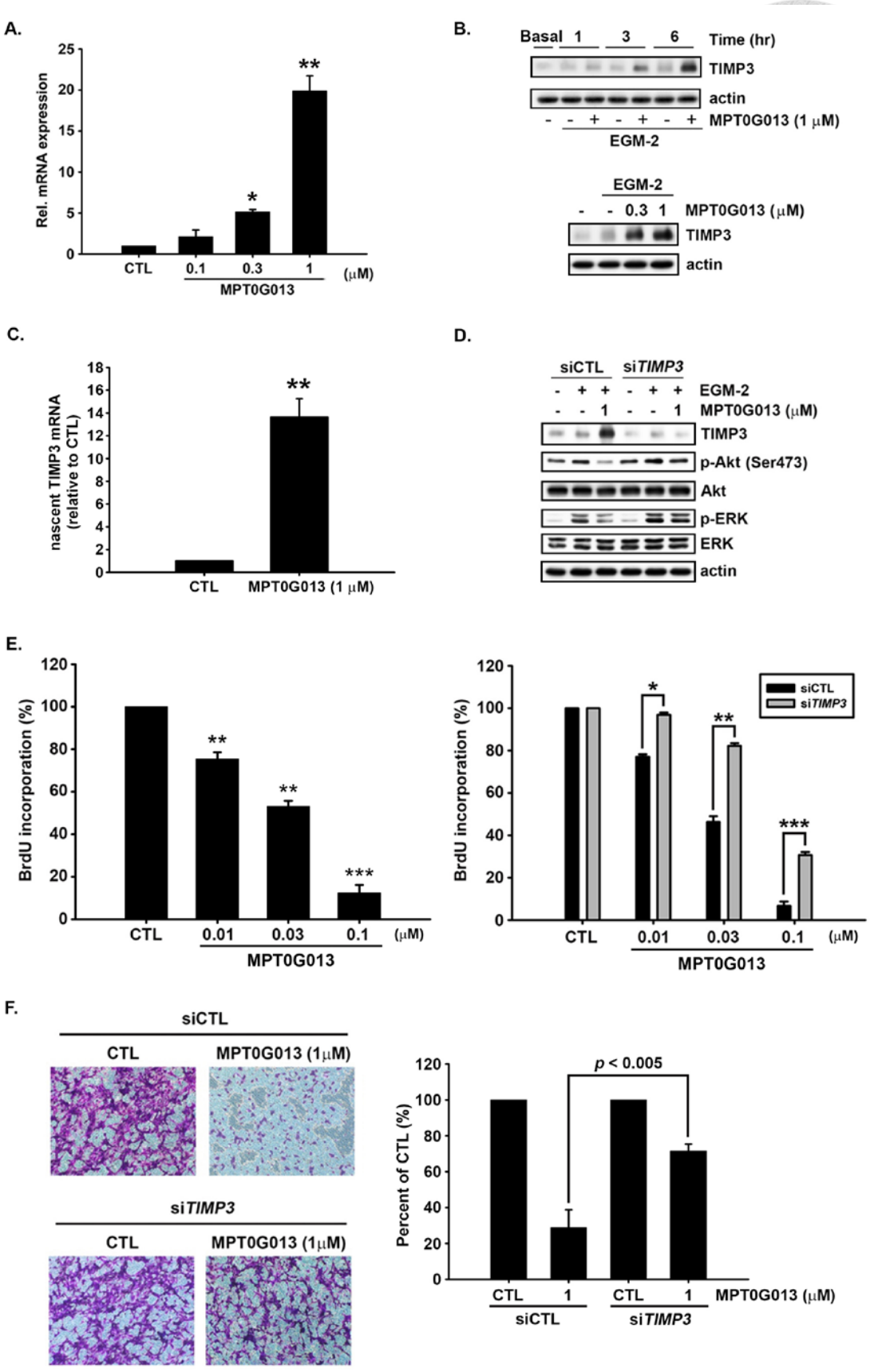

Figure 4-3. Induction of TIMP3 expression by MPT0G013 inhibits angiogenesis.

A, Quantitative RT-PCR analysis of TIMP3 mRNA expression in endothelial cells treated with or without MPT0G013 for 6 h. B, *Top panel*, Western blot showing induction of TIMP3 protein expression by MPT0G013 at indicated times. *Bottom panel*, The dose-dependent induction of TIMP3 protein in HUVECs treated with or without MPT0G013 at indicated concentrations for 6 h. C, Nascent RNA was labeled and isolated from HUVECs using Click-iT Nascent RNA Label and Capture Kit (Invitrogen), and then the nascent TIMP3 mRNA was measured using Quantitative RT-PCR. In A and C, 100% = $2^{(-C_T)}$. D, Western blot showing that silencing TIMP3 reversed the inhibition effect of phosphorylated Akt and ERK induced by MPT0G013. E, BrdU incorporation assay. *Left panel*, MPT0G013 dose-dependently inhibited BrdU incorporation after 18 h incubation. *Right panel*, HUVECs tranfected with siTIMP3 increased DNA synthesis after treatment with MPT0G013 for 18 h. F, *Left panel*, boyden chamber chemotaxis assay. Silencing TIMP3 in HUVES rescued the inhibitory effect of MPT0G013 on migration. *Right panel*, quantitative analysis of the migrated cell numbers. Sodium citrate was used to solve crystal violet and then detected absorbance with 550 nm wavelength. In E and F, 100% = OD. Data represent the mean ± SEM from three independent experiments. * $P < 0.05$, ** $P < 0.005$ and *** $P < 0.001$ versus control.

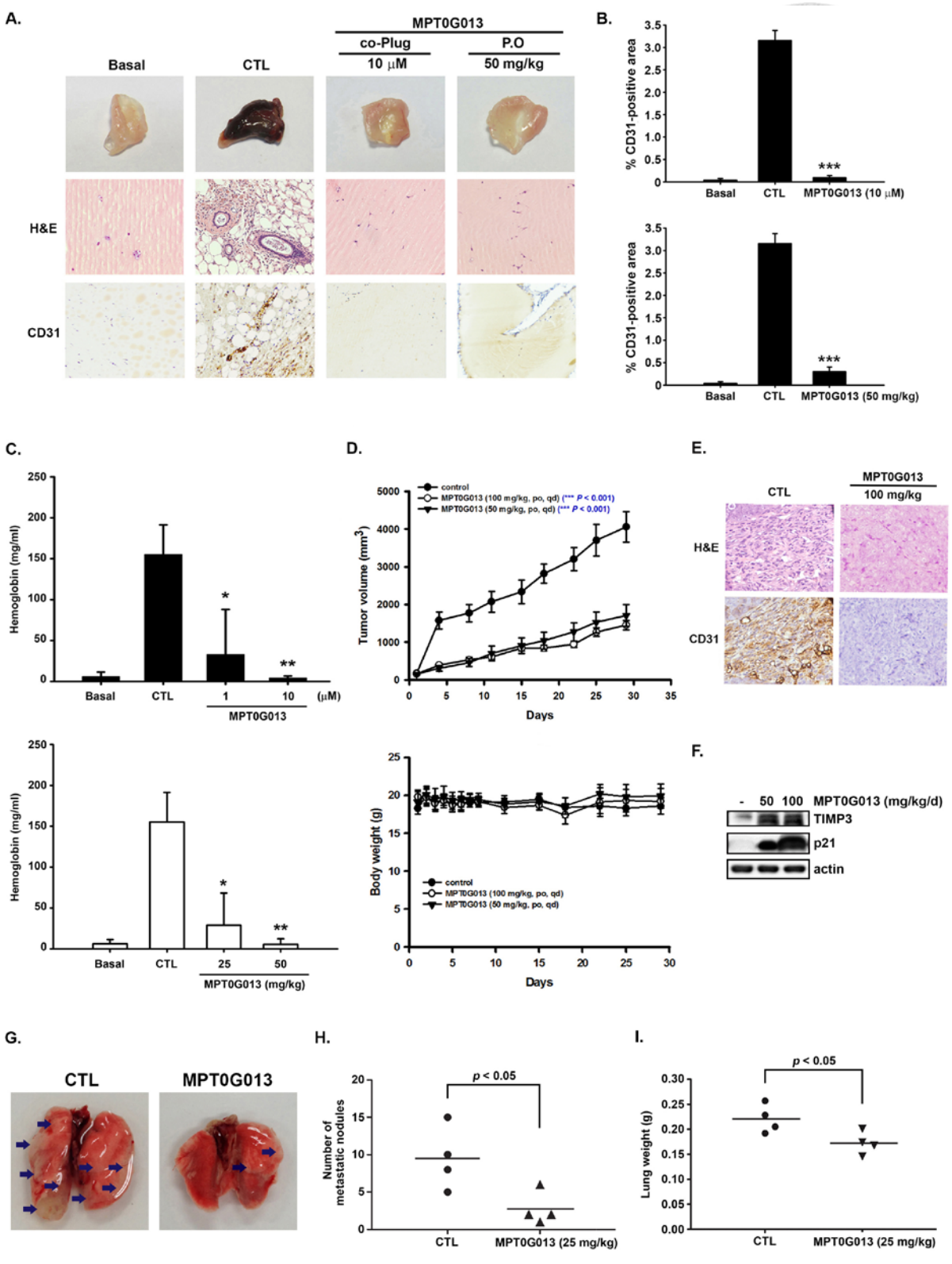

Figure 4-4. MPT0G013 inhibits the *in vivo* angiogenesis and tumor growth.

A, Nude mice were injected subcutaneously with matrigel mixed without (control, CTL) or with MPT0G013 (1 μM and 10 μM) or oral (p.o.) administration with

MPT0G013 (50 mg/kg/d). Plugs were excised from the mice after a week and photographed. Sections of H&E stained Matrigel plugs were examined by light microscopy. The Matrigel plugs were subjected to CD31 immunohistochemical staining. *Brown color,* CD31-positive blood vessels. B, Quantification of CD31-positive area. 100% = pixels. The data are representative of five randomly chosen independent fields using the National Institutes of Health (NIH) Image J software (Bethesda, MD). ***, $p < 0.001$ as compared with the control group. C, Quantification of the hemoglobin content of matrigel plugs by spectrophotometer measured at 540 nm. 100% = OD. Data represent the mean ± SEM from five independent experiments. * $P < 0.05$ and ** $P < 0.005$ versus control. D, Effect of MPT0G013 on the growth of HCT116 colon tumor xenografts in BALB/c nude mice. *Top panel,* Tumor growth is presented as the mean tumor volume (mm^3) ± S.E. Tumor volume was determined by caliper measurements and was calculated as the product of 1⁄2 x length x $width^2$. *Bottom panel,* body weight (g) of the mice. Each value represents the mean of at least five animals. ***, $p < 0.001$ as compared with the control group. E, CD31-stained sections of blood vessels from a xenograft tumor. *Brown color,* CD31-positive blood vessels. F, Western blot analysis of TIMP3 and p21 expression in tumor tissue. G, MPT0G013 reduced lung cancer cell metastasis *in vivo*. Proliferating HCT-116 cells were injected into the lateral tail vein of SCID mice that received vehicle or MPT0G013 (25mg/kg) by oral administration every other day (n = 4 in each group). Representative images of metastatic lung nodules from mice after treated without (control, CTL) or with MPT0G013 for 6 weeks. Arrows indicate surface lung nodules. H, Macroscopic lung surface nodules (Φ > 1 mm) were counted under a dissected microscope (Optima) in each group. Black bar represent the average. I, Quantification of gross weight of individual lungs.

Table 4-1. Anti-proliferative effects of MPT0G013 and several synthetic arylsulfonamide derivative compounds in HUVECs.

Compound	GI_{50} (μM ± SD)
MPT0G013	0.14 ± 0.01
MPT0G017	0.60 ± 0.05
MPT0G018	0.98 ± 0.28
MPT0G019	1.40 ± 0.14
MPT0G031	4.63 ± 0.15
MPT0G032	3.64 ± 0.25
MPT0G033	4.34 ± 0.22
MPT0G034	6.49 ± 0.12
MPT0G036	1.45 ± 0.07
MPT0G037	2.03 ± 0.06
MPT0G038	15.75 ± 0.08
MPT0G039	14.45 ± 0.09
MPT0E014	0.47 ± 0.02
MPT0E028	0.15 ± 0.01

Mean ± SD (n = 3)

Table 4-2. Angiogenic-related genes down-regulated and up-regulated by MPT0G013 in endothelial cells.

Accession no.	Gene name	Symbol	Log_2 ratio	*P* value
NM_001118887.1 *	angiopoietin 2	*ANGPT2*	-5.070807	1.775799E-33
NM_003868.1	fibroblast growth factor 16	*FGF16*	-3.335650	1.230107E-24
NM_001005377.2 **	plasminogen activator, urokinase receptor	*PLAUR*	-2.804592	6.221146E-19
NM_002632.4	placental growth factor	*PGF*	-2.720818	2.332189E-14
NM_002006.4	fibroblast growth factor 2 (basic)	*FGF2*	-2.678274	5.808877E-16
NM_002658.3 ***	plasminogen activator, urokinase	*PLAU*	-2.296566	1.236864E-6
NM_001160031.1 #	fms-related tyrosine kinase 1 (vascular endothelial growth factor receptor)	*FLT1*	-1.494546	8.563744E-08
NM_000245.2 ¥	met proto-oncogene (hepatocyte growth factor receptor)	*MET*	-1.305731	2.999884E-7
NM_001146.3 £	angiopoietin 1	*ANGPT1*	-1.137254	0.0004765304
NM_001024847.2 †	transforming growth factor, beta receptor II (70/80kDa)	*TGFBR2*	-1.055459	5.674958E-7
NM_203339.1 ‡	clusterin	*CLU*	1.844688	2.429692E-6
NM_000362.4	TIMP metallopeptidase inhibitor 3	*TIMP3*	3.415408	1.198377E-22
NM_000598.4 §	insulin-like growth factor binding protein 3	*IGFBP3*	4.038052	3.817849E-34

HUVECs were treated with 10 μM MPT0G013 for 24 hr, then the total RNA was extracted for microarray analysis. Each unique splice variant of the gene was also tested. Different accession numbers are given.

* ANGPT2: NM_001147.2,NM_001118888.1
** PLAUR: NM_002659.3
*** PLAU: NM_001145031.1
# FLT1: NM_001160030.1
¥ MET: NM_001127500.1
£ ANGPT1: NM_001199859.1
† TGFBR2: NM_003242.5
‡ CLU: NM_001831.2,NM_001171138.1
§ IGFBP3: NM_001013398.1

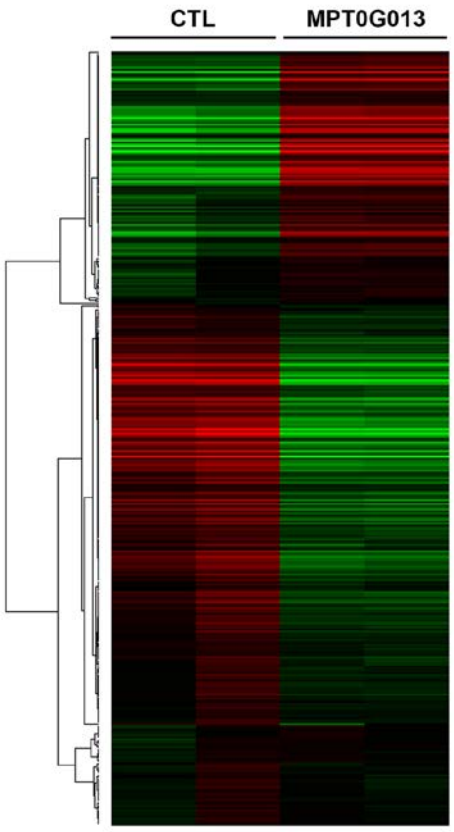

Supplementary Figure 4-1. Hierarchical clustering analysis of microarray data comparing MPT0G013-treated group and untreated in HUVECs. Total RNA of HUVECs treated with or without 10 μM MPT0G013 for 24 hours was extracted and analyzed by Human OneArray. Genes significantly different, with $P < 0.05$ after the treatment, were pooled and used to generate heat maps. Up-regulated and downregulated genes are represented in red and green, respectively.

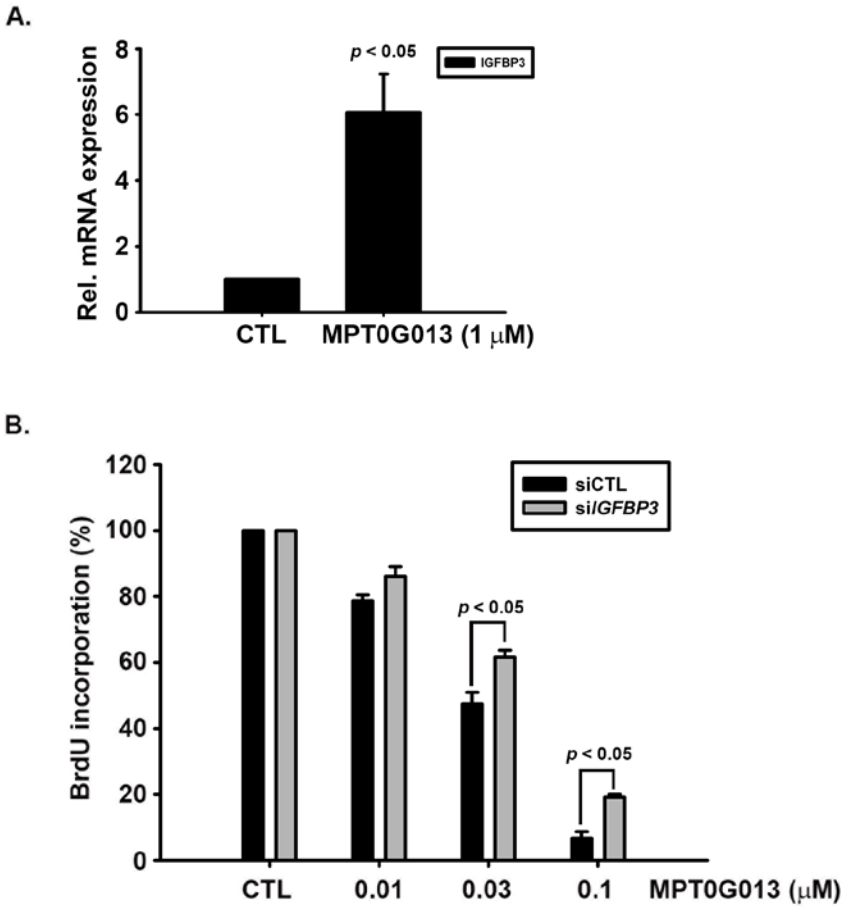

Supplementary Figure 4-2. A, Quantitative RT-PCR analysis of IGFBP3 mRNA expression in endothelial cells treated without (control, CTL) or with MPT0G013 for 12 hr. B, BrdU incorporation assay. HUVECs tranfected with siIGFBP3 slightly increased DNA synthesis after treated with MPT0G013 for 18 hr.

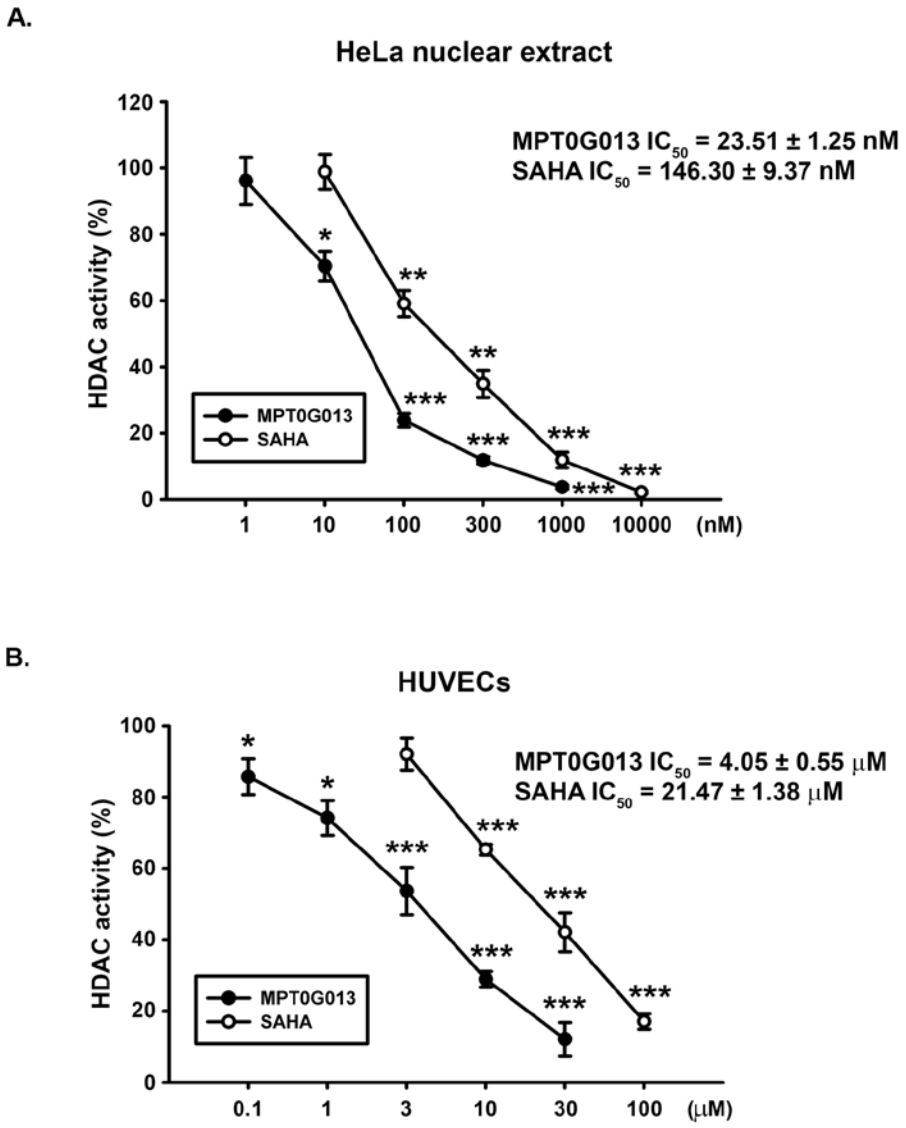

Supplementary Figure 4-3. HDAC assay with HeLa or HUVECs nuclear extract was carried out by using the HDAC Fluorescent Activity Assay Kit (BioVision, CA, USA) according to manufacturer's instructions. A, Inhibitory effects of pan-HDAC activity in MPT0G013- and SAHA-treated HeLa nuclear extract protein. B, Inhibition of pan-HDAC activity by MPT0G013 and SAHA. After treated with the indicated concentrations of MPT0E013 or SAHA for 24 h, the nuclear proteins from HUVECs were extracted to analysis the inhibition of pan-HDAC activity. Data represent the mean ± SEM from three independent experiments. * $P < 0.05$, ** $P < 0.01$ and *** $P < 0.001$ versus control.

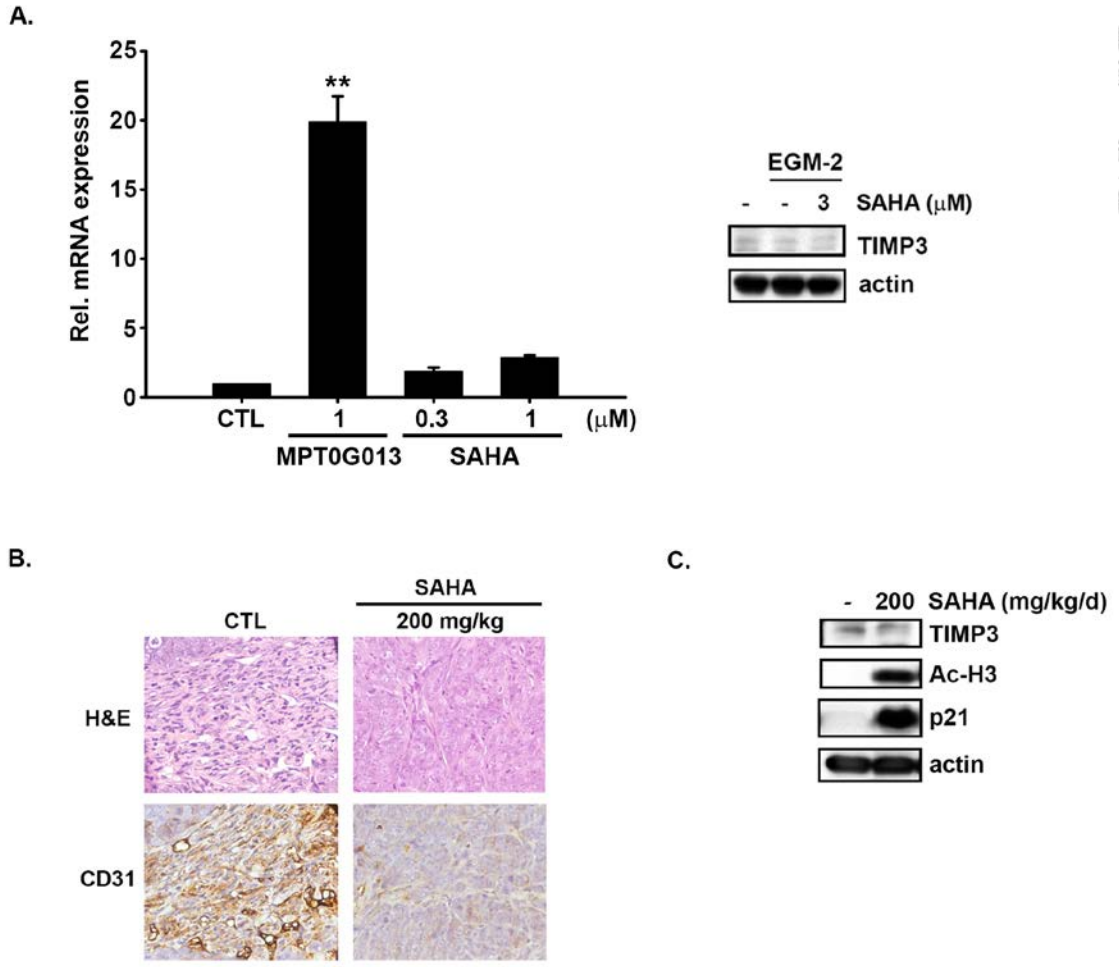

Supplementary Figure 4-4

A, *Left Panel,* quantitative RT-PCR analysis of TIMP3 mRNA expression in endothelial cells treated without (control, CTL) or with MPT0G013 and SAHA for 6 hr. *Right panel,* Western blot showing induction of TIMP3 protein expression by SAHA at indicated concentration. B, CD31-stained sections of blood vessels from a xenograft tumor. *Brown color,* CD31-positive blood vessels. C, Western blot analysis of TIMP3, Ac-H3 and p21 expression in tumor tissue.

Supplemental Table 4-1. Inhibitory effect on HDAC activity by MPT0G013 and SAHA.

Compound	HDAC1	HDAC2	HDAC8	HDAC4	HDAC6
	Class I			Class IIa	Class IIb
	IC_{50} (nM ± SE)				
MPT0G013	56.7 ± 2.5	125.9 ± 5.1	3322.8 ± 480.5	>10000	56.5 ± 2.6
SAHA	118.4 ± 11.1	506.5 ± 35.6	>10000	>10000	113.5 ± 2.8

Supplemental Table 4-2. Anti-proliferative effects of MPT0G013 in various cancer cell lines.

Cell line	GI_{50} (μM ± SD)
A549	0.44 ± 0.029
HCT-116	0.34 ± 0.027
Hep3B	0.57 ± 0.049
MDA-MB-231	0.32 ± 0.014
PC-3	0.42 ± 0.014
SK-OV-3	0.35 ± 0.019

Mean ± SD (n = 3)

第五章

口服活性微管標靶藥物MPT0B271單獨及與erlotinib合併使用於治療人類非小型細胞肺癌之探討

Orally active microtubule-targeting agent, MPT0B271, for the treatment of human non-small cell lung cancer, alone and in combination with erlotinib

Cell Death Dis. 2014 Apr 10;5:e1162.

中文摘要

目前被用來治療癌症的taxanes及vinca生物鹼等微管結合藥物，缺點為抗藥性的產生及必須透過靜脈注射投與，因此迫切需要研發新的藥物，MPT0B271 (N-[1-(4-Methoxy-benzenesulfonyl)-2,3-dihydro-1H-indol-7-yl]-1-oxy-isonicotinamide) ，是一個口服生體可用率佳的微管標靶全合成藥物，在體內及體外具有強力的抗癌效果，微管聚合實驗及免疫螢光染色實驗顯示MPT0B271導致微管的去聚合，MPT0B271在nanomolar濃度下就能抑制許多癌細胞株生長及降低存活率，這些細胞株包括multidrug-resistant癌細胞株NCI/ADR-RES。進一步利用流式細胞儀分析rhodamine-123 (Rh-123) 的輸出及利用calcein acetoxymethyl ester (calcein AM) assay，發現MPT0B271不是p-glycoprotein (p-gp) 的受質。此外，MPT0B271也會誘導細胞G2/M期停滯，並增加cyclin B1、p-Thr161 Cdc2/p34、serine/threonine kinases polo-like kinase 1、aurora kinase A和B以及減少Cdc25C、p-Tyr15 Cdc2/p34蛋白表現。MPM2的增加及cyclin B1轉移至核內也表示M期的週期停滯。再者，MPT0B271能濃度相關性地誘導細胞凋亡，並減少Bcl-2、Bcl-xL和Mcl-1，增加caspase-3、caspase-7和poly (ADP-ribose) polymerase (PARP) 的切割。最後，本研究發現在體內及體外，與單獨給藥相較之下，MPT0B271合併erlotinib能明顯抑制人類非小細胞肺癌A549細胞的生長，這些結果證實MPT0B271是一個具有潛力治療各種癌症的新穎微管結合藥物。

英文摘要

Microtubule-binding agents, such as taxanes and vinca alkaloids, are used in the treatment of cancer. The limitations of these treatments, such as resistance to therapy and the need for intravenous administration, have encouraged the development of new agents. MPT0B271 (N-[1-(4-Methoxy-benzenesulfonyl)-2,3-dihydro-1H-indol-7-yl] -1-oxy-isonicotinamide), an orally active microtubule-targeting agent, is a completely synthetic compound that possesses potent anticancer effects in vitro and in vivo. Tubulin polymerization assay and immunofluorescence experiment showed that MPT0B271 caused depolymerization of tubulin at both molecular and cellular levels. MPT0B271 reduced cell growth and viability at nanomolar concentrations in numerous cancer cell lines, including a multidrug-resistant cancer cell line NCI/ADR-RES. Further studies indicated that MPT0B271 is not a substrate of p-glycoprotein (p-gp), as determined by flow cytometric analysis of rhodamine-123 (Rh-123) dye efflux and the calcein acetoxymethyl ester (calcein AM) assay. MPT0B271 also caused G2/M cell-cycle arrest, accompanied by the up-regulation of cyclin B1, p-Thr161 Cdc2/p34, serine/threonine kinases polo-like kinase 1, aurora kinase A and B and the downregulation of Cdc25C and p-Tyr15 Cdc2/p34 protein levels. The appearance of MPM2 and the nuclear translocation of cyclin B1 denoted M phase arrest in MPT0B271-treated cells. Moreover, MPT0B271 induced cell apoptosis in a concentration-dependent manner; it also reduced the expression of Bcl-2, Bcl-xL, and Mcl-1 and increased the cleavage of caspase-3 and -7 and poly (ADP-ribose) polymerase (PARP). Finally, this study demonstrated that MPT0B271 in combination with erlotinib significantly inhibits the growth of the human non-small

cell lung cancer A549 cells as compared with erlotinib treatment alone, both in vitro and in vivo. These findings identify MPT0B271 as a promising new tubulin-binding compound for the treatment of various cancers.

第一節 緒言

微管是細胞骨架的主要成分，並且在細胞分裂、細胞內運輸、細胞活動佔有必要的角色 (Hawkins *et al.*, 2010) ，許多臨床上重要的微管標靶藥物，例如taxanes及vinca生物鹼，能夠與微管結合，因此改變其正常動態平衡並導致微管的穩定或去穩定化 (Stanton *et al.*, 2011) ，破壞微管的構型會誘導細胞週期停滯在G2/M期，並步入細胞凋亡或非凋亡死亡路徑 (Mollinedo *et al.*, 2003; Schmidt *et al.*, 2007)。

即使微管標靶藥物在臨床上被用來治療癌症病人，這些藥物仍有實質上的缺陷：抗藥性的產生(Perez, 2009) 。抗藥性產生方式可能是內生性的，首次化療就無反應而失敗，或是首次化療有效，但第二輪化療失敗 (Gottesman, 2002)。不論哪一種方式，都造成腫瘤難以治療和棘手。Taxanes及其他微管標靶藥物最常見的抗藥性是過度表現輸出幫浦p-glycoprotein (p-gp)/ multidrug resistance (MDR) protein (Dumontet *et al.*, 1999) ，臨床上使用的微管標靶藥物paclitaxel及vinblastine都是p-gp的受質，因此，研發能夠躲避這些抗藥性機轉的微管標靶藥物是迫切需要的，而能夠治療帶有抗藥性腫瘤的病人 (Fojo *et al.*, 2007; Kavallaris, 2010; Murray *et al.*, 2012)，此外，另一個缺陷是目前這些藥物必須使用靜脈注射給予，而導致過敏感反應 (Gelderblom *et al.*, 2001; Koolen *et al.*, 2010)。

在本篇研究中，我們利用非小細胞肺癌細胞株，探討MPT0B271 (N-[1-(4-methoxy-benzenesulfonyl)-2,3-dihydro-1H-indol-7-yl]-1-oxy-isonicotinamide) 的抗癌效果，在體內及體外，MPT0B271能抑制許多癌細胞株的生長及存活率，破壞微管的聚合，並且能躲避p-gp導致的抗藥性，此外，MPT0B271與erlotinib合併使用有更強的抗癌效果，進一步證實MPT0B271是一個具有潛力的抗癌候選藥物。

第二節 結果

MPT0B271 抑制細胞微管聚合

在 *in vitro* polymerization assay 中，MPT0B271 (Figure 5-1A) 能夠抑制微管聚合 (Figure 5-1B)，此作用效果與微管去穩定藥物 (microtubule-destabilizing agents) colchicine 及 vincristine 相似；另外使用微管穩定藥物 (microtubule-stabilizing agents) paclitaxel 能促進微管聚合 (Figure 5-1B)。再者，利用免疫螢光染色與共軛焦顯微鏡來觀察 MPT0B271 對於細胞內的微管排列與分布，Figure 5-1C 顯示 MPT0B271 能破壞 A549 細胞的微管細胞骨架，這些結果顯示 MPT0B271 在癌細胞中會造成微管的去聚合。

MPT0B271 在 *in vivo* 中是口服生體可用的腫瘤生長抑制劑

Figure 5-1D 顯示 CD-1 老鼠靜脈注射及口服 MPT0B271 後，體內血液濃度與時間的關係。結果顯示，MPT0B271 口服的半衰期為 2 小時，相較靜脈注射較長，並且絕對口服生體可用率為 26%。當口服給予老鼠 20 mg/kg MPT0B271，能被快速吸收並且達到最大血中濃度只需要 15 分鐘，MPT0B271 的平均 Cmax 及 $AUC_{(0\text{-}27)}$ 分別是 402 ng/ml 及 558 ng·h/ml，進一步利用人類 NSCLC cell line A549 的腫瘤異體移植實驗，來評估 MPT0B271 在 *in vivo* 的作用，Figure 5-1E 顯示口服給予 MPT0B271 能造成劑量相關性地腫瘤生長抑制作用，並且不影響小鼠的體重 10%。

MPT0B271 在 *in vitro* 抑制癌細胞生長及誘導細胞毒殺

利用Sulforhodamine B (SRB) assay來評估MPT0B271抑制癌細胞生長的作用，Figure 5-2A 顯示 MPT0B271 在 A549、AsPC-1、HCT116、Hep3B、

MDA-MB-231、PC3、SKOV3以及NCI/ADR-RES細胞的GI_{50}分別為27.9、23.3、21.0、35.5、19.0、20.4、18.5及18 nM。利用3-(4,5-dimethylthiazol-2-yl)-2,5-diphenyltetrazolium bromide (MTT) assay評估MPT0B271，發現能顯著抑制人類癌細胞株的存活率，IC_{50}範圍在21-73 nM (Figure 5-2B)。

Paclitaxel及vincristine對於NCI/ADR-RES細胞生長的作用

從SRB及MTT assay中，發現MPT0B271在multidrug-resistant cancer cell line NCI/ADR-RES同樣具有強抑制效果，反之，paclitaxel及vincristine在NCI/ADR-RES細胞中的GI_{50}分別是7.67 ± 1.23 μM及8.16 ± 0.85 μM (Figure 5-2C)，表示MPT0B271的毒殺效果比paclitaxel及vincristine強很多。接下來，我們利用流式細胞儀評估MPT0B271對於rhodamine-123 (Rh-123) 在NCI/ADR-RES細胞累積的影響，rhodamine-123 (Rh-123) 是p-gp的螢光染劑受質，將細胞處理p-gp抑制劑verapamil及cyclosporine A，能夠明顯增加Rh-123的累積，然而，MPT0B271卻沒有此作用 (Figure 5-2D)，calcein acetoxymethyl ester (calcein AM)是p-gp的螢光受質，可用來評估p-gp的運輸活性，因此抑制p-gp的作用可以藉由Multidrug Resistant Assay中calcein AM的累積來測量，如Figure 5-2E所示，verapamil或cyclosporine A明顯增加細胞內的螢光表現，相反地，MPT0B271並不影響calcein AM的流出。我們進一步利用SRB assay測試verapamil與MPT0B271合併處理NCI/ADR-RES細胞的影響 (Supplementary Figure 5-1)，發現verapamil並不會增加MPT0B271抑制細胞增生的作用，這些結果顯示MPT0B271能躲避p-gp造成的抗藥性。

MPT0B271使細胞週期停留在M期

大部分微管標靶藥物都會誘導細胞週期停滯，因此我們利用流式細胞儀來評

估MPT0B271對細胞週期進行的影響，將A549細胞以MPT0B271處理0至72小時，能時間相關性地使細胞累積在G2/M期，接著明顯增加低倍體sub-G1細胞量，表示細胞凋亡 (Figure 5-3A)。為了瞭解MPT0B271誘導G2/M期細胞停滯的機轉，我們利用西方墨點法分析G2/M期調控蛋白，發現MPT0B271誘導cyclin B1、p-Thr161 Cdc2/p34、serine/threonine kinases polo-like kinase 1 (PLK1) 以及aurora kinase A、aurora kinase B的蛋白表現，減少Cdc25C、p-Tyr15 Cdc2/p34蛋白表現，以及明顯大量增加mitosis-specific MPM2蛋白表現 (Figure 5-3B)，此外，將A549細胞處理MPT0B271則能顯著地增加細胞核內cyclin B1的蛋白累積 (Figure 5-3C) 。

MPT0B271誘導A549細胞凋亡

我們利用 Cell Death Detection ELISA^{Plus} kit 藉由測定 cytoplasmic histone-associated DNA fragments來評估MPT0B271誘導的細胞凋亡。結果顯示，MPT0B271處理48小時後能濃度相關性地增加A549細胞的DNA fragments (Figure 5-4A)；另外，MPT0B271能以濃度相關性地誘導caspase-3及其下游poly (ADP-Ribose) polymerase (PARP) 的活性 (Figure 5-4B)。我們進一步探討MPT0B271對於抗細胞凋亡蛋白的影響，發現MPT0B271能時間相關性地減少A549細胞中Bcl-2、Bcl-xL及Mcl-1的表現 (Figure 5-4C)。此外，將A549細胞過度表現Mcl-1能夠反轉PARP的活化及細胞存活率，表示MPT0B271是透過抑制Mcl-1的表現來誘導細胞凋亡 (Figure 5-4D)。

MPT0B271增加A549細胞p53的活化

我們進一步利用西方墨點法評估MPT0B271對於p53的影響，發現將A549細胞處理MPT0B271能明顯增加p53蛋白及p53在Ser15磷酸化的表現 (Figure 5-5A) ，然而，使用p53 small interfering RNA (siRNA) 抑制細胞的p53基因表現，

並無法反轉PARP的活化及細胞存活率 (Figure 5-5B)。此外，我們進一步評估MPT0B271在其它human NSCLC cell lines的體外細胞毒殺活性。利用MTT assay，發現將H1299 細胞株 (null p53) 及H226 細胞株 (mutant p53) 處理MPT0B271，能明顯減少細胞存活率，具有濃度相關性，IC_{50}分別為0.110 ± 0.014 μM and 0.046 ± 0.003 μM (Figure 5-5C)。

MPT0B271抑制A549細胞中持續性活化的STAT3

接下來，我們探討MPT0B271對於A549細胞中持續性磷酸化的STAT3的影響。如Figure 5-5D所示，MPT0B271能以時間相關性地明顯抑制STAT3在tyrosine705的磷酸化，利用PathScan Phospho-STAT3 (Tyr705) Sandwich ELISA kit，也再度證實MPT0B271抑制STAT3 tyrosine磷酸化的作用 (Figure 5-5E) ，然而，將細胞轉染持續性活化的STAT3只能些微地逆轉A549的細胞存活率 (Figure 5-5F)。

MPT0B271與erlotinib合併使用能在體內及體外增加抑制癌細胞生長的作用

Erlotinib已被證實能有效治療advanced NSCLC，但是卻會產生抗藥性 (Wang *et al.*, 2012b)，因此，我們探討是否MPT0B271與erlotinib合併處理能更有效抑制erlotinib-resistant human NSCLC A549細胞生長，如Figure 5-6A及Supplementary Figure 5-2所示，利用enzyme immunoassay評估histone-associated DNA fragments，erlotinib (5 μM) 與MPT0B271 (0.0125或0.025 μM) 合併處理細胞的組別，與藥物單獨給予的組別相較之下，能導致更明顯的細胞死亡，最後，在A549腫瘤異體移植的實驗中，MPT0B271與erlotinib合併治療比單獨給藥能導致更明顯的腫瘤生長抑制效果，並且不影響小鼠的體重 (Figure 5-6B and 6C)。這些結果顯示合併MPT0B271與erlotinib對於erlotinib-resistant NSCLC cell lines有更好的抑制腫瘤生長效果。

第三節 討論

在本研究中，MPT0B271被證實是一個抑制微管聚合的藥物，並且在各種癌細胞株中包括抗藥性細胞株，都展現明顯的抗腫瘤活性，過去研究指出在各種的細胞外及細胞內壓力，例如DNA損傷、致癌作用及微管破壞，p53在細胞反應中扮演一個重要的角色 (Stewart *et al.*, 2001)，本研究結果顯示，MPT0B271以時間相關性地誘導p53蛋白表現，但是，利用siRNA抑制p53基因表現並無法阻止MPT0B271造成的細胞凋亡，此外，MPT0B271在A549 (wild-type p53)、H1299 (p53 null) 以及 H226 (p53 mutant) 有相似的IC_{50}值，表示MPT0B271的抗癌作用與p53的表現無直接相關性。臨床上使用的傳統微管標靶藥物，例如paclitaxel，需要長期的靜脈注射給予療法，導致病人身心的疲苦及降低病人的生活品質，此外，這類藥物會導致過敏感反應及神經病變 (Dumontet *et al.*, 2010; Gelderblom *et al.*, 2001)，而在這篇研究中，MPT0B271改善了傳統微管標靶藥物溶解度，並且是一個口服生體可用及在體內對於NSCLC腫瘤異體移植是有效的藥物。

抗藥性一直是微管標靶藥物在臨床使用上的嚴重問題，MDR p-gp是在multidrug-resistant tumor cells過度表現的細胞膜蛋白，並且是化療藥物治療成功的主要障礙，MDR蛋白導致藥物從標靶細胞內輸出，而造成抗藥性 (Nieto Montesinos *et al.*, 2012)，許多微管標靶藥物都是p-gp的受質，因此在multidrug-resistant cancer cells中，需要投予更高的劑量才能達到適當的細胞內濃度 (Fojo *et al.*, 2007)，我們利用p-gp及multidrug resistance-associated protein (MRP)的受質，Rh-123及calcein AM，當作探針來偵測化合物與MDR蛋白的交互作用，在活細胞中，esterase能夠將calcein AM脂解生成calcein，而釋放出強的綠色螢光 (Canitrot *et al.*, 1995; Shapiro *et al.*, 1998; Szakacs *et al.*, 1998)，我們的結果顯示在NCI/ADR-RES細胞中，MPT0B271不影響Rh-123的累積或calcein在細胞內的螢

光，我們也利用SRB assay測試了verapamil與MPT0B271合併在NCI/ADR細胞中的作用 (Supplementary Figure 5-1)，verapamil與MPT0B271合併的GI_{50}為16 nM，表示合併使用的生長抑制效果與單獨處理相似，這些結果顯示MPT0B271可能不是p-gp輸出幫浦的受質或調節者。

如同其它的微管標靶藥物，藉由流式細胞儀分析發現MPT0B271誘導濃度相關性地G2/M期阻斷，並且增加有絲分裂特定標記蛋白MPM-2的蛋白表現，另一個G2/M期的標記蛋白是cyclin B1，G2期時留在細胞質內，當有絲分裂開始會快速移動至細胞核內 (Gavet *et al.*, 2010)，從西方墨點法分析顯示MPT0B271明顯增加cyclin B1在細胞核內的蛋白表現，暗示著MPT0B271處理的細胞停滯在有絲分裂期，Cdc2/p34是一個細胞週期激酶，能夠調控真核細胞G2期的進行及G2/M期的轉換，過去有報導指出Cdc2/p34 kinase的活性必須依賴其與cyclin B1的結合以及其本身磷酸化的狀態 (Coulonval *et al.*, 2011)，我們發現MPT0B271明顯減少p-Tyr15 Cdc2/p34及增加p-Thr161 Cdc2/p34的表現，以及cyclin B1的增加，但是對Cdc2/p34的表現不影響，PLK-1及aurora kinase A and B在有絲分裂時是活化態的 (Malumbres, 2011)，在哺乳細胞中，PLK-1是G2/M期轉換的早期促進蛋白，並且參與調控了不同的過程，包括有絲分裂的起始、紡錘絲體的形成及細胞質分裂 (cytokinesis)，Aurora kinase A及B對於中心體的分離、有絲分裂紡錘絲體的集合、染色體在主軸上的雙向位置以及細胞質分裂是必須的 (Andrews *et al.*, 2003; Lens *et al.*, 2010)，本研究結果顯示MPT0B271以時間相關性地增加PLK-1、Aurora kinase A及B的蛋白表現，更加支持了我們的論點，MPT0B271誘導A549細胞停滯在M期。

我們的結果顯示除了誘導細胞週期停滯在有絲分裂期，MPT0B271 能夠造成低倍體細胞群的增加 (細胞凋亡 sub-G1 期)，我們也發現 MPT0B271 明顯增加 cytoplasmic histone-associated DNA fragments，更加證實了 MPT0B271 誘導了 A549 細胞凋亡。Cysteine proteases (caspases) 經由蛋白水解特定的蛋白，而在細

胞凋亡中占有相當重要的角色，death receptor-mediated pathway 及 mitochondrial-mediated pathway 都會活化 caspase-3，並接著導致 PARP 的切割 (Fan *et al.*, 2005) ，我們的結果顯示 MPT0B271 在 A549 細胞中，明顯導致 caspase-3 及-7 的活化，但卻無法促進 caspase-8 及-9 的切割，caspase-8 及-9 可能在 A549 細胞凋亡中，屬於次要的角色。Mcl-1 能夠阻止內在及外在路徑誘導的細胞凋亡 (Thomas *et al.*, 2010)，將細胞處理 MPT0B271 明顯減少 Mcl-1 在 A549 細胞中的表現，此外，過度表現 Mcl-1 能救援細胞凋亡的現象，象徵 Mcl-1 降解在 MPT0B271 誘導細胞凋亡的重要角色。

STAT3 在大部分的癌細胞中是持續性活化的，並且與化療與放療的抗藥性相關，acetyl STAT3 會移至細胞核內，經由活化基因的表現來促進細胞增生及存活，此外，STAT3 也能與微管及粒線體結合，調控細胞行為，從過去的文獻已經發現微管標靶藥物減少癌細胞中 tyrosine phosphorylation-induced activation of STAT3 (Tyr705)，減少 STAT3 活化的基因，與其細胞毒殺的作用相關 (Aggarwal *et al.*, 2006; Liu *et al.*, 2011; Walker *et al.*, 2010)，在本研究中，我們發現 MPT0B271 特定減少 STAT3 在 Tyr705 的磷酸化，在 A549 細胞轉染 STAT3-C 質體，只能些微部分逆轉細胞的毒殺作用，表示 STAT3 在 MPT0B271 誘導的 A549 細胞凋亡是較次要的角色，其他的機轉可能參與在此現象中。

從過去的文獻報導中，已經知道在很多的人類癌症包括 NSCLC，會過度表現 EGFR，並且是預後不良的指標，口服 EGFR tyrosine kinase inhibitor Erlotinib (Terceva, Roche, Mannheim, Germany) 能夠可逆性地與 EGFR 的細胞內 domain 結合，並且阻礙 EGFR 的自體磷酸化，抑制其下游誘發癌細胞失控生長的訊息路徑，雖然 erlotinib 被證實在轉移的 NSCLC 具有療效，並且被報導對於帶有 EGFR 突變的 advanced NSCLC 病人，能夠延長存活率，但是抗藥性卻常發生並減少其療效 (Francis *et al.*, 2010; Sangodkar *et al.*, 2010; Uribe *et al.*, 2012)，為了克服抗藥性的問題，我們將微管結合藥物 MPT0B271 與 erlotinib 合併處理 erlotinib-resistant

human NSCLC A549 細胞株，能增加抗癌效果，我們利用 cell death detection ELISA assay kit，結果顯示單獨使用 erlotinib 無法明顯造成 A549 細胞死亡，然而，MPT0B271 與 erlotinib 合併療法具有加成作用，在 A549 異體移植小鼠實驗中也看到一樣的結果，erlotinib 無法抑制腫瘤的進展，但是與 MPT0B271 合併卻產生強力的抑癌效果，這些結果指出 MPT0B271 與 erlotinib 合併在 advanced NSCLC 是有效及有益處的合併療法。

總結以上所述，我們的結果指出 MPT0B271 是一個對於 p-gp 具有低感受性、強力細胞毒殺活性及口服有效的微管去穩定藥物，MPT0B271 在 human NSCLC 細胞中，能抑制微管聚合、導致細胞週期停滯在有絲分裂並促進細胞凋亡訊息路徑，此外，不論在體內或體外，MPT0B271 與 erlotininb 合併抑制腫瘤生長的作用，明顯比單獨給藥更有效，這些結果顯示 MPT0B271 在 NSCLC 擁有成為新穎療法的潛力。

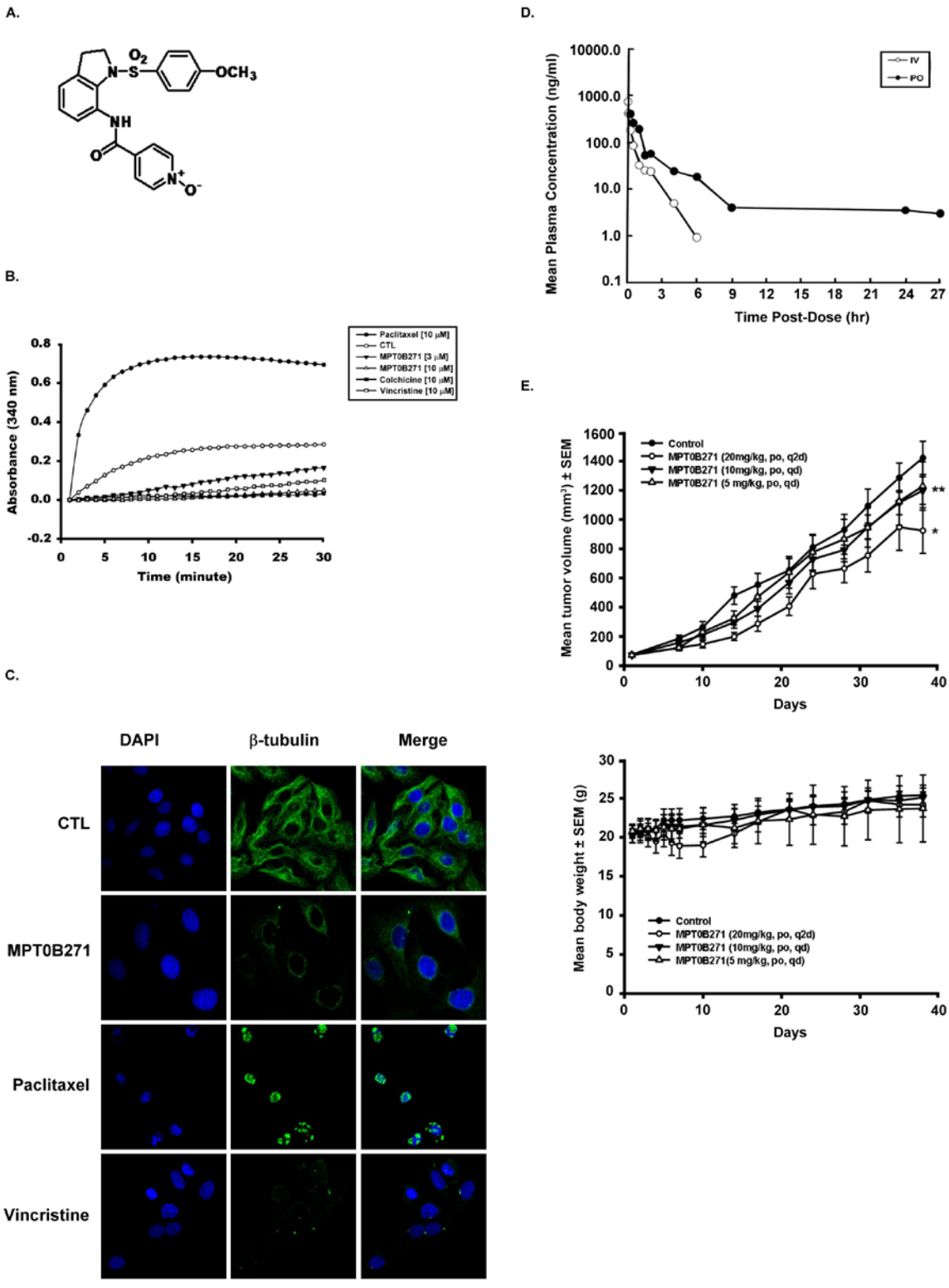

Figure 5-1. A, chemical structure of MPT0B271. B, effect of MPT0B271 on tubulin polymerization. Purified tubulin in reaction buffer was incubated at 37°C in the absence (control, CTL) or presence of increasing concentrations of MPT0B271, 10 μM paclitaxel, 10 μM colchicine or 10 μM vincristine. Assembly of microtubules was

then measured over 30 min at 1-min intervals at an absorbance of 340 nm using a spectrophotometer. C, immunofluorescence staining of microtubules in A549 cells. Cells were treated with vehicle (DMSO), 0.3 μM MPT0B271, paclitaxel or vincristine for 24 h. Cells were labeled with a β-tubulin antibody and a FITC-conjugated anti-mouse IgG antibody, were counterstained with 4,6-diamidino-2-phenylindole (DAPI) and observed by confocal microscopy. *Left*, DAPI; *middle*, microtubule network; *right*, merged microtubule network and DAPI. D, PK properties, plasma concentration versus time profiles of MPT0B271 after i.v. (2 mg/kg) and p.o. (20 mg/kg) dosing of fasted male CD-1 (*Crl.*) mice. E. efficacy of MPT0B271, dosed orally, on tumor xenografts. *Upper panel*, tumor growth of A549 xenografts in nude mice that were orally treated with or without MPT0B271 (5, 10, 20 mg/kg). Tumor growth is presented as the mean tumor volume (mm^3) ± S.E. Tumor volume was determined using caliper measurements and was calculated as the product of 1/2 x length x $width^2$. *Lower panel*, body weight (g) of the mice. *, $p < 0.05$ and ** $p < 0.01$ as compared with the control group.

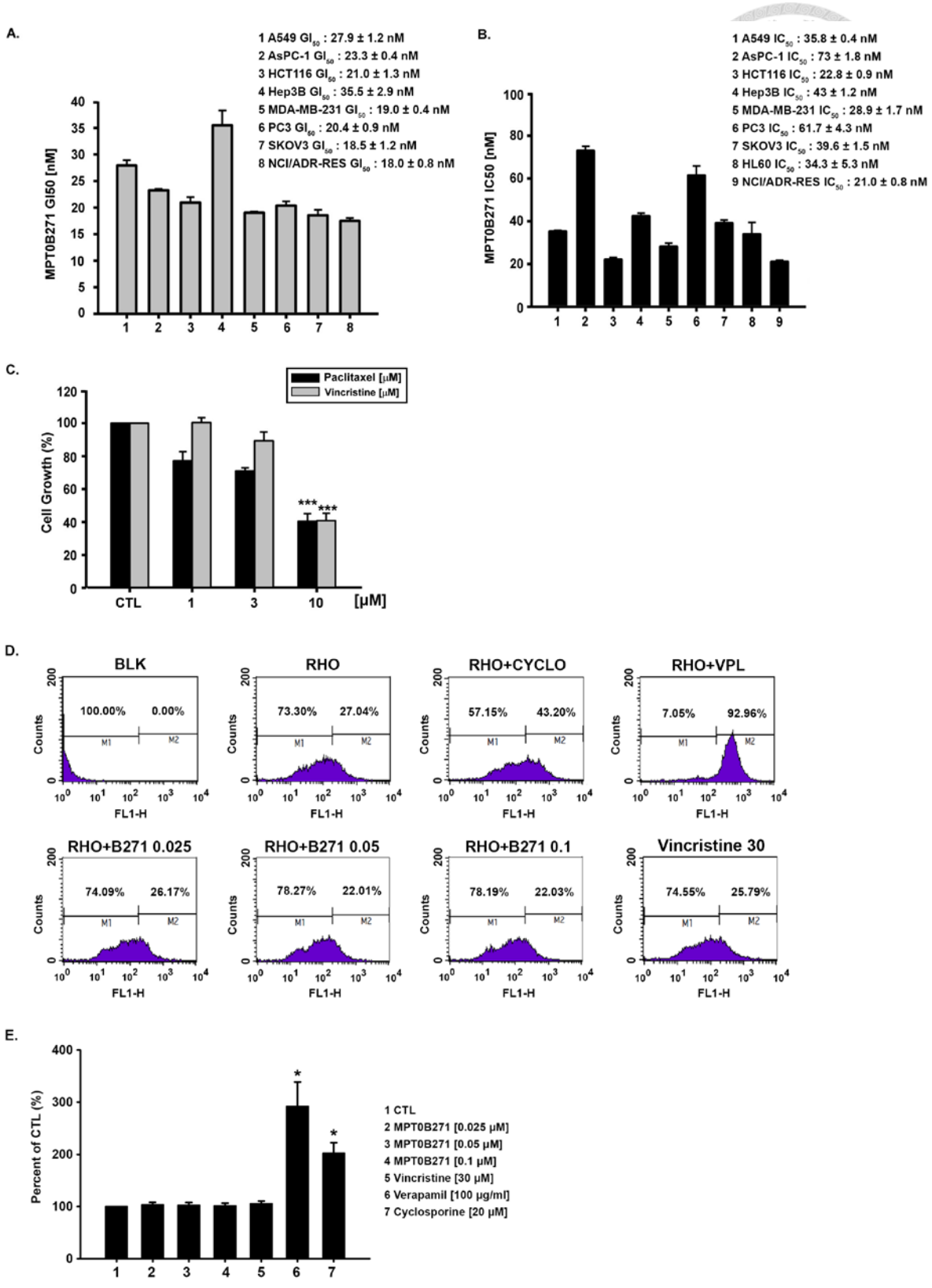

Figure 5-2. A, various types of human cancer cells were treated without (control, CTL) or with the indicated concentrations of MPT0B271 for 48 h. Then, cell growth

inhibition was determined using the SRB assay, and the GI_{50} of each cell line is expressed as the mean ± S.E. of four independent determinations. B, the cytotoxic effects of various human cancer cell lines were determined using an MTT assay. The IC_{50} of each cell line is expressed as the mean ± S.E. of four independent determinations. C, NCI/ADR-RES cells were treated with the indicated concentration of paclitaxel or vincristine for 48 h, and cell growth was determined by the SRB assay. Data are expressed as the mean ± S.E. of at least three independent experiments. *** $p < 0.01$ as compared with the control group. D, effect of MPT0B271 on p-gp activity. NCI/ADR-RES cells were pre-treated with or without MPT0B271 (0.025, 0.05, 0.1 μM), verapamil (50 μM), cyclosporine A (10 μM) or vincristine (30 μM) for 1 h and then co-treated with 10 μM rhodamine 123 (Rh-123). After 1 h incubation at 37°C, cells were washed with PBS, collected by trypsinization and detected by flow cytometry. E, NCI/ADR-RES cells were incubated in the absence or presence of the indicated agents for 30 min and then stained with calcein AM fluorescent dye. Fluorescence was measured at an excitation wavelength of 485 nm and an emission wavelength of 535 nm.

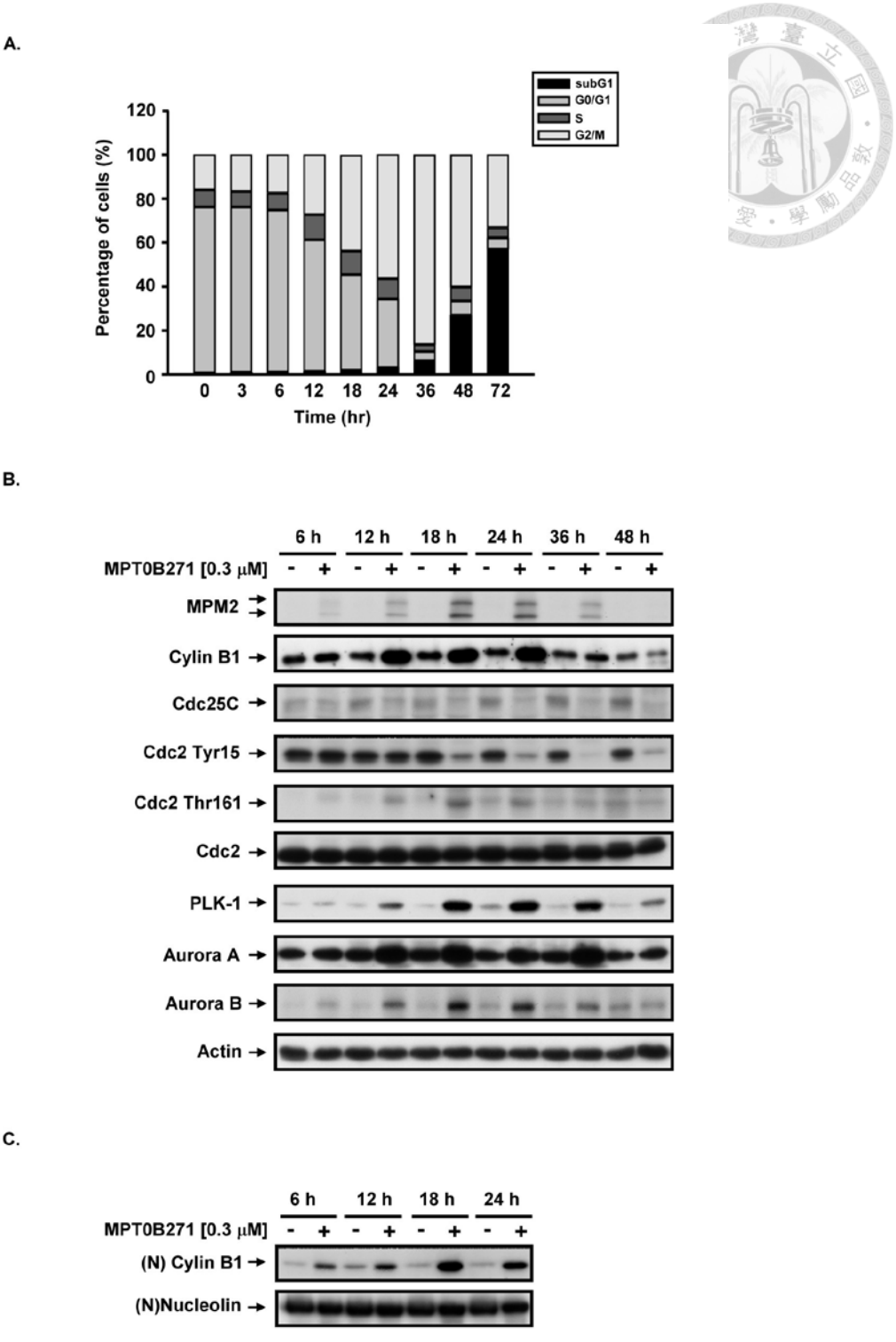

Figure 5-3. A, effect of MPT0B271 on cell cycle progression. A549 cells were exposed to 0.3 μM MPT0B271 for the indicated times and then stained with PI to determine the proportion of DNA. Data acquisition and analysis were performed on a FACScan flow cytometer. The data are expressed as the mean ± S.E. of at least three independent experiments. B, the effect of MPT0B271 on G2/M cell cycle regulatory

proteins. A549 cells were treated with 0.3 μM MPT0B271 for the indicated times. Whole cell extracts were subjected to SDS-PAGE and immunoblotted with the indicated antibodies. C, treatment with 0.3 μM MPT0B271 for the indicated times. Nuclear lysates were subjected to Western blot analysis using an antibody specific for cyclin B1.

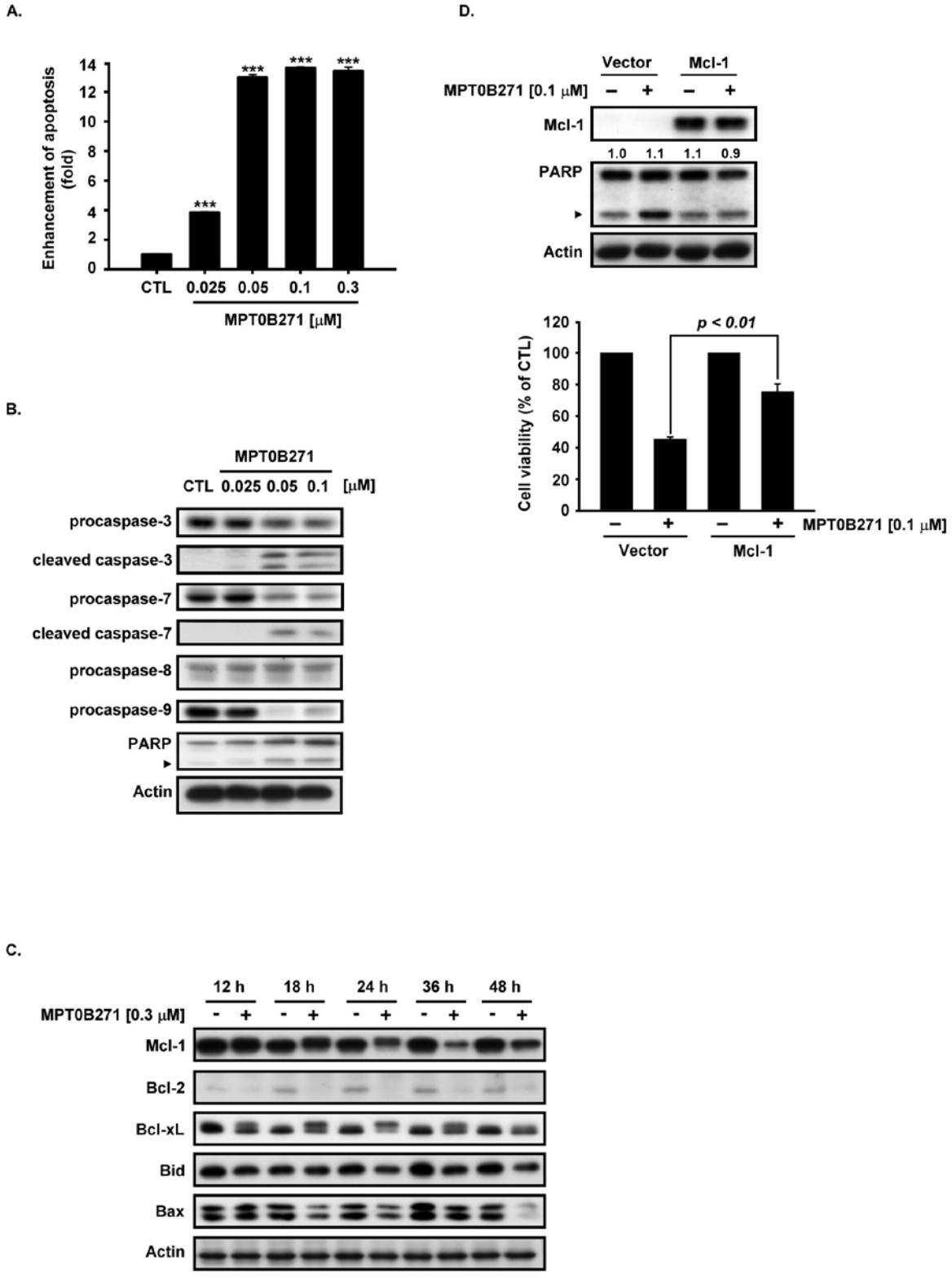

Figure 5-4. A, measurement of apoptosis. A549 cells were treated without (control, CTL) or with the indicated concentration of MPT0B271, and oligonucleosomal DNA fragmentation was quantitatively assessed with the Cell Death ELISA^{PLUS} kit.

Apoptosis was enhanced in relation to control cells. Data are expressed as the mean ± S.E. of at least three independent experiments. ***, $p < 0.001$, as compared with the control group. B, A549 cells were exposed to serial concentrations of MPT0B271 for 48 h, and whole cell lysates were collected and immunoblotted with antibodies against caspase-3, -7, -8 and -9 and PARP. C, after treatment with vehicle or MPT0B271 (0.3 μM) for the indicated times, A549 cells were harvested and lysed. Equal amounts of lysate protein were run on an SDS-PAGE gel, transferred to nitrocellulose membrane and incubated with the indicated antibodies. D, effect of ectopic Mcl-1 on MPT0B271-induced cell apoptosis. A549 cells were transfected with vector or Mcl-1 plasmid for 24 h and then incubated with or without MPT0B271 for 48 h. Whole cell lysates were subjected to Western blot analysis, and cell viability was measured by the SRB assay.

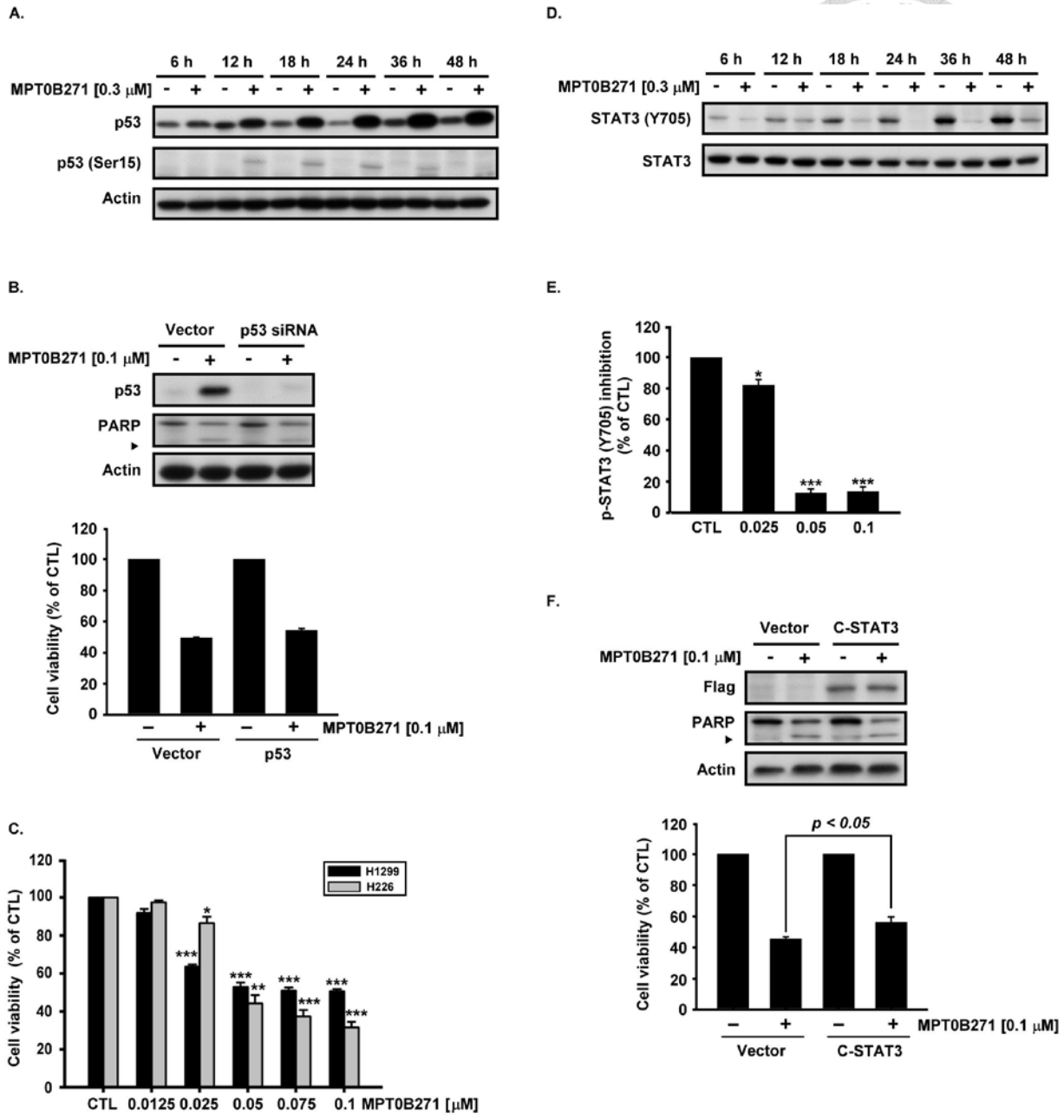

Figure 5-5. A, the effect of MPT0B271 on p53 expression and phosphorylation in A549 cells. Cells were treated without (control, CTL) or with MPT0B271 (0.3 μM) for the indicated times, and whole cell extracts were prepared and underwent Western blot analysis using the indicated antibodies. B, A549 cells were pretreated with or without p53 siRNA for 24 h and then incubated with or without MPT0B271 (0.1 μM) for 48 h. *Upper panel*, total cellular lysates were subjected to Western blot analysis of p53 and PARP. *Lower panel*, cell viability was measured by the SRB assay and expressed as a percentage of the untreated control. C, concentration-dependent effect of MPT0B271 on cell viability. H1299 and H226 cells were treated with or without

the indicated concentration of MPT0B271 for 48 h, and the cytotoxic effect was determined with the MTT assay. Data are expressed as the mean ± S.E. of at least three independent experiments. *, $p < 0.05$; ** $p < 0.01$ and *** $p < 0.001$ as compared with the control group. D, the effect of MPT0B271 on STAT3 phosphorylation in A549 cells. Cells were treated with MPT0B271 (0.3 μM) for the indicated times, and whole cell extracts were prepared and analyzed for STAT-3 phosphorylation (at Tyr^{705}). E, A549 cells were treated with various concentrations (0.025-0.1 μM) of MPT0B271 for 24 h, after which the level of STAT3 tyrosine phosphorylation in cells were measured using the PathScan® Phospho-Stat3 (Try705) Sandwich ELISA kit and spectrophotometry at 450 nm. Data represent the mean ± S.E. of at least three independent experiments. *, $p < 0.05$; *** $p < 0.001$ as compared with the control group. F, the effect of ectopic STAT3 on MPT0B271-induced cell apoptosis. A549 cells were transfected with vector or STAT3 plasmid for 24 h and then incubated with or without MPT0B271 for 48 h. Whole cell lysates were subjected to Western blot analysis, and cell viability was measured by the SRB assay.

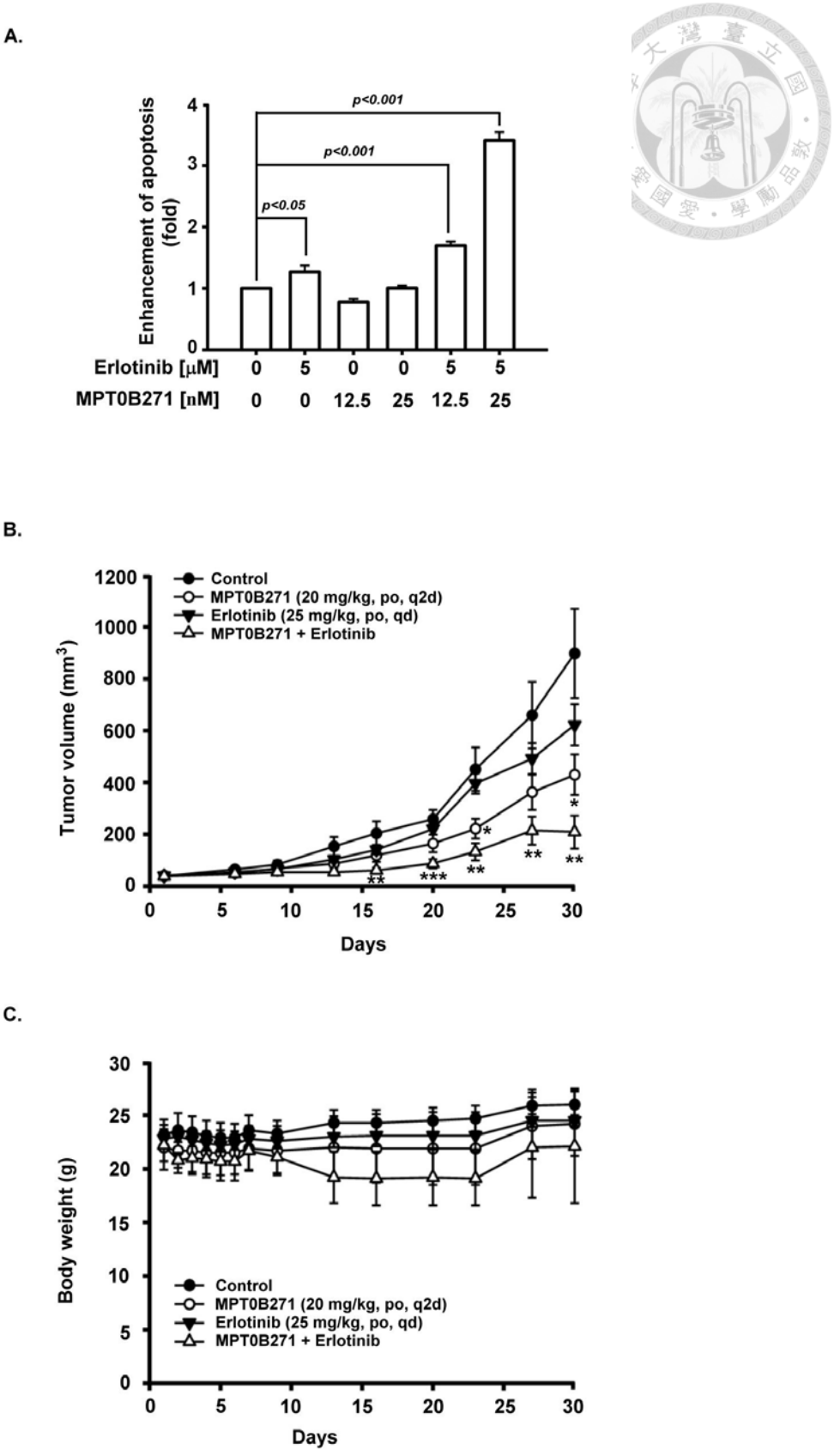

Figure 5-6. *In vitro* and *in vivo* antitumor activity of MPT0B271 in combination with

erlotinib. A, A549 cells were treated with erlotinib (5 μM) in combination with MPT0B271 (0.0125 or 0.025 μM) for 48 h, and cell apoptosis was measured using the Cell Death ELISA^{PLUS} kit. Data are expressed as the mean ± S.E. of at least three independent determinations. B, A549 xenograft model. A549-tumor-bearing nude mice were treated with vehicle, MPT0B271 (20 mg/kg/d by oral gavage q2d), erlotinib (25 mg/kg/d by oral gavage once a day), or MPT0B271 in combination with erlotinib. Tumor was excised when the tumor size reached 1200 mm^3. C, the body weight of the mice measured daily during the first week and then at the days of administration. *, $p < 0.05$; ** $p < 0.01$ and *** $p < 0.001$ as compared with the control group.

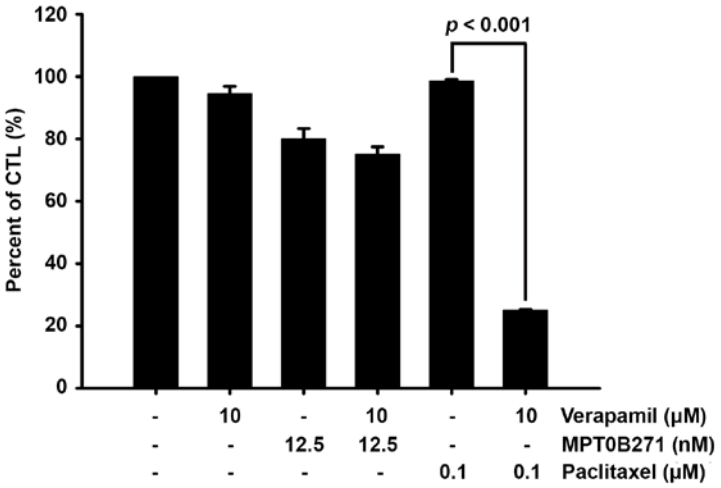

Supplemental figure 5-1. Antiproliferative effect of MPT0B271 in combination with erlotinib in NCI/ADR-RES cells using SRB assay. NCI/ADR-RES cells were treated without (control, CTL) or with verapamil, MPT0B271 or paclitaxel at indicated concentrations for 48 hours. And then cells were fixed and stained with SRB. The protein-bound dye was subsequently extracted with 10 mM trizma base to determine the absorbance at a wavelength of 515 nm.

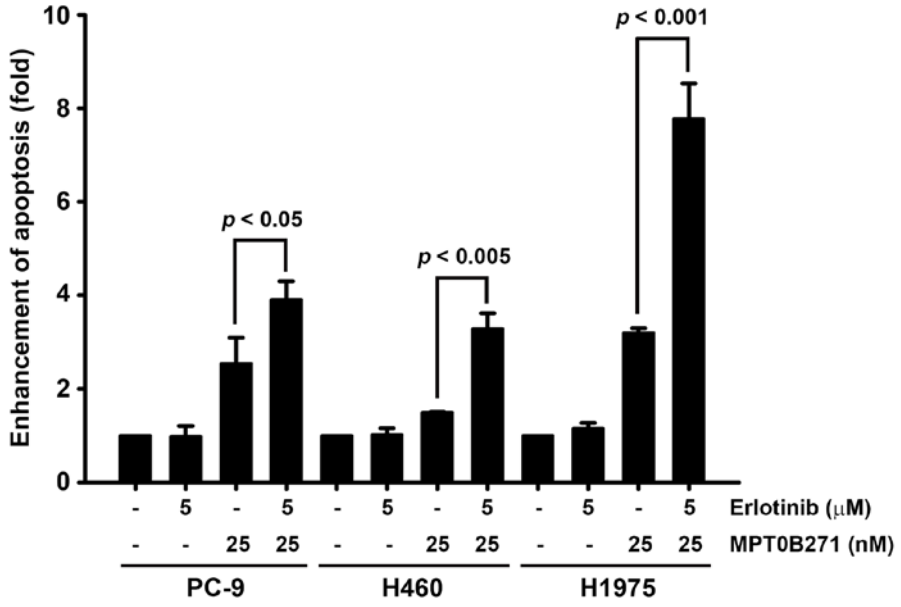

Supplemental figure 5-2. Apoptotic effects of MPT0B271 in combination with erlotinib in several human non-small cell lung cancer cells. PC-9, H460 and H1975 NSCLC cells were treated with or without erlotinib, MPT0B271, and combination of MPT0B271 and erlotinib for 24 hours. Cell apooptosis was analyzed by Cell Death Detection ELISA^{PLUS} kit (Roche Diagnostics).

第六章 總結與展望

癌症是目前三十二年來蟬聯第一名的國人死亡殺手，罹癌患者年齡層亦有逐年下降之趨勢，多數病人在診斷時已近晚期，且常因無法有效治療而導致死亡。隨著醫學、藥理學、分子生物研究領域發展日新月異，不同機轉的化學療法能夠有效治療各種癌症，但是卻因為藥物的缺點、毒性、副作用及抗藥性的產生，而限制了藥物的應用和治療效果，降低了病人的生活品質。為了改善這些問題，小分子標靶療法 (molecular targeted therapy) 成為科學界和藥廠的研發對象，是癌症治療的新紀元，經由基礎研究了解癌細胞與正常細胞間某些關鍵「標靶」的表現差異，運用抗體或小分子等藥物來有效阻斷癌細胞異常活化或過度表現之重要標靶相關路徑，達到治療的目的，其中，抗血管新生療法即屬於標靶療法之一。

過度的血管新生會造成許多疾病，尤其在癌症中，是腫瘤持續生長的關鍵，血管內皮細胞在血管新生過程扮演中樞的角色，內皮細胞的增生、類血管管腔形成、移行更是其中的關鍵，在本篇論文中，我們利用臍靜脈內皮細胞為研究對象，探討中草藥物萃取成分與化學合成物質的藥理機轉，並且發現了兩個具有發展潛力的小分子藥物：Dehydrocostuslactone 與 MPT0G013。Dehydrocostuslactone 可以經由抑制 Akt/GSK3-β/cyclin D1 路徑及 mTOR 訊息傳遞而影響細胞增生、tube formation (Figure 6-1)，並在動物實驗中，證明確實對血管生長因子引起的血管新生具有抑制作用。MPT0G013 則透過誘導活化抗血管新生內生性蛋白 TIMP3、IGFBP3 的基因轉錄，抑制血管新生受體與配體的結合，進而抑制下游 Akt 和 ERK 的訊息傳遞，達到抗血管新生的作用，進而抑制腫瘤的生長，然而，MPT0G013 如何活化 TIMP3 基因轉錄仍有待進一步釐清 (Figure 6-1)。中草藥物的專利則取得不易，若是能作為先導藥物 (lead compound)，將其化學結構進一步優化，以提高藥力、選擇性、減低毒性，或許能發展為理想的血管新生抑制劑。

口服 gefitinib 或 erlotinib 對以鉑化合物 (cisplatin/carboplatin) 為主之化療藥物，對已失效之非小細胞肺癌患者仍有約 18.4% 腫瘤緩解率，對未曾使用過化療之晚期 NSCLC 患者，第一線使用口服 gefitinib 或 erlotinib，可達超過 50% 腫瘤緩解率，對東方女性 (含台灣、日本等)、非吸煙 (non-smokers)、肺腺癌 (adenocarcinoma) 患者口服 gefitinib 或 erlotinib，腫瘤緩解率尤其更高。但是仍然在許多患者中，產生了對標靶藥物的抗藥性。在本篇論文中，口服生體可用 MPT0B271 能夠透誘發細胞凋亡，並且在體內及體外，與 erlotinib 合併使用能更明顯抑制 erlotinib-sensitive 癌細胞的生長，具有加成性細胞毒殺的作用 (Figure 6-1)，此外，與傳統微管標靶藥物不同的是，MPT0B271 具有抑制微管聚合的作用，但能躲避 p-gp 造成的抗藥性，顯示 MPT0B271 是一個極具有發展潛力的藥物，若能進一步釐清對於其他訊息傳導路徑的抑制效果，以及與 erlotininb 如何增加 EGFR- resistant mutation 癌細胞的細胞毒殺機轉，極有潛力成為非小細胞肺癌治療上的新療法，並期望能帶給治療病人更多的選擇。

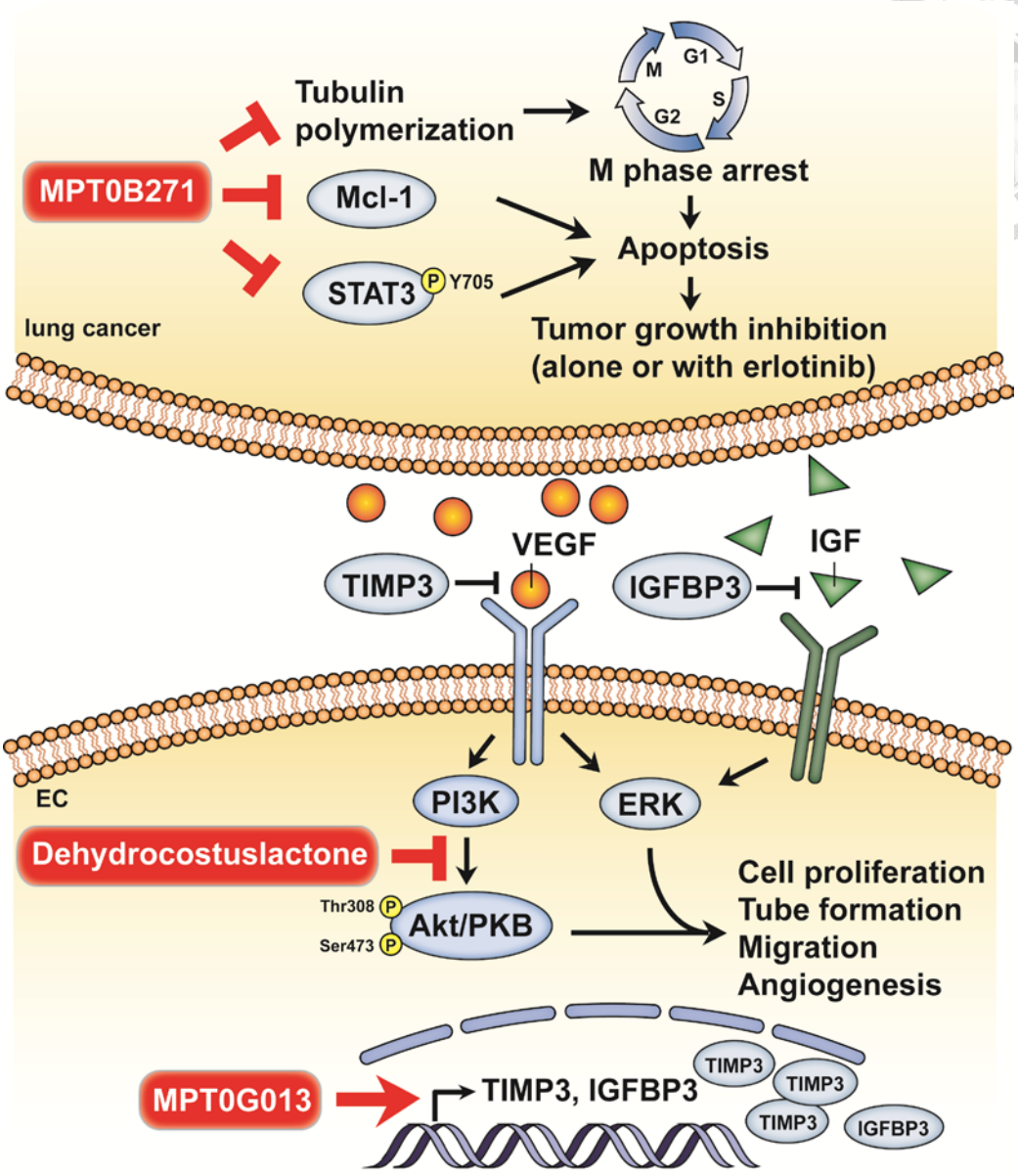

Figure 6-1. Summary of anti-angiogenic and anti-tumor mechanisms of DHC, MPT0G013 and MPT0B271.

參考文獻

Aggarwal BB, Sethi G, Ahn KS, Sandur SK, Pandey MK, Kunnumakkara AB, *et al.* (2006). Targeting signal-transducer-and-activator-of-transcription-3 for prevention and therapy of cancer: modern target but ancient solution. *Annals of the New York Academy of Sciences* **1091:** 151-169.

Ahonen M, Poukkula M, Baker AH, Kashiwagi M, Nagase H, Eriksson JE, *et al.* (2003). Tissue inhibitor of metalloproteinases-3 induces apoptosis in melanoma cells by stabilization of death receptors. *Oncogene* **22**(14)**:** 2121-2134.

Akahane T, Akahane M, Shah A, Connor CM, Thorgeirsson UP (2004). TIMP-1 inhibits microvascular endothelial cell migration by MMP-dependent and MMP-independent mechanisms. *Experimental cell research* **301**(2)**:** 158-167.

Algire GH, Chalkley HW, Earle WE, Legallais FY, Park HD, Shelton E, *et al.* (1950). Vascular reactions of normal and malignant tissues in vivo. III. Vascular reactions' of mice to fibroblasts treated in vitro with methylcholanthrene. *Journal of the National Cancer Institute* **11**(3)**:** 555-580.

Andrews PD, Knatko E, Moore WJ, Swedlow JR (2003). Mitotic mechanics: the auroras come into view. *Current opinion in cell biology* **15**(6)**:** 672-683.

Balak MN, Gong Y, Riely GJ, Somwar R, Li AR, Zakowski MF, *et al.* (2006). Novel D761Y and common secondary T790M mutations in epidermal growth factor receptor-mutant lung adenocarcinomas with acquired resistance to kinase inhibitors. *Clinical cancer research : an official journal of the American Association for Cancer Research* **12**(21)**:** 6494-6501.

BenEzra D (1997). Inhibition of angiogenesis by tissue inhibitor of metalloproteinase-3. *Investigative ophthalmology & visual science* **38**(12)**:** 2433-2434.

Bond M, Murphy G, Bennett MR, Amour A, Knauper V, Newby AC, *et al.* (2000). Localization of the death domain of tissue inhibitor of metalloproteinase-3 to the N

terminus. Metalloproteinase inhibition is associated with proapoptotic activity. *The Journal of biological chemistry* **275**(52)**:** 41358-41363.

Bond M, Murphy G, Bennett MR, Newby AC, Baker AH (2002). Tissue inhibitor of metalloproteinase-3 induces a Fas-associated death domain-dependent type II apoptotic pathway. *The Journal of biological chemistry* **277**(16)**:** 13787-13795.

Breuninger LM, Paul S, Gaughan K, Miki T, Chan A, Aaronson SA, *et al.* (1995). Expression of multidrug resistance-associated protein in NIH/3T3 cells confers multidrug resistance associated with increased drug efflux and altered intracellular drug distribution. *Cancer research* **55**(22)**:** 5342-5347.

Burgering BM, Coffer PJ (1995). Protein kinase B (c-Akt) in phosphatidylinositol-3-OH kinase signal transduction. *Nature* **376**(6541)**:** 599-602.

Canitrot Y, Lautier D (1995). [Use of rhodamine 123 for the detection of multidrug resistance]. *Bulletin du cancer* **82**(9)**:** 687-697.

Carmeliet P (2003). Angiogenesis in health and disease. *Nature medicine* **9**(6)**:** 653-660.

Carmeliet P, Jain RK (2011). Molecular mechanisms and clinical applications of angiogenesis. *Nature* **473**(7347)**:** 298-307.

Chang F, Lee JT, Navolanic PM, Steelman LS, Shelton JG, Blalock WL, *et al.* (2003). Involvement of PI3K/Akt pathway in cell cycle progression, apoptosis, and neoplastic transformation: a target for cancer chemotherapy. *Leukemia* **17**(3)**:** 590-603.

Chen YY, Brown NJ, Jones R, Lewis CE, Mujamammi AH, Muthana M, *et al.* (2014). A peptide derived from TIMP-3 inhibits multiple angiogenic growth factor receptors and tumour growth and inflammatory arthritis in mice. *Angiogenesis* **17**(1)**:** 207-219.

Chung AS, Lee J, Ferrara N (2010). Targeting the tumour vasculature: insights from physiological angiogenesis. *Nature reviews. Cancer* **10**(7)**:** 505-514.

Costa DB, Halmos B, Kumar A, Schumer ST, Huberman MS, Boggon TJ, *et al.* (2007). BIM mediates EGFR tyrosine kinase inhibitor-induced apoptosis in lung

cancers with oncogenic EGFR mutations. *PLoS medicine* **4**(10)**:** 1669-1679; discussion 1680.

Coulonval K, Kooken H, Roger PP (2011). Coupling of T161 and T14 phosphorylations protects cyclin B-CDK1 from premature activation. *Molecular biology of the cell* **22**(21)**:** 3971-3985.

Davidson G, Niehrs C (2010). Emerging links between CDK cell cycle regulators and Wnt signaling. *Trends in cell biology* **20**(8)**:** 453-460.

Della NG, Campochiaro PA, Zack DJ (1996). Localization of TIMP-3 mRNA expression to the retinal pigment epithelium. *Investigative ophthalmology & visual science* **37**(9)**:** 1921-1924.

Diehl JA, Cheng M, Roussel MF, Sherr CJ (1998). Glycogen synthase kinase-3beta regulates cyclin D1 proteolysis and subcellular localization. *Genes & development* **12**(22)**:** 3499-3511.

Diehl JA, Zindy F, Sherr CJ (1997). Inhibition of cyclin D1 phosphorylation on threonine-286 prevents its rapid degradation via the ubiquitin-proteasome pathway. *Genes & development* **11**(8)**:** 957-972.

Dumontet C, Jordan MA (2010). Microtubule-binding agents: a dynamic field of cancer therapeutics. *Nature reviews. Drug discovery* **9**(10)**:** 790-803.

Dumontet C, Sikic BI (1999). Mechanisms of action of and resistance to antitubulin agents: microtubule dynamics, drug transport, and cell death. *Journal of clinical oncology : official journal of the American Society of Clinical Oncology* **17**(3)**:** 1061-1070.

Ebos JM, Lee CR, Cruz-Munoz W, Bjarnason GA, Christensen JG, Kerbel RS (2009). Accelerated metastasis after short-term treatment with a potent inhibitor of tumor angiogenesis. *Cancer cell* **15**(3)**:** 232-239.

El Sayed KA (2005). Natural products as angiogenesis modulators. *Mini reviews in medicinal chemistry* **5**(11)**:** 971-993.

Ellis LM, Hicklin DJ (2008). VEGF-targeted therapy: mechanisms of anti-tumour activity. *Nature reviews. Cancer* **8**(8)**:** 579-591.

Engelman JA (2009). Targeting PI3K signalling in cancer: opportunities, challenges and limitations. *Nature reviews. Cancer* **9**(8)**:** 550-562.

Fan TJ, Han LH, Cong RS, Liang J (2005). Caspase family proteases and apoptosis. *Acta biochimica et biophysica Sinica* **37**(11)**:** 719-727.

Ferrara N, Kerbel RS (2005). Angiogenesis as a therapeutic target. *Nature* **438**(7070)**:** 967-974.

Fojo T, Menefee M (2007). Mechanisms of multidrug resistance: the potential role of microtubule-stabilizing agents. *Annals of oncology : official journal of the European Society for Medical Oncology / ESMO* **18 Suppl 5:** v3-8.

Folkman J (2007). Angiogenesis: an organizing principle for drug discovery? *Nature reviews. Drug discovery* **6**(4)**:** 273-286.

Folkman J (2002). Role of angiogenesis in tumor growth and metastasis. *Seminars in oncology* **29**(6 Suppl 16)**:** 15-18.

Folkman J (1971). Tumor angiogenesis: therapeutic implications. *The New England journal of medicine* **285**(21)**:** 1182-1186.

Francis H, Solomon B (2010). The current status of targeted therapy for non-small cell lung cancer. *Internal medicine journal* **40**(9)**:** 611-618.

Franke TF, Yang SI, Chan TO, Datta K, Kazlauskas A, Morrison DK, *et al.* (1995). The protein kinase encoded by the Akt proto-oncogene is a target of the PDGF-activated phosphatidylinositol 3-kinase. *Cell* **81**(5)**:** 727-736.

Franklin SL, Ferry RJ, Jr., Cohen P (2003). Rapid insulin-like growth factor (IGF)-independent effects of IGF binding protein-3 on endothelial cell survival. *The Journal of clinical endocrinology and metabolism* **88**(2)**:** 900-907.

Fu M, Wang C, Li Z, Sakamaki T, Pestell RG (2004). Minireview: Cyclin D1: normal

and abnormal functions. *Endocrinology* **145**(12)**:** 5439-5447.

Gavet O, Pines J (2010). Activation of cyclin B1-Cdk1 synchronizes events in the nucleus and the cytoplasm at mitosis. *The Journal of cell biology* **189**(2)**:** 247-259.

Gelderblom H, Verweij J, Nooter K, Sparreboom A (2001). Cremophor EL: the drawbacks and advantages of vehicle selection for drug formulation. *Eur J Cancer* **37**(13)**:** 1590-1598.

Gerber HP, McMurtrey A, Kowalski J, Yan M, Keyt BA, Dixit V, *et al.* (1998). Vascular endothelial growth factor regulates endothelial cell survival through the phosphatidylinositol 3'-kinase/Akt signal transduction pathway. Requirement for Flk-1/KDR activation. *The Journal of biological chemistry* **273**(46)**:** 30336-30343.

Gingras AC, Kennedy SG, O'Leary MA, Sonenberg N, Hay N (1998). 4E-BP1, a repressor of mRNA translation, is phosphorylated and inactivated by the Akt(PKB) signaling pathway. *Genes & development* **12**(4)**:** 502-513.

Gottesman MM (2002). Mechanisms of cancer drug resistance. *Annual review of medicine* **53:** 615-627.

Gu P, Xing X, Tanzer M, Rocken C, Weichert W, Ivanauskas A, *et al.* (2008). Frequent loss of TIMP-3 expression in progression of esophageal and gastric adenocarcinomas. *Neoplasia* **10**(6)**:** 563-572.

Hahn-Windgassen A, Nogueira V, Chen CC, Skeen JE, Sonenberg N, Hay N (2005). Akt activates the mammalian target of rapamycin by regulating cellular ATP level and AMPK activity. *The Journal of biological chemistry* **280**(37)**:** 32081-32089.

Hamada K, Sasaki T, Koni PA, Natsui M, Kishimoto H, Sasaki J, *et al.* (2005). The PTEN/PI3K pathway governs normal vascular development and tumor angiogenesis. *Genes & development* **19**(17)**:** 2054-2065.

Hanai J, Dhanabal M, Karumanchi SA, Albanese C, Waterman M, Chan B, *et al.* (2002). Endostatin causes G1 arrest of endothelial cells through inhibition of cyclin D1. *The Journal of biological chemistry* **277**(19)**:** 16464-16469.

Hawkins T, Mirigian M, Selcuk Yasar M, Ross JL (2010). Mechanics of microtubules. *Journal of biomechanics* **43**(1)**:** 23-30.

Herbert SP, Stainier DY (2011). Molecular control of endothelial cell behaviour during blood vessel morphogenesis. *Nature reviews. Molecular cell biology* **12**(9)**:** 551-564.

Herbst RS, Heymach JV, Lippman SM (2008). Lung cancer. *The New England journal of medicine* **359**(13)**:** 1367-1380.

Hoegy SE, Oh HR, Corcoran ML, Stetler-Stevenson WG (2001). Tissue inhibitor of metalloproteinases-2 (TIMP-2) suppresses TKR-growth factor signaling independent of metalloproteinase inhibition. *The Journal of biological chemistry* **276**(5)**:** 3203-3214.

Hopper-Borge E, Chen ZS, Shchaveleva I, Belinsky MG, Kruh GD (2004). Analysis of the drug resistance profile of multidrug resistance protein 7 (ABCC10): resistance to docetaxel. *Cancer research* **64**(14)**:** 4927-4930.

Hsu YL, Wu LY, Kuo PL (2009). Dehydrocostuslactone, a medicinal plant-derived sesquiterpene lactone, induces apoptosis coupled to endoplasmic reticulum stress in liver cancer cells. *The Journal of pharmacology and experimental therapeutics* **329**(2)**:** 808-819.

Huisman MT, Chhatta AA, van Tellingen O, Beijnen JH, Schinkel AH (2005). MRP2 (ABCC2) transports taxanes and confers paclitaxel resistance and both processes are stimulated by probenecid. *International journal of cancer. Journal international du cancer* **116**(5)**:** 824-829.

Hung JY, Hsu YL, Ni WC, Tsai YM, Yang CJ, Kuo PL, *et al.* (2010). Oxidative and endoplasmic reticulum stress signaling are involved in dehydrocostuslactone-mediated apoptosis in human non-small cell lung cancer cells. *Lung Cancer* **68**(3)**:** 355-365.

Ide AG, Baker, N.H. & Warren, S.L. (1939). Vascularization of the Brown Pearce rabbit epithelioma transplant as seen in the transparent ear chamber. *Am. J. Roentgenol* **42:** 891-899.

Ivy SP, Wick JY, Kaufman BM (2009). An overview of small-molecule inhibitors of VEGFR signaling. *Nature reviews. Clinical oncology* **6**(10)**:** 569-579.

Iwatsuki K, Tanaka K, Kaneko T, Kazama R, Okamoto S, Nakayama Y, *et al*. (2005). Runx1 promotes angiogenesis by downregulation of insulin-like growth factor-binding protein-3. *Oncogene* **24**(7)**:** 1129-1137.

Jiang BH, Liu LZ (2008). AKT signaling in regulating angiogenesis. *Current cancer drug targets* **8**(1)**:** 19-26.

Jiang BH, Zheng JZ, Aoki M, Vogt PK (2000). Phosphatidylinositol 3-kinase signaling mediates angiogenesis and expression of vascular endothelial growth factor in endothelial cells. *Proceedings of the National Academy of Sciences of the United States of America* **97**(4)**:** 1749-1753.

Kanda S, Hodgkin MN, Woodfield RJ, Wakelam MJ, Thomas G, Claesson-Welsh L (1997). Phosphatidylinositol 3'-kinase-independent p70 S6 kinase activation by fibroblast growth factor receptor-1 is important for proliferation but not differentiation of endothelial cells. *The Journal of biological chemistry* **272**(37)**:** 23347-23353.

Kavallaris M (2010). Microtubules and resistance to tubulin-binding agents. *Nature reviews. Cancer* **10**(3)**:** 194-204.

Kobayashi S, Boggon TJ, Dayaram T, Janne PA, Kocher O, Meyerson M, *et al.* (2005). EGFR mutation and resistance of non-small-cell lung cancer to gefitinib. *The New England journal of medicine* **352**(8)**:** 786-792.

Koers-Wunrau C, Wehmeyer C, Hillmann A, Pap T, Dankbar B (2013). Cell surface-bound TIMP3 induces apoptosis in mesenchymal Cal78 cells through ligand-independent activation of death receptor signaling and blockade of survival pathways. *PloS one* **8**(7)**:** e70709.

Koolen SL, Beijnen JH, Schellens JH (2010). Intravenous-to-oral switch in anticancer chemotherapy: a focus on docetaxel and paclitaxel. *Clinical pharmacology and therapeutics* **87**(1)**:** 126-129.

Kuo PL, Ni WC, Tsai EM, Hsu YL (2009). Dehydrocostuslactone disrupts signal transducers and activators of transcription 3 through up-regulation of suppressor of cytokine signaling in breast cancer cells. *Molecular cancer therapeutics* **8**(5)**:** 1328-1339.

Lai MJ, Huang HL, Pan SL, Liu YM, Peng CY, Lee HY, *et al.* (2012). Synthesis and biological evaluation of 1-arylsulfonyl-5-(N-hydroxyacrylamide)indoles as potent histone deacetylase inhibitors with antitumor activity in vivo. *Journal of medicinal chemistry* **55**(8)**:** 3777-3791.

Langton KP, McKie N, Curtis A, Goodship JA, Bond PM, Barker MD, *et al.* (2000). A novel tissue inhibitor of metalloproteinases-3 mutation reveals a common molecular phenotype in Sorsby's fundus dystrophy. *The Journal of biological chemistry* **275**(35)**:** 27027-27031.

Lens SM, Voest EE, Medema RH (2010). Shared and separate functions of polo-like kinases and aurora kinases in cancer. *Nature reviews. Cancer* **10**(12)**:** 825-841.

Liu H, Tekle C, Chen YW, Kristian A, Zhao Y, Zhou M, *et al.* (2011). B7-H3 silencing increases paclitaxel sensitivity by abrogating Jak2/Stat3 phosphorylation. *Molecular cancer therapeutics* **10**(6)**:** 960-971.

Lockhart AC, Braun RD, Yu D, Ross JR, Dewhirst MW, Humphrey JS, *et al.* (2003). Reduction of wound angiogenesis in patients treated with BMS-275291, a broad spectrum matrix metalloproteinase inhibitor. *Clinical cancer research : an official journal of the American Association for Cancer Research* **9**(2)**:** 586-593.

Malumbres M (2011). Physiological relevance of cell cycle kinases. *Physiological reviews* **91**(3)**:** 973-1007.

Miao ZH, Feng JM, Ding J (2012). Newly discovered angiogenesis inhibitors and their mechanisms of action. *Acta pharmacologica Sinica* **33**(9)**:** 1103-1111.

Mollinedo F, Gajate C (2003). Microtubules, microtubule-interfering agents and apoptosis. *Apoptosis : an international journal on programmed cell death* **8**(5)**:** 413-450.

Murphy DA, Makonnen S, Lassoued W, Feldman MD, Carter C, Lee WM (2006). Inhibition of tumor endothelial ERK activation, angiogenesis, and tumor growth by sorafenib (BAY43-9006). *The American journal of pathology* **169**(5)**:** 1875-1885.

Murray S, Briasoulis E, Linardou H, Bafaloukos D, Papadimitriou C (2012). Taxane resistance in breast cancer: mechanisms, predictive biomarkers and circumvention strategies. *Cancer treatment reviews* **38**(7)**:** 890-903.

Murthy A, Defamie V, Smookler DS, Di Grappa MA, Horiuchi K, Federici M, *et al.* (2010). Ectodomain shedding of EGFR ligands and TNFR1 dictates hepatocyte apoptosis during fulminant hepatitis in mice. *The Journal of clinical investigation* **120**(8)**:** 2731-2744.

Musgrove EA, Caldon CE, Barraclough J, Stone A, Sutherland RL (2011). Cyclin D as a therapeutic target in cancer. *Nature reviews. Cancer* **11**(8)**:** 558-572.

Nagase H, Visse R, Murphy G (2006). Structure and function of matrix metalloproteinases and TIMPs. *Cardiovascular research* **69**(3)**:** 562-573.

Nelsen CJ, Rickheim DG, Tucker MM, Hansen LK, Albrecht JH (2003). Evidence that cyclin D1 mediates both growth and proliferation downstream of TOR in hepatocytes. *The Journal of biological chemistry* **278**(6)**:** 3656-3663.

Nguyen KS, Kobayashi S, Costa DB (2009). Acquired resistance to epidermal growth factor receptor tyrosine kinase inhibitors in non-small-cell lung cancers dependent on the epidermal growth factor receptor pathway. *Clinical lung cancer* **10**(4)**:** 281-289.

Nieto Montesinos R, Beduneau A, Pellequer Y, Lamprecht A (2012). Delivery of P-glycoprotein substrates using chemosensitizers and nanotechnology for selective and efficient therapeutic outcomes. *Journal of controlled release : official journal of the Controlled Release Society* **161**(1)**:** 50-61.

Oh GS, Pae HO, Chung HT, Kwon JW, Lee JH, Kwon TO, *et al.* (2004). Dehydrocostus lactone enhances tumor necrosis factor-alpha-induced apoptosis of human leukemia HL-60 cells. *Immunopharmacology and immunotoxicology* **26**(2)**:** 163-175.

Paez-Ribes M, Allen E, Hudock J, Takeda T, Okuyama H, Vinals F, *et al.* (2009). Antiangiogenic therapy elicits malignant progression of tumors to increased local invasion and distant metastasis. *Cancer cell* **15**(3)**:** 220-231.

Pao W, Miller VA, Politi KA, Riely GJ, Somwar R, Zakowski MF, *et al.* (2005). Acquired resistance of lung adenocarcinomas to gefitinib or erlotinib is associated with a second mutation in the EGFR kinase domain. *PLoS medicine* **2**(3)**:** e73.

Pavloff N, Staskus PW, Kishnani NS, Hawkes SP (1992). A new inhibitor of metalloproteinases from chicken: ChIMP-3. A third member of the TIMP family. *The Journal of biological chemistry* **267**(24)**:** 17321-17326.

Perez EA (2009). Microtubule inhibitors: Differentiating tubulin-inhibiting agents based on mechanisms of action, clinical activity, and resistance. *Molecular cancer therapeutics* **8**(8)**:** 2086-2095.

Phung TL, Ziv K, Dabydeen D, Eyiah-Mensah G, Riveros M, Perruzzi C, *et al.* (2006). Pathological angiogenesis is induced by sustained Akt signaling and inhibited by rapamycin. *Cancer cell* **10**(2)**:** 159-170.

Potente M, Gerhardt H, Carmeliet P (2011). Basic and therapeutic aspects of angiogenesis. *Cell* **146**(6)**:** 873-887.

Qi JH, Ebrahem Q, Moore N, Murphy G, Claesson-Welsh L, Bond M, *et al.* (2003). A novel function for tissue inhibitor of metalloproteinases-3 (TIMP3): inhibition of angiogenesis by blockage of VEGF binding to VEGF receptor-2. *Nature medicine* **9**(4)**:** 407-415.

Qi JH, Ebrahem Q, Yeow K, Edwards DR, Fox PL, Anand-Apte B (2002). Expression of Sorsby's fundus dystrophy mutations in human retinal pigment epithelial cells reduces matrix metalloproteinase inhibition and may promote angiogenesis. *The Journal of biological chemistry* **277**(16)**:** 13394-13400.

Rosenwald IB, Kaspar R, Rousseau D, Gehrke L, Leboulch P, Chen JJ, *et al.* (1995). Eukaryotic translation initiation factor 4E regulates expression of cyclin D1 at transcriptional and post-transcriptional levels. *The Journal of biological chemistry* **270**(36)**:** 21176-21180.

Sangodkar J, Katz S, Melville H, Narla G (2010). Lung adenocarcinoma: lessons in translation from bench to bedside. *The Mount Sinai journal of medicine, New York* **77**(6)**:** 597-605.

Sarbassov DD, Guertin DA, Ali SM, Sabatini DM (2005). Phosphorylation and regulation of Akt/PKB by the rictor-mTOR complex. *Science* **307**(5712)**:** 1098-1101.

Schmidt M, Bastians H (2007). Mitotic drug targets and the development of novel anti-mitotic anticancer drugs. *Drug resistance updates : reviews and commentaries in antimicrobial and anticancer chemotherapy* **10**(4-5)**:** 162-181.

Schnell CR, Stauffer F, Allegrini PR, O'Reilly T, McSheehy PM, Dartois C, *et al.* (2008). Effects of the dual phosphatidylinositol 3-kinase/mammalian target of rapamycin inhibitor NVP-BEZ235 on the tumor vasculature: implications for clinical imaging. *Cancer research* **68**(16)**:** 6598-6607.

Shapiro AB, Ling V (1998). The mechanism of ATP-dependent multidrug transport by P-glycoprotein. *Acta physiologica Scandinavica. Supplementum* **643:** 227-234.

Shinojima T, Yu Q, Huang SK, Li M, Mizuno R, Liu ET, *et al.* (2012). Heterogeneous epigenetic regulation of TIMP3 in prostate cancer. *Epigenetics : official journal of the DNA Methylation Society* **7**(11)**:** 1279-1289.

Skeen JE, Bhaskar PT, Chen CC, Chen WS, Peng XD, Nogueira V, *et al.* (2006). Akt deficiency impairs normal cell proliferation and suppresses oncogenesis in a p53-independent and mTORC1-dependent manner. *Cancer cell* **10**(4)**:** 269-280.

Stanton RA, Gernert KM, Nettles JH, Aneja R (2011). Drugs that target dynamic microtubules: a new molecular perspective. *Medicinal research reviews* **31**(3)**:** 443-481.

Stewart ZA, Tang LJ, Pietenpol JA (2001). Increased p53 phosphorylation after microtubule disruption is mediated in a microtubule inhibitor- and cell-specific manner. *Oncogene* **20**(1)**:** 113-124.

Szakacs G, Jakab K, Antal F, Sarkadi B (1998). Diagnostics of multidrug resistance in

cancer. *Pathology oncology research : POR* **4**(4)**:** 251-257.

Tabata Y, Isashiki Y, Kamimura K, Nakao K, Ohba N (1998). A novel splice site mutation in the tissue inhibitor of the metalloproteinases-3 gene in Sorsby's fundus dystrophy with unusual clinical features. *Human genetics* **103**(2)**:** 179-182.

Taylor RC, Cullen SP, Martin SJ (2008). Apoptosis: controlled demolition at the cellular level. *Nature reviews. Molecular cell biology* **9**(3)**:** 231-241.

Thomas LW, Lam C, Edwards SW (2010). Mcl-1; the molecular regulation of protein function. *FEBS letters* **584**(14)**:** 2981-2989.

Tsai AC, Pan SL, Liao CH, Guh JH, Wang SW, Sun HL, *et al.* (2010). Moscatilin, a bibenzyl derivative from the India orchid Dendrobrium loddigesii, suppresses tumor angiogenesis and growth in vitro and in vivo. *Cancer letters* **292**(2)**:** 163-170.

Uribe MC, Grier HJ, Parenti LR (2012). Ovarian structure and oogenesis of the oviparous goodeids Crenichthys baileyi (Gilbert, 1893) and Empetrichthys latos Miller, 1948 (teleostei, Cyprinodontiformes). *Journal of morphology* **273**(4)**:** 371-387.

Ussar S, Voss T (2004). MEK1 and MEK2, different regulators of the G1/S transition. *The Journal of biological chemistry* **279**(42)**:** 43861-43869.

Walker SR, Chaudhury M, Nelson EA, Frank DA (2010). Microtubule-targeted chemotherapeutic agents inhibit signal transducer and activator of transcription 3 (STAT3) signaling. *Molecular pharmacology* **78**(5)**:** 903-908.

Wang CY, Tsai AC, Peng CY, Chang YL, Lee KH, Teng CM, *et al.* (2012a). Dehydrocostuslactone suppresses angiogenesis in vitro and in vivo through inhibition of Akt/GSK-3beta and mTOR signaling pathways. *PloS one* **7**(2)**:** e31195.

Wang M, Zhao J, Zhang LM, Li H, Yu JP, Ren XB, *et al.* (2012b). Combined Erlotinib and Cetuximab overcome the acquired resistance to epidermal growth factor receptors tyrosine kinase inhibitor in non-small-cell lung cancer. *Journal of cancer research and clinical oncology* **138**(12)**:** 2069-2077.

Weber BH, Vogt G, Pruett RC, Stohr H, Felbor U (1994). Mutations in the tissue inhibitor of metalloproteinases-3 (TIMP3) in patients with Sorsby's fundus dystrophy. *Nature genetics* **8**(4)**:** 352-356.

Yasui M, Yamamoto H, Ngan CY, Damdinsuren B, Sugita Y, Fukunaga H, *et al*. (2006). Antisense to cyclin D1 inhibits vascular endothelial growth factor-stimulated growth of vascular endothelial cells: implication of tumor vascularization. *Clinical cancer research : an official journal of the American Association for Cancer Research* **12**(15)**:** 4720-4729.

Yuan TL, Choi HS, Matsui A, Benes C, Lifshits E, Luo J, *et al.* (2008). Class 1A PI3K regulates vessel integrity during development and tumorigenesis. *Proceedings of the National Academy of Sciences of the United States of America* **105**(28)**:** 9739-9744.

Zeng Y, Rosborough RC, Li Y, Gupta AR, Bennett J (1998). Temporal and spatial regulation of gene expression mediated by the promoter for the human tissue inhibitor of metalloproteinases-3 (TIMP-3)-encoding gene. *Developmental dynamics : an official publication of the American Association of Anatomists* **211**(3)**:** 228-237.

著作

Wang CY, Liou JP, Tsai AC, Lai MJ, Liu YM, Lee HY, Wang JC, Pan SL, Teng CM. A novel action mechanism for MPT0G013, a derivative of arylsulfonamide, inhibits tumor angiogenesis through up-regulaiton of TIMP3 expression. Oncotarget 2014 revised.

Wang MJ, Liu YQ, Chang LC, **Wang CY**, Zhao YL, Zhao XB, Qian K, Nan X, Yang L, Yang XM, Hung HY, Yang JS, Kuo DH, Goto M, Morris-Natschke SL, Pan SL, Teng CM, Kuo SC, Wu TS, Wu YC, Lee KH. Design, Synthesis, Mechanisms of Action, and Toxicity of Novel 20(S)-Sulfonylamidine Derivatives of Camptothecin as Potent Antitumor Agents. J Med Chem. 2014 Jul 8.

Tsai AC, Pai HC, **Wang CY**, Liou JP, Teng CM, Wang JC, Pan SL. In vitro and in vivo anti-tumour effects of MPT0B014, a novel derivative aroylquinoline, and in combination with erlotinib in human non-small-cell lung cancer cells. Br J Pharmacol. 2014 Jan;171(1):122-33.

Tsai AC*, **Wang CY***, Liou JP, Pai HC, Hsiao CJ, Chang JY, Wang JC, Teng CM, Pan SL. Orally active microtubule-targeting agent, MPT0B271, for the treatment of human non-small cell lung cancer, alone and in combination with erlotinib. Cell Death Dis. 2014 Apr 10;5:e1162. (*: equal contribution)

Li WQ, Wang XL, Qian K, Liu YQ, **Wang CY**, Yang L, Tian J, Morris-Natschke SL, Zhou XW, Lee KH. Design, synthesis and potent cytotoxic activity of novel podophyllotoxin derivatives. Bioorg Med Chem. 2013 Apr 15;21(8):2363-9.

Liu Y, Qian K, **Wang CY**, Chen CH, Yang X, Lee KH. Design and one-pot synthesis of new 7-acyl camptothecin derivatives as potent cytotoxic agents. Bioorg Med Chem Lett. 2012 Dec 15;22(24):7659-61.

Yang X, Shi Q, Lai CY, Chen CY, Ohkoshi E, Yang SC, **Wang CY**, Bastow KF, Wu TS, Pan SL, Teng CM, Yang PC, Lee KH. Antitumor agents 295. E-ring hydroxylated antofine and cryptopleurine analogues as antiproliferative agents: design, synthesis, and mechanistic studies. J Med Chem. 2012 Aug 9;55(15):6751-61.

Wang CY, Tsai AC, Peng CY, Chang YL, Lee KH, Teng CM, Pan SL. Dehydrocostuslactone suppresses angiogenesis in vitro and in vivo through inhibition of Akt/GSK-3β and mTOR signaling pathways. PLoS One. 2012;7(2):e31195.

Tsai AC, Pan SL, Lai CY, **Wang CY**, Chen CC, Shen CC, Teng CM. The inhibition of angiogenesis and tumor growth by denbinobin is associated with the blocking of insulin-like growth factor-1 receptor signaling. J Nutr Biochem. 2011 Jul;22(7):625-33.

Tsai AC, Pan SL, Sun HL, **Wang CY**, Peng CY, Wang SW, Chang YL, Kuo SC, Lee KH, Teng CM. CHM-1, a new vascular targeting agent, induces apoptosis of human umbilical vein endothelial cells via p53-mediated death receptor 5 up-regulation. J Biol Chem. 2010 Feb 19;285(8):5497-506.